Tampere University

Elias D. Tervonen

EFFECTS OF HOUSEHOLD PHOTOVOLTAIC SYSTEMS WITH ENERGY STORAGE SYSTEMS ON THE LOW VOLTAGE GRID

Master of Science Thesis
Faculty of Information Technology and Communication Sciences
Examiner 1: Assistant Professor Kari Lappalainen
Examiner 2: Professor Seppo Valkealahti
April 2023

ABSTRACT

Elias D. Tervonen: Effects of household photovoltaic systems with energy storage systems on the low voltage grid
Master of Science Thesis
Tampere University
Master's Degree Programme in Electrical Engineering
April 2023

This thesis was done to better understand and study issues caused by a high quantity of photovoltaic (PV) systems in low-voltage grids by the low voltage (LV) feeder simulations. Other focus was studying the effect of energy storage systems (ESSs) in avoiding issues and grid violations during high-level PV penetrations.

PV modules are connected in series as a PV system to increase PV production. The value of PV production are determined by environmental parameters, mainly global irradiance received by solar cells and cell temperatures of the cells. Favoring a 3-phase grid connection and the optimal sizing of a PV inverter helps to maximize PV production and diminish issues caused to both the PV system and grid operations.

PV systems as a part of the electrical distribution grid have been studied and tested for the last decades but a new trend of multiple PV systems located in the same feeder has caused grid issues. A peak production during the midday with low consumption in the feeder causes overvoltages in the grid points. Other issues caused by PV systems include thermal capacity limit violations in feeder lines due to reverse power flow (RPF), harmonic injections, voltage phase unbalances and undervoltages in grid components, like feeder lines and transformers. The level of PV production can be determined using the term hosting capacity (HC) based on different parameters. The parameter used in this thesis is the peak load of 180 kW of the feeder during the two simulation dates. The level of HC is restricted by lengths of feeder lines, number and capacity of loads and issues mentioned earlier. HC enhancement tools include voltage control, active power curtailment, reactive power control and transformer applications, like off-load and on-load tap changers.

ESS technologies alter by price, capacity and operational attributes. Different algorithms and topologies of ESSs are chosen based on a wanted performance of PV systems. Centralized and de-centralized topologies of ESS are chosen depending on the number and separate shading conditions of the PV systems in the region. For household PV systems, battery energy storage systems are favored due to their physical size and lower investment costs when compared to other ESS technologies.

In this thesis, the levels of PV capacity are simulated using $Matlab^{TM}$ Simulink program with the PV data measured in the solar PV research power plant in the Hervanta Campus of Tampere University. The PV data from the two simulation dates was added to the simulation model consisting of 21 residential buildings in the 285 m low voltage feeder. PV capacities were integrated starting from the transformer towards the end of the feeder in three cases. The operation states of ESSs were integrated with the settings of 2 %/min and 10 %/min ramp rate limits as the power control tool. In case 3, grid violations of the thermal capacity limit of feeder lines and +5% of the nominal overvoltages in distribution cabinets were recorded with over 120 % PV capacity. RPF was recorded at 77.69 % PV capacity. Grid violations could be avoided using de-centralized ESS applications in PV systems. The 2 %/min ramp rate limit would enable the LV feeder to avoid grid violations. But the 10 %/min ramp rate limit could not avoid grid violations on the other simulation date.

Keywords: photovoltaic (PV) systems, energy storage systems (ESSs), hosting capacity (HC) and low voltage (LV)

TIIVISTELMÄ

Elias D. Tervonen: Kotitalouksien aurinkovoima- ja energiavarastojärjestelmien vaikutukset pienjänniteverkossa
Diplomityö
Tampereen yliopisto
Tieto- ja sähkötekniikan koulutus
Sähkötekniikan DI-ohjelma
Huhtikuu 2023

Tämän opinnäytetyön tarkoituksena oli tutkia ja ymmärtää paremmin pienjänniteverkoissa suurissa määrissä esiintyvien aurinkovoimajärjestelmien aiheuttamia ongelmia. Toisena pääkohtana oli simuloida verkon sietokykyä ja energiavarastojärjestelmien vaikutusta verkkorajojen rikkoumisen välttämisessä korkean tason aurinkovoimatuotannon aikana.

Aurinkovoimajärjestelmän tuotannon määrään ja laatuun vaikuttavat ympäristötekijät, pääasiassa aurinkokennojen saama valoisuus ja lämpötila. Aurinkovoimajärjestelmän moduulit voidaan järjestää eri topologioilla parantamaan saatavan tuotannon määrää. Kolmivaiheisen verkkoliitynnän ja invertterin optimaalinen mitoituksen suosiminen auttavat maksimoimaan tuotantoa ja vähentämään tuotannossa ja jakeluverkkotoiminnassa esiintyviä ongelmia.

Aurinkovoimajärjestelmät eivät ole täysin uusi tai vähässä käytössä oleva teknologia, mutta uusi ilmiö on ilmaantunut sähköntuotannossa, jossa normaalisti kuluttajiksi profiloituneet kotitaloudet ovat hankkineet aurinvoimajärjestelmien moduuleja katoilleen kasvavissa määrin. Suuresta tuotannosta, erityisesti keskipäivisin, on syntynyt verkkohäiriöitä, yleisimpinä ylijännitepisteet ja verkkojohtojen kuumeneminen. Muita haittailmiöitä ovat käänteinen tehonvirtaus (englanniksi reverse power flow) tehonkulussa, harmoniset yliaallot, vaihejännitteiden epätasapaino ja alijännitteet. Tuotannon taso voidaan paremmin suhteuttaa verkkoarvoihin käyttämällä englannin kielen termiä Hosting capacity (HC). HC perustuu johonkin verkkoparametriin ja tässä työssä käytetään simulointimallin hetkellistä huippukulutusta 180 kW. HC:n arvoa rajoittavat johtimien pituudet, kotitalouksien kuormitusten arvot ja lukumäärä verkkohaaralla sekä aikaisemmin mainittujen haittatekijöiden arvot. HC:n arvoa kasvattavat työkalut ovat tehonhallinta, jännitteiden hallinta ja muuntajan jännitteen hallintalaitteet. Myös näiden hallintalaitteiden yhteiskäyttöratkaisuja käytetään paremmin kasvattamaan aurinkovoiman tuotantoa.

Energiavarastojärjestelmät vaihtelevat investointihinnan, kapasiteetin ja käyttö-ominaisuuksien mukaan. Erilaisia järjestelmäalgoritmeja ja topologioita valitaan aurinkovoimajärjestelmien halutun suorituskyvyn perusteella. Kotitalouksien aurinkovoimajärjestelmien energiavarastojärjestelmien ratkaisuissa suositaan akkuteknologioita niiden pienemmän fyysisen kokojen ja alhaisempien investointihintojen vuoksi muihin teknologioihin verrattaessa.

Tässä opinnäytetyössä aurinkovoimatuotantoa simuloitiin $Matlab^{TM}$ Simulink-ohjelmalla Tampereen yliopiston Hervannan kampuksen aurinkovoimatutkimuslaitoksessa mitatuilla arvoilla. Arvot lisättiin simulointimalliin, joka koostui 21 asuinrakennuksesta 285 metrin pienjänniverkkohaaralla kahden simulointipäivän aikana. Aurinkovoimakapasiteettia kasvatettiin kolmessa simulointitapauksessa rakennus kerrallaan alkaen muuntajalta. Verkkorajat menivät rikki yli 120% aurinkovoimajärjestelmän tuotannon arvolla 3. tapauksessa, jossa oli asennettu aurinkopaneeleja kotitalouksien, autotallien ja autokatosten etelän puoleisille katoille. Verkkorikkomukset ilmaantuivat verkkohaaran alkupään johtimien ylikuumenisena ja loppupään jakelukaappien ja sulakekaappien ylijännitteinä. Vastaikkaisvirtaus tehonjakelussa havaittiin yli 77.69 % tuotannon arvoilla. Verkkorikkomukset pystyttiin välttämään käyttämällä energiavarastojärjestelmän asetusta perustuen tehon muutosnopeuden rajoittamiseen 2 %/min arvolla, mutta 10 %/min arvolla ei pystynyt estämään ylijännitteiden syntymistä verkkohaaran loppupään kotitalouksien sulakekaapeissa toisena simulointipäivänä.

Avainsanat: aurinkovoimajärjestelmät (photovoltaic systems), energiavarastojärjestelmät (energy storage systems) , pienjänniteverkko (low voltage grid) ja ylijännitteet (overvoltages).

PREFACE

This thesis was developed in the unit of electrical engineering of Tampere University in the Hervanta Campus. Assistant Professor Kari Lappalainen supervised the thesis and examined it with Professor Seppo Valkealahti.

The topic of the thesis is interesting and topical to the current economic and geopolitical situation we are living in 2023. The target audience is not only the personnel of the electrical industry and distribution system operators but also consumers considering or already having PV modules on their rooftops. I hope that this thesis not only helps to better understand the potential of PV systems at low voltage levels but also helps to realize that the role of electric distribution grids is changing. In the future, the focus of grid reinforcement should be on having stabilized and trustworthy operation states of regional grids where the need for power transfer from outside of the distribution grid is minimized due to a high level of residential and industrial PV production.

Firstly, I wish to thank Kari Lappalainen and Hossein Hafesi from Tampere University for helping and guiding me in building the Matlab™ Simulink simulation model. I also wish to thank Lappalainen for the idea, referencing literature for the thesis and calculating the PV and ESS data used in the simulation model. I wish my thanks and regards to the university personnel and private sector workers stationed in the E and F wings of the Sähkötalo building of Hervanta Campus. I had lovely time discussing about multiple subjects and sharing unique moments in the coffee room.

In October 2022, I broke my ankle due to the incident. I give my gratitude and wishes to the medical personnel of Hospital Nova in Jyväskylä, Tampere University Hospital and Hatanpää Health Center in Tampere for the professional and high-quality service that I received.

Lastly, I want to give thanks to my family: father Jouko, mother Marja-Riitta and brother Joel for giving me support during my engineering studies in 2016–2023.

Rakkaus voittaa aina.

Elias D. Tervonen
elias.tervonen@gmail.com

Puuppola, 6th April 2023.

TABLE OF CONTENTS

SYMBOLS AND ABBREVIATIONS

Symbols

A	Ideality factor of a diode
B	Temperature independent constant of saturation current
d_0, d_1	Polynomial coefficients of a photovoltaic inverter
$E_{\mathrm{ESS,\ min}}$	Minimum charging of the energy storage system
E_G	Energy band gap
$E_{G,\ 0}$	Linearly extrapolated zero temperature band gap of semiconductor
G_0	Reference level of irradiance
I_0	Saturation current of a diode
I_{MPP}	Current of maximum power point of a photovoltaic cell or module
I_{SC}	Short-circuit current
k	Boltzmann constant
P_{ESS}	Active power fed to the energy storage system
P_{grid}	Active power fed to the grid
$P_{\mathrm{grid,\ max}}$	Maximum active power fed to the grid
P_{inv}	Active power fed to the inverter
$P_{\mathrm{peak\ load}}$	Peak active power load
P_{MPP}	Active power of maximum power point of the photovoltaic module
P_{PV}	Active power of a photovoltaic module or system
$P_{\mathrm{PV,\ nom}}$	Nominal active power of a photovoltaic module or system
p_{PV}	Injected active power of a photovoltaic inverter

$p_{\mathrm{PV,\ peak}}$	Peak injected active power of a photovoltaic inverter
q	Elementary charge
q_{PV}	Injected reactive power of a photovoltaic inverter
$q_{\mathrm{PV,\ peak}}$	Peak injected reactive power of a photovoltaic inverter
$\mathrm{RR}_{\mathrm{limit}}$	Ramp rate limit
U^{-}	Negative sequence voltage magnitude
U^{+}	Positive sequence voltage magnitude
U_{MAX}	Maximum voltage
U_{MIN}	Minimum voltage
U_{MPP}	Voltage of maximum power point of a photovoltaic module
U_{MV}	Medium grid voltage
U_{N}	Nominal voltage
U_{OC}	Open-circuit voltage
γ	Temperature dependence of parameters of the dark saturation current
ϕ	Angle difference

Abbrevations

AC	Alternative current
APC	Active power curtailment
BESS	Battery energy storage system
CES	Cold and cryogenic energy storage
CAES	Compressed air energy storage
DC	Direct current
DFT	Discrete Fourier transform

DG	Distributed generation
DSO	Distribution system operator
EMD	Empirical mode decompensation
ESS	Energy storage system
LPF	Low-pass filter
HC	Hosting capacity
HV	High voltage
HVDC	High voltage direct current
LV	Low voltage
MPP	Maximum power point
MPPT	Maximum power point tracking
MV	Medium voltage
n-type	Negative semiconductor
OfLTR	Off-load tap changer
OLTR	On-load tap changer
PV	Photovoltaic
PCC	Point of common-coupling
p-n junction	Positive-negative semiconductor junction
p-type	Positive semiconductor
PF	Power factor
PQ	Power quality
PHS	Pumped hydro storage
PTES	Pumped thermal electricity storage
RR	Ramp rate

RPC	Reactive power control
REG	Renewable energy generation
RPF	Reverse power flow
STC	Standard test conditions
SG	Synchronous generator
TES	Thermal energy storage
VUF	Voltage unbalance factor

1 INTRODUCTION

Electricity was first strange but not unknown to men during ancient history. Some might have understood thunder and following fast lightning as a natural phenomenon. But for most, it must have been a terrifying phenomenon and had some superstitious reasoning behind it. The early electrical battery was invented in the current Baghdad, Iraq early as in the Parthian era (~ 250 BC). The battery might have functioned as an electrochemical battery and it was built inside of a clay pot and consisted of copper and iron parts dunked in citrus or acetic acid. [1, p. 15] The overcut of the clay pot is shown in Figure 1.1. The internal mix between acid and metals could store an electric charge. The replica of clay pot functions was done by the study groups at the University of Singapore. One group could light up to 5 modern light-emitted diodes with the highest average voltage measured 11.7 V and the highest average current measured 3.6 mA. [2] The usage of the clay pot is unknown but the builders understood the potential difference between materials, commonly known as voltage. This clay pot was the first recorded electrochemical battery [1]. But it took over two thousand years before electricity usage was enhanced to colossal levels. This was done by adding a simple component between two or more potentials, a metal wire as a conductor. Electricity is an excellent solution for energy storage and distribution. Electricity distribution may not cause major climate change pollution if renewable energy generations (REGs) are favored. The overall benefits of electricity are better than energy production methods, like gas, hydro, and oil storage. The only disadvantage of storing electricity is more difficult to contain a high level of charge [3].

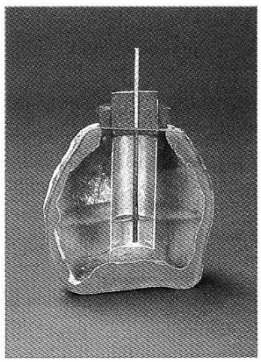

Figure 1.1. *Overcut of the clay pot copy that is believed to function as the first recorded electrochemical battery [1].*

Photovoltaic (PV) systems have become an interesting investment for all members of society today. Before a single PV system in a distribution grid had a negligible effect on the grid operation states and values [4]. But a high level of PV systems installed in distribution feeders has caused concern and issues with grid operations. During a high PV penetration in a low voltage (LV) grid, the thermal limit of conductors and the load rate of a transformer may be violated due

to the effects of reverse power flow (RPF). RPF occurs when power is transferred from generally profiled load points to the transformer in distribution feeders. [5]–[7] Overvoltages are the main problem of high PV penetration [5], [8]–[11]. Undervoltages, thermal capacity limit violations of feeders and high overloading of transformers are major issues of high PV production as well [8], [10], [12], [13]. The interest in household PV systems is amplified by the rising cost of living in western countries and the unstable geopolitical situation of today. Can a household PV system in a LV grid have higher or even unlimited production with an installed energy storage system (ESS) application? Can it be done without grid code violations?

This thesis was done to better understand the different factors of household PV systems located in LV feeders and the effect of integrated ESSs in PV systems as the power control tool. The topic area is wide and includes multiple theories, not only of PV systems and EESs but also of the electric power grid and the effects of PV system operations on it. All these theory areas are wide. The goal is to make the reader understand that none of the theories can be left out or ignored. The best way is to realize and understand that PV systems on household rooftops still need more development before both grid stability and maximal PV production are achieved.

Household PV systems are still a new technology that has multiple factors that can affect distribution grid operations and values. These factors are mentioned briefly. The focus remains on small- and medium-scaled PV systems with the modules located on the rooftops of the residential buildings in the simulated LV feeder. The LV feeder has 4 underground cable lines starting from the transformer and 4 distribution cabinets which are designed to distribute power to 21 residential buildings. The simulations were simple and done by using the $Matlab^{TM}$ Simulink program and add the power values of PV data in the simulation model. The active power of the PV data was measured from the solar PV power research plant located on the rooftop of the Sähkötalo building in Hervanta Campus of Tampere University. The research plant consists of the weather station and 69 PV modules [14]. The data was measured from the PV string of 23 modules on two dates: 7th August 2021 and 27th April 2022. The first step of the simulation was to find the maximum value of PV penetration, id est the threshold of the feeder. This safe limit is called hosting capacity (HC). And secondly, see how the ESS applications located in PV systems with the de-centralized topology could avoid these issues when the PV capacity is increased beyond the determined threshold of the LV feeder. The ESS applications used two ramp rate (RR) limit settings: 2 %/min and 10 %/min based on the PV data during the two simulation dates. The simulation uses the calculated values of ESS applications and ignores the choice of ESS technology.

Chapter 2 discusses the PV theory. The theory mentions major environmental parameters in PV production, grid-connections types, topologies and components of a PV system. The environmental factors in the research plant on the Hervanta campus are presented at the end of Chapter 2. The electric power grid is discussed in Chapter 3. The backgrounds of transmission and distribution grids are presented. Two grid components, conductors and transformer, are discussed. HC factors and improvement methods in the literature are discussed as well. In Chapter 4, different ESS technologies based on capacities and operational attributes are presented. Different ESS algorithms and topologies in general use are presented and discussed. Different ESS-

integrated PV systems already in use are presented. The simulation model and data are presented in Chapter 5. Components and measurement instruments of the research plant are presented. The layout of the simulation model and the load profiles of the LV feeder are discussed. In Chapter 6, the results of three simulation cases with different PV capacities are presented. The ESS applications are used in Case 3 when the threshold of the LV feeder is violated. The results and PV systems in distribution grids are discussed at the end of Chapter 6. Lastly, the conclusions are presented in Chapter 7.

2 PHOTOVOLTAIC POWER SYSTEMS

The early 21st century witnessed the rise of REG systems due to the concerns caused by climate change. This has been noted by the industry, for example, grid component designers have taken actions to decrease carbon dioxide emissions in their production methods to slow down climate change [15]. Solar power-based PV systems are one of two major distribution generation (DG) solutions with wind power. The total PV capacity globally reached 480 GW in 2018. Asia dominated the market with half of the global PV capacity. The leading continents with existing and planned PV capacity by 2050 are Asia (280 & 4 837 GW), Europe (121 & 891 GW), North America (55 & 1 728 GW), Oceania (10 & 109 GW), Middle East and Africa (8 & 673 GW) and Latin America and Caribbean (7 & 281 GW) in 2018, respectively. [16, p. 24] China has stated that it will have a PV capacity of 1300 GW by 2055 [17]. The Finnish government has decided to pass the initiative to increase the level of renewable resources to satisfy the 50% of the annual energy consumption of the nation by 2030 [18]. The capacity of grid-connected PV systems in the Finnish power grid was 395 MW at the end of 2021, according to the Finnish distribution grid operators (DSOs). The capacity increased by over 100 MW from 2020. [19] The town of Utajärvi, Finland has stated that they are planning the solar power park of 350,000 PV modules with an annual produced energy of 200,000 MWh. The production is planned to satisfy the consumption of the large industrial region and the construction is planned to start as early as 2023. [20]

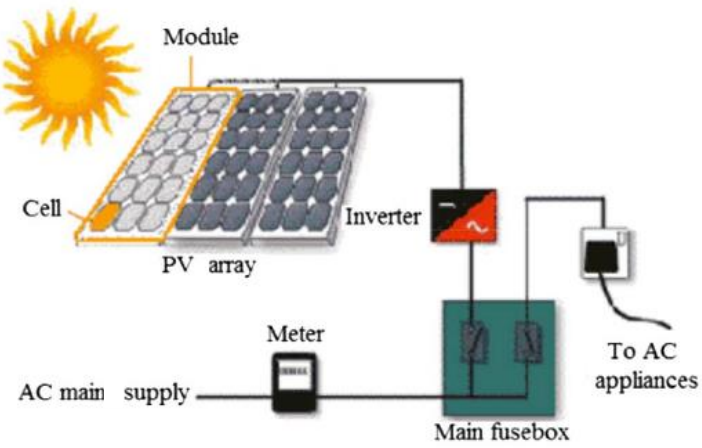

Figure 2.1. *Layout of a household photovoltaic system [21].*

The typical layout of a PV system installed in a household is shown in Figure 2.1. Modules consist of solar cells and PV systems have multiple modules depending on a size of an available platform area and a wanted production. The inverter converts direct current (DC) produced by a PV system to alternative current (AC) to match the grid requirements. AC power can be consumed locally by AC appliances or fed to the power grid (AC main supply in Figure 2.1.). [21]

DG units by capacities can be divided into small-scaled up to 10 kW, medium-scaled between 10–1000 kW, and larger utility-scaled between 1–10 MW [22]. These technologies were

developed as an alternative energy source outside of traditional AC power networks to compensate for small, usually household, power consumption. DG solutions are rapidly increasing in number and replacing traditional synchronous generators (SGs), like oil- and coal-powered ones, in the power grid. The decreasing amount of SGs and increasing quantity of grid-connected PV systems have caused inertia and frequency control issues in power grids. The generation exchange between SGs and DGs in power grids has awakened a need for SGs to adapt their production according to changes in DGs to maintain grid stability and control. [23] Voltage flickers due to high wind power penetration are considered one of the most serious issues caused by wind power production to distribution grids [24]. Voltage flickers are more likely to be an issue in distribution grids with high PV concentrations [7, p. 16785]. A large quantity of DG units with a slow response time may cause an unintentional islanding mode in an LV grid [25, p. 5]. DSOs are also interested in the impacts and finding solutions to characteristical problems of a high quantity of household PV systems in their LV feeders [12, p. 336].

In earlier years, the main issue of grid-connected PV systems was investment costs due to the low supply of PV modules in the market [26]. The availability of PV modules to residential households and companies has become easier during the last decade when module production has increased which has led to lower unit prices [7]. Household PV systems in LV grids can have a positive effect on decreasing the usage of non-renewable resources in power production avoiding forming gas emissions [27, p. 217], low need for cooling solutions and are a silent method of power production [28]. The main drawback of PV modules is causing unbalance between production and consumption in the grid due to rapidly changing irradiance caused by the shading of PV modules. Other minor drawbacks are low energy densities and an investment cost. [26] But the cost has been decreasing with more PV module manufacturers in the market [7].

Chapter 2 is discussing the PV theory and general factors considering PV systems. Firstly, the PV theory is presented and discussed. The components of solar cells and modules are presented. The role of external factors, mainly irradiance and temperature, affecting solar power production is discussed. In the second part, the structure and factors of the PV module are discussed. Thirdly, the PV inverter is presented. This part discusses different operation applications and general factors in the sizing of PV inverters. The operation states of PV inverters are not used in this thesis and the PV inverters are assumed to function without losses in the simulations. Topologies and grid-connection types of PV systems are discussed in the fourth part. Lastly, the environmental factors of the solar PV power research plant located at the Hervanta campus of Tampere University are discussed.

2.1 Photovoltaic theory

PV systems generate electric power through the PV effect by the cells receiving solar irradiance. The semiconductor solar cell absorbs irradiance and converts it to electrical energy by electrical current carriers in semiconductor materials: electrons and holes [29]. The effect can be done also by artificial light as well under optimal conditions [30]. The first to find the PV effect was

Becquerel who had done observations of photovoltaism in 1839. The first PV device to gain attention and practical use was designed by Fritts in 1883. The modern PV cell, with the founding of p-n (positive-negative semiconductor) junction between two semiconductors, was founded by Bell Laboratories in 1940s. [26, pp. 4, 5] This chapter presents the PV theory, presents different PV cell technologies but focuses more on silicon (Si)-based PV cells.

Light travels from the Sun to the atmosphere of the Earth where a portion of the light is absorbed and scattered before the rest of the irradiance reaches the surface of the Earth. PV cells and modules receive the global horizontal irradiance which is the combination of two components: direct and diffused irradiances. Direct irradiance is direct sunlight received by PV cells without being reflected from any surfaces. Diffused irradiance is scattered light that travels either first to the surface of the Earth and reflects or is reflected from clouds and structures to PV cells. [30] PV systems are designed to operate under clear sky conditions where the nominal output power is based. But the output power of PV systems can exceed based on the global irradiance received by PV modules due to the cloud enhancement phenomenon. The cloud enhancement phenomenon occurs during different conditions. The effect is the increments of either global irradiance due to light magnified from cloud edges or diffused irradiance before and after the effect and light penetrating a thin layer of clouds. The cloud enchantment phenomenon can cause an increment of PV production over 30% of the nominal capacity of the PV system under standard test conditions (STC). Overall, the cloud enchantment phenomenon has been proven to not cause major issues in the PV system operations. [31]

A PV cell consists of two semiconductor materials: positive (p-type) and negative (n-type). p-type has a majority of holes as electrical carries in the valence band and n-type has a majority of electrons in the conduction band. When these two semiconductors are brought to contact, a p-n junction is created. Both semiconductor types can have totally or partially occupied by electrons in their valence and conduction bands. Generally is assumed that energy bands have electrons fully occupying the conduction band and zero electrons in the conduction band under STC. [29] The absorbed light, photons with greater energy than the energy band gap E_G, causes excited electrons to travel from the valence to the conduction band and holes from the conduction band to the valence band in the p-n junction to form electron-hole pairs. This creates DC power. [26] This process is called fundamental absorption. The PV cell operates as the semiconductor diode where the electrical current moves in one direction. The direct bandgap semiconductor is shown in Figure 2.2 where the minimum value of the conduction band equals as the maximum value of the valence band according to the same crystal momentum value. Other bandgaps with different crystal momentum values between the two bands are called indirect bandgaps. [29, pp. 87, 92, 103] This thesis does not include different bandgaps in the PV cells of the PV systems in the simulations but understanding that the creation of electron-hole pairs between two bands is an essential process in irradiance converted to electrical energy.

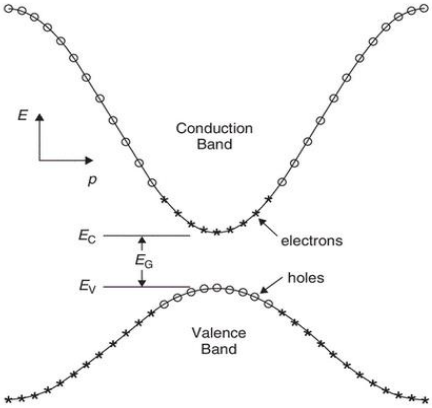

Figure 2.2. *Direct bandgap between semiconductors [29].*

The cross-section of the solar cell is shown in Figure 2.3 [32]. If an electron falls back to the valence band from an electron-hole pair in the conduction band, due to a semiconductor shifting out of thermal equilibrium, the process is called recombination. Recombination is the unwanted process that lowers the efficiency of a PV cell in PV production and high levels of recombination shorten the lifetime of the PV cell. [29, pp. 94, 95]

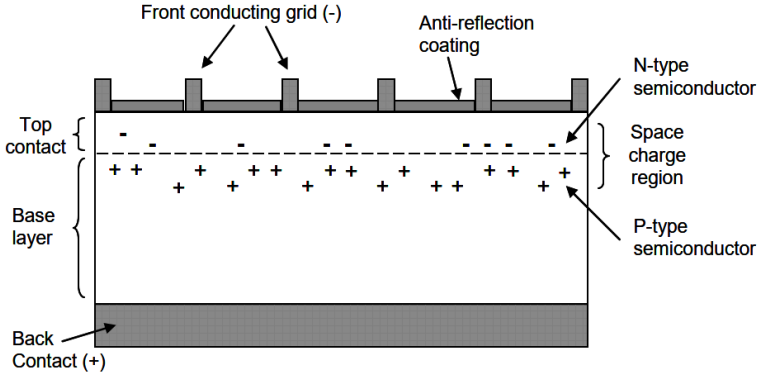

Figure 2.3. *Cross-section structure sketch of a PV cell [32].*

A PV cell has an anti-reflection coating to maximize the received global irradiance by increasing the amount of irradiance received by the semiconductor [29]. The most popular solar cell technologies are Si-cells: singular or multi-crystalline and amorphous [26], [33]. Other solar cell technologies are gallium arsenide (GaAs), indium gallium phosphide (GaInP), copper indium gallium selenide ($\mathrm{Cu(InGa)Se_2}$) and cadmium telluride (CdTe) cells, just giving a few examples. [29] This chapter focuses more on the theory of Si-based PV cells. To gain electric power from a PV cell, an electric load, an external resistor, is added between the contacts of semiconductors to enable a current flow [34].

The electric values of the PV cell, current (I) and the open-circuit voltage (U_{OC}) are defined by Equations 2.1 and 2.2. Equation 2.1 defines the current-voltage ($I-U$) curve of the cell:

$$I = I_{\mathrm{SC}} - I_0\left(e^{\frac{qU}{AkT}} - 1\right), \tag{2.1}$$

where I_{SC} is the short-circuit current at zero voltage, U the voltage and T the temperature of a PV cell. q is the elementary charge, I_0 is the saturation current of the diode, A the ideality factor of the diode and k is the Boltzmann constant. U_{OC} at zero current of the PV cell is defined by

$$U_{OC} = \frac{AkT}{q} ln\left(1 + \frac{I_{SC}}{I_0}\right) \approx \frac{AkT}{q} ln\left(\frac{I_{SC}}{I_0}\right). \quad (2.2)$$

To gain better performance of the PV cell, U_{OC} and I_{SC} should have values as large as possible. [26] The *I–U* and power–voltage (*P–U*) curves of the PV cell are presented in Figure 2.4. The *I–U* and *P–U* curves are values that help in planning and maximizing the production of PV cells. The point of the maximum production of a PV cell is known as maximum power point (MPP). The noticeable is that the MPP is achieved the current value under I_{SC} and decreasing current with rising voltage.

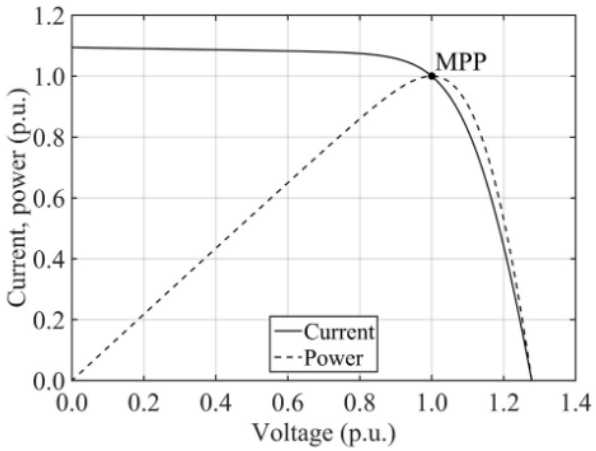

Figure 2.4. *I–U and P–U curves of PV cell with the MPP [35].*

An ideal situation would be all PV cells operating with identical conditions and characteristics but every cell has its unique operation conditions, like individual MPPs, which cause power losses called mismatch losses in the PV system. Mismatch losses are determined as a difference between the sum of the maximum power of each PV cell or module of a PV system operating apart from others and the maximum power of the PV system as a whole. [35, p. 18] Mismatch losses tell how the placement and different environmental conditions of PV modules affect the production of the PV system. PV cells have internal reducing factors that affect operating PV modules and systems.

With multiple factors affecting the operations of PV cells, the two global factors affect production greatly. Solar irradiance G and cell temperature T are the two most restricting factors. The short-circuit I_{SC} of the PV cell is directly proportional to irradiance G, as seen in:

$$I_{\mathrm{SC}}(G) = \left(\frac{G}{G_0}\right) I_{\mathrm{SC}}(G_0), \quad (2.3)$$

where G_0 is the reference level of irradiance. Equation 2.3 shows that having higher irradiance is desirable when maximizing PV production. [32] Solar irradiance variations are the main reason for rapid changes in PV production due to fast-changing cloud shading on PV modules [36] and other weather-related conditions [7]. Power fluctuations caused by changing PV production are a

challenge from the point of view of grid operations because this forces to find power from somewhere else to compensate the loads in the grid. The cell temperature T affects the open-circuit voltage U_{OC} as seen in

$$U_{\mathrm{OC}} \approx \frac{E_{G,\ 0}}{q} - \frac{kT}{q} ln\left(\frac{BT^{\gamma}}{I_{\mathrm{SC}}}\right), \tag{2.4}$$

where $E_{G,\ 0}$ is the linearly extrapolated zero temperature band gap of the semiconductor, B the temperature independent constant of saturation current and γ the temperature dependence of parameters of the dark saturation current. Equation 2.4 shows that the cell temperature T of a PV cell, and thus a PV module, affects the open-circuit voltage U_{OC}. To gain a better performance of PV systems, conditions with a low cell temperature and a high solar irradiance are optimal. [32, pp. 14–16] Increasing the cell temperature of PV cells and modules causes the biggest performance loss in Si-based PV cells [29, p. 302]. Even when solar irradiance increases during a hot summer day, production cannot be maximized due to an increased cell temperature. An example case of the PV module with three different irradiance values: 400, 800 and 1200 W/m^2 is shown in (a) of Figure 2.5. It also shows the cell temperature difference of the PV module receiving the constant irradiance 800 W/m^2 (b) of Figure 2.5. It shows that the PV module has higher currents with higher irradiance, as proven by Equation 2.3. The cell temperature differences follow Equation 2.4. Even when 25℃ temperature has a higher I_{SC} value than in colder temperatures, the current of PV modules drops faster with raising the voltage. The highest MPP of the PV module is achieved under the coldest temperature -25℃.

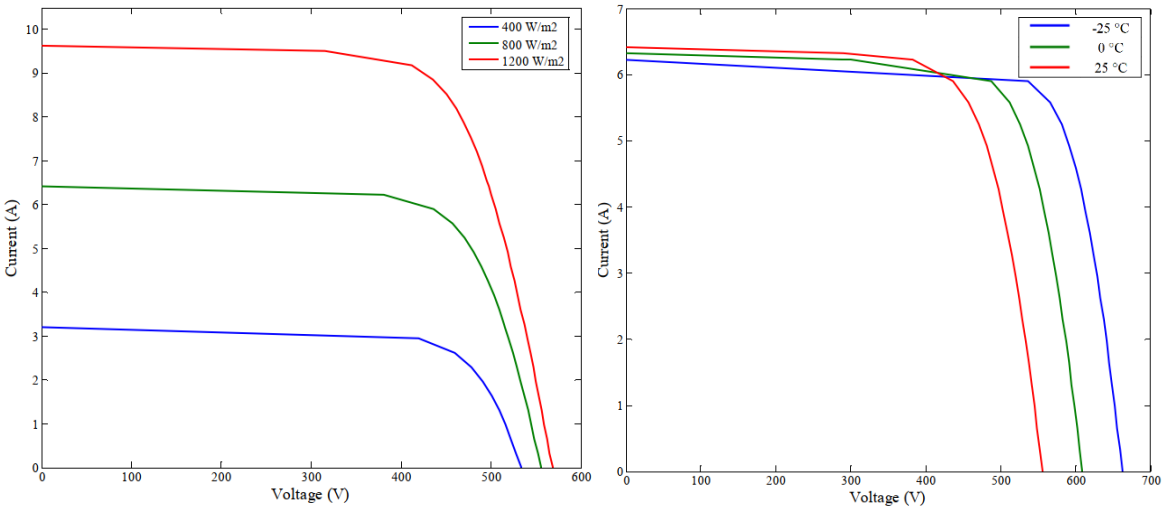

(a) **(b)**

Figure 2.5. *I–V curves of the PV module with (a) three different irradiance values and (b) three different cell temperatures with the constant irradiance of 800 W/m^2 [32].*

This thesis uses the PV data measured from the solar PV power research plant located on the rooftop of the Sähkötalo building in the Hervanta Campus of Tampere University. Tampere region has changing weather conditions between seasons and the structures around the research plant can cause significant changes in the PV production of individual PV modules and strings due to changing shading conditions. The PV modules of the research plant receive the major

portion of the annual solar radiation during summer. Sun goes down for a few hours and daytime can last up to 20 hours depending on a geometrical location, especially in the northern parts of Finland. The optimal angle for a PV module can be calculated by adding 15° to the latitude of the research plant during winter and subtracting 15° from it during summer. The fixed position of PV strings causes irradiance to be lost during morning and evening hours when sunlight shines on the back of PV modules during summer. The optimal angle of the PV modules is between 22–35° from May to August. The optimal angle drops to 22° in June and increases towards the end of the year. The optimal angle of the PV module in the plant is between 72–80° from November to February. The optimal angle peaks in December and drops afterward. The optimal angle can be achieved by changing the angle manually which is not preferable due to extra work. The optimal angle can be achieved automatically by using a sun-tracking system that adjusts the inclination and orientation of PV modules. The system has an active sun-tracker application that optimizes the tilt and orientation of PV modules. The sun-tracker adjusts the angle of PV modules periodically to gain optimal PV production and an active sun-tracker is concerned to be the best solution for angle optimization. Sun rises briefly over the horizon in southern Finland during winter. PV modules with the fixed angle of 45° receive more irradiance than the measurements on the horizontal surface during winter. Formated ice on the lower parts of PV modules causes PV modules to have multiple MPPs. Extreme cold weather, snow and ice cause stress and damage to the mobile parts of trackers on PV modules which can halt their use. This can be avoided with a fixed position but it causes power losses due to the incapability to change the angle of PV modules to maximize the PV production all year round. The annual solar energy of the research plant is similar to northern Germany with the fixed angle and to southern Germany with a sun-tracking application when compared to the annual irradiance levels of these regions. [14, pp. 2, 5, 7–9]

2.2 The structure of the photovoltaic module

The main component of PV systems is PV modules, also known as PV panels, that are connected in series to increase the output power of a PV system. These are called PV strings. A PV cell with the lowest current, due to shading or a fault, restricts the current of a PV module and thus the current of series-connected modules of PV string [35]. Possible parallel strings are connected to increase the power production of the PV system [32]. Figure 2.6. shows a layout of 36 PV cells with two parallel bypass diodes [37, p. 305].

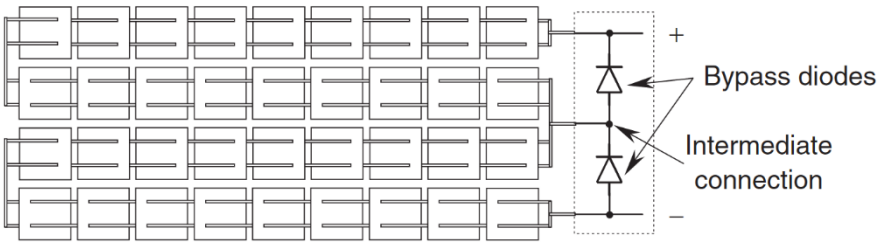

Figure 2.6. *Layout of series-connected 36 PV cells with two parallel bypass diodes [37].*

Shading of a single module decreases produced DC power by all PV modules connected in series in the PV string [38]. Shaded and faulty PV cells operating under the current of a series-connected PV string will act as a load and cause overheating and hot spots in solar cells with lower currents in the worst case. To avoid unnecessary power losses and overheating of PV cells, PV modules and strings have parallel bypass diodes. The bypass diodes protect a group of PV cells or modules from unwanted operation states and maximize power production, even with partial or total shading or during fault situations of PV cells. Bypass diodes have been also noted in decreasing mismatch losses of a PV system. [35, pp. 18, 19]

The solar cell efficiency research is shown in Figure 2.7. It shows the measured efficiencies of solar cell types under laboratory conditions. 47.1% and 44.4% efficiencies are achieved with two types of three-junction cells. Single-junction solar cell types were measured at around 30% efficiency. The third highest efficiencies are measured with crystalline Si-cells (21.2%–27.6%). Thin-film technologies have measured efficiencies between 22.2%–23.4%. And efficiencies of the emerging PV technologies alter more with the lowest value being 13% and the highest-value 31.3%. [39] Even though the efficiency of PV cells of a PV system might have a high-values, power losses, like mismatch losses, will decrease the efficiency of the PV system. Current commercial PV modules have an efficiency of around 20% [38].

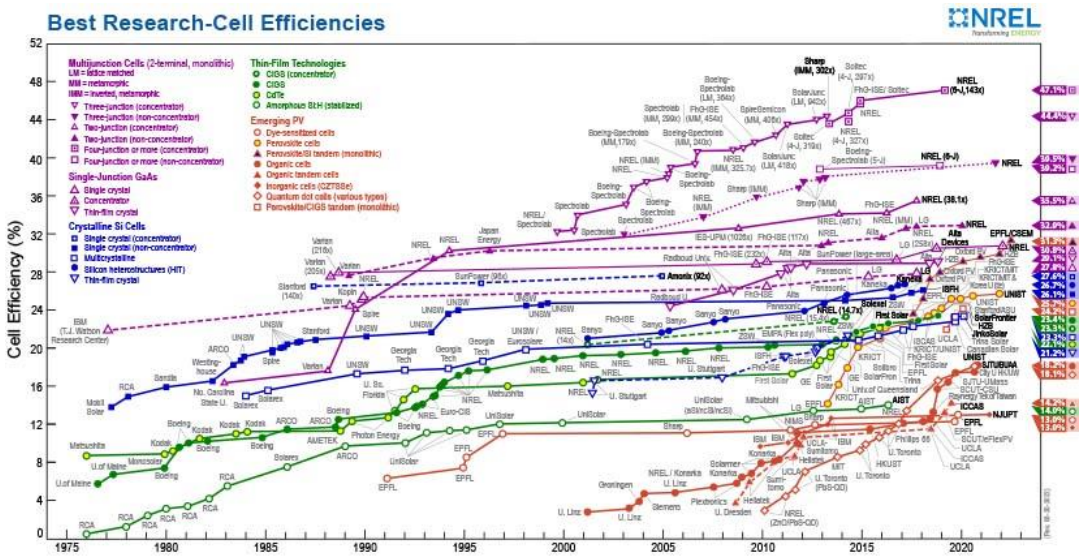

Figure 2.7. *The best research solar cells effiencies [39].*

PV modules installed on the rooftops are recommended to have an air gap to enable better cooling. Cell temperature is the second most restrictive factor in PV production after irradiance, as mentioned earlier. Having a cooling option for PV modules is an attractive and effective method to enhance the production of PV modules under high external temperatures. The cell temperature depends on wind speeds and lengths of air gaps under PV modules. A building-integrated PV system is a possible solution that has the primary energy produced by PV modules and the additional thermal energy recovery from the air under the PV modules. The final air temperature exiting under PV modules can reach over 30℃ more than the external air temperature. Heat can be

converted to electrical energy by the building-integrated PV system. [40] This and other solutions also improve the efficiency of PV systems.

2.3 The operations and features of photovoltaic inverter

A PV inverter is the most important component of a PV system after PV modules because the task of the PV inverter is to convert DC power produced by modules to match the AC power form of a power system or a connected grid. The PV inverter is responsible for maintaining the efficiency of the PV system and protecting both the PV system and the connected power system from fault situations. This part briefly presents the role of the PV inverter as a part of a PV system and discusses general variables and applications of inverters. These can be used to both increase the efficiency of the PV system and an opportunity to attribute in performing as a grid control solution to some level. Also, the vulnerability of a PV inverter or a PV system becoming an issue during a separate fault situation in the grid and different solutions to rebel against them are mentioned briefly.

The modern distribution grid transfers and distributes electricity in an AC form and PV cells produce DC power. The conversion from DC to AC is done by a PV inverter. The PV inverter converts the DC power produced by PV modules which is fed to the grid as an AC power. The important features of PV inverters are MPP Tracking (MPPT), power measurements, anti-island detection and operating under grid-fault conditions [41]. No inverter has the perfect conversion rate efficiency from DC to AC, the DC/AC ratio, of 100%. The performance efficiency of an inverter has been determined as 85–96% depending on the quality of equipment used in the inverter while power generation is kept close to the nominal value of the PV system. [42, p. 126]

Traditional PV system inverters, string inverters connecting multiple PV modules, can be replaced with microinverters installed on every individual module. The trend of using microinverters has gained great interest in the last few years. Microinverters can feed power from the PV module to the grid without the need for connecting modules in a PV string. But the price and cost-effectiveness of a PV system with multiple microinverters may come into jeopardy depending on the pricing and the nominal power of modules. [38] But overall benefits of microinverters are the reason why favoring them over traditional PV inverters in PV systems has increased [13].

Failures in PV inverters are the most frequent reason behind PV system incidents. Incidents are caused mostly due first-generation production issues, like inexperience in design. But PV incidents can be also caused by error situations in a grid. [42] The three main reasons for disconnecting PV inverters from the grid are due to overcurrents, soaring DC voltages and losing the synchronization. The inverter tries to balance between output and input of an exceeding DC power of a PV generator. This causes currents and DC voltages to increase which leads to the disconnection of the PV system from the grid.

The power-limiting mode is a state of a PV inverter where a PV system produces more power than the maximum power capacity of the inverter. Power-limiting mode is the non-favorable operation state that causes surplus PV power to be lost when the PV system can not be able to feed the total power to the grid due to the limitation caused by the sizing of the PV inverter. Other

longer-term negative effects are the decrement in the lifetimes of PV inverters and capacitors under higher power production states. Power losses and the negative effects mentioned can be avoided by optimal sizing of PV inverters. The sizing parameter used is called the DC/AC ratio where DC-generated PV production is rated to the AC capacity of the inverter. Literature states that the DC/AC ratio values under 1.0 do not cause power curtailments. The ratio is recommended to be kept between 1.1–1.7. The need for optimal sizing of inverters becomes a necessity in a region with multiple, rapid irradiance changes due to multiple shading conditions. [43, p. 1367]

PV systems have been noted to cause problems in fault detection at the distribution grid level. The short-circuit current values of relays might be measured only based on the grid-connection values without taking into account the role of PV systems in an isolated grid. This can cause relays not to detect faults in an island mode. [44, p. 189] This is why short-circuit current values of the fault detection should be determined to at least two modes: grid-connected and island mode. One major function of both grid-connected and PV systems with an island mode is the fault detection attribute. This attribute comes crucial in local grid control. The fault detection in a PV system operating in island mode may cause “blind spots” with insignificant fault current setting values [5], [45]. This blind spot causes the PV system to inject fault current through a bypass path to the delicate parts of a PV system and a local distribution grid. This causes unwanted stress and damage on grid components which will eventually break. The use of the MPPT during low irradiance conditions causes difficulties in fault detection. This can be eliminated by determining an efficient fault detection technique. [45, p. 12] Inverters can be used also to enhance the performance of a PV system. Reactive current injection of PV inverter can give better performances to the PV system when measured in the point of common-coupling (PCC) under a prolonged, large area grid fault [23, p. 982]. Reactive power control (RPC) of PV inverters is mentioned more in Chapter 3.5.2.

All current commercial PV inverters have an anti-islanding protection solution [44]. PV inverters also must have frequency stability with a maximum 2% frequency change during a fault situation [45, p. 7]. Every commercial grid-connected PV system is required to have the low voltage ride through solution where the PV system notices and withstands a single fault situation in a connected LV grid. Studies show that the PV inverters might require a fault current contribution solution in near future to better adjust fault situations in the grid and protect the PV system. [7, p. 16785] PV systems contribute to a major part of fault currents during a fault situation in the distribution grid level [27, p. 229]. If a part of a LV grid with DG units, is not remeasured and set the new safe values to better mitigate fault currents, the current fed from DG units can cause unnecessary fuse breaks in residential switchboards [25, p. 3]. The traditional fault detection solutions of electric power grids may not be effective enough to detect and isolate a fault caused by a larger number of grid-connected PV systems. This can be a topical issue with high-impedance faults measuring solutions, like overcurrent and distance protection [25]. The issue can spread to a larger grid region when a current fed from a LV grid can prolong fault situations on a medium voltage (MV) grid [46].

Another feature of PV inverters is the harmonics cancellation. Harmonic cancellation features have been used in inverters at the industry level [47] and should be easy to integrate into PV systems located in residential grid feeders. PV inverters can be used to eliminate harmonics in LV grids but other grid control components, like active and passive filters, are preferred by DSOs and private companies as well [45, p. 7]. Harmonic canceling features decrease power losses and voltage drops in the power grid which enhances the voltage profile of the grid [47]. Installing the harmonics cancellation feature in PV inverters should not be a technical issue but there is no statement to enforce it in PV systems at the distribution grid level [41]. Harmonic injections caused by PV inverters to distribution grids are mentioned more in Chapter 3.4. The role of the PV inverter as a RPC tool is mentioned in Chapter 3.5.2.

2.4 Grid connections and topologies

External factors play a key role with the PV components in increasing the production of a PV system. These can be simple as a choice of a grid connection or a more challenging choice between different layouts of PV systems. This part focuses on the two grid-connection choices: single-phase, id est the unbalanced, and 3-phase, id est the balanced connection. Lastly, PV system topologies are presented and discussed.

Most PV systems located on rooftops of households and commercial buildings are grid-connected to the LV grid [8, p. 3] favoring a single-phase connection [48, p. 2965]. 70% of the PV capacity of Europe is connected to LV grids [18]. New PV installations were grid-connected as high as 99% internationally in 2013, respectively [7, p. 16785]. Grid-connected PV systems operate in balanced conditions occasionally [42] as they operate in unbalanced conditions the most of time. Unbalanced conditions cause changes in the amplitude and frequency of PV penetration which has an impact on the grid operations and electrical values in the grid. High PV penetration levels have four major weakening impacts on the factors of the distribution grid: power quality (PQ), voltages, stability, and both protection systems and their components [45]. A safe limit of PV penetration, the term HC, fed to the grid by 3-phase grid-connected PV systems with high power capacity is limited usually by the thermal limit capacity of feeder lines [9]. High currents in the feeders cause thermal damage to phase lines and the distribution transformer which can limit the HC of PV systems [49].

As more and more households are buying PV systems and more PV modules in existing ones on their rooftops, most of these PV systems use mostly single-phase grid connections. The single-phase grid connections can be connected between two phases or a phase and the neutral wire [50, p. 15]. The production of single-phase connected PV systems is limited by the current limit id est ampacity of transformer windings when transformer loading violations occur during peak PV production [18, p. 1712]. The functions and operation states of a PV system can affect any electrical value limits, mainly voltage and current limits of grid components, at the distribution grid level. This can affect greatly phase voltage balance and stability of a feeder during a high PV penetration level and a low load situation in a grid. Higher PV penetrations from multiple single-phase grid-connected PV systems will unbalance the phase voltages in the feeders and most

significantly at the transformer terminals. The unbalanced phases lead to poorer power factor (PF) and PQ values in the grid. A high PV penetration from a single single-phase connected PV system can lead to the shifting of a neutral point and enhance RPF. [9, p. 1581] During situations when there is a great difference between consumption and production, phase voltages can alter greatly [49, p. 2689]. The issue can be amplified by raising the number of single-phase PV systems in the grid which leads to increasing the voltage unbalance factor (VUF) value [18, p. 1712]. Unbalanced load states with single-phase connections cause heating in 3-phase generators on the level of consumers [51, p. 442]. Single-phase PV inverters inject harmonic distortions into the grid causing greater voltage unbalances [52].

Depending on a grid topology and components of a LV grid, a high voltage of a single phase may violate the grid code and even lead to under voltages in the other phases. But the household PV systems have relatively small capacities and maximum production of PV systems could occur only a couple of days per month. The study by Wajahat et al. [48] confirms that the scenarios where single-phase PV systems were connected to multiple or evenly between grid phases had higher HC levels. Multiple single-phase PV systems in the LV grid, the worst being to all systems share the same phase, will cause serious voltage fluctuations and other electrical value violations. A more restrictive factor in increasing HC of single-phase PV systems was not overvoltages but phase voltage unbalance. [48]

Simultaneous over- and undervoltage situations can occur when an automated On-Load-Tap Changer (OLTC) located in the transformer will detect the phase overvoltage and tries to lower phase voltage values in the LV grid. But two other phases within allowed voltage limit values can be lowered too much and lead to undervoltage values in these phases. [44, p. 187] Using different voltage and grid control tools, like OLTC, can mitigate voltage rises caused by single-phase PV systems effectively. There is mentioned more about voltage control tools in Chapter 3.5.1.

The locations and sizing of PV systems are the major factors in the planning and enabling stability of grid operations [45, p. 9]. Different topology layouts of grid-connected PV systems are shown in Figure 2.8.A centralized (central in Figure 2.8.) inverter topology has been favored in the past as the topology of PV systems with a large quantity of PV modules with multiple strings. PV modules share similar environmental conditions, mainly shading. The topology enables a PV system to have higher voltages and power production. Voltage fluctuations inside modules are smaller due to the higher string voltage opposite to a lower string voltage which is more vulnerable to possible issues caused by rapidly changing shading conditions. The centralized topology has a low cost-per-ratio from a financial point of view. Major disadvantages of the centralized topology are power losses due to centralized MPPT, higher losses in string diodes, losses and security risks in high voltage direct current (HVDC) cables and small flexibility caused by the design. String topology is a single PV string that gives an easier solution, like the AC module topology, than other topologies for determining values of the MPPT of a PV string. String topology is also a more flexible design by adding individual PV strings to the grid. Multi-string topology is the further de-

velopment of string topology by combining the advantages of string and centralized inverter topologies. Multiple PV strings with individual DC/DC inverters and MPPTs can be connected parallel to each other while sharing the same grid-connected DC/AC inverter. This enables high efficiency but also increases a cost of a large-scale DC/AC inverter due to high power production. Multi-string and string topologies are better options for PV systems with multiple and changing environmental conditions of PV modules. The AC module is the most simple topology containing a single or few PV modules and a shared inverter. This gives an optional adjustment between two components with no mismatch losses. The disadvantages of AC module topology are high per-energy cost and relatively high voltage fluctuations due to a lower voltage that can cause efficiency issues. The AC module topology is the best solution for those who wish to connect PV systems to the grid per a system at the time. [32, pp. 12–14], [35, pp. 23, 24]

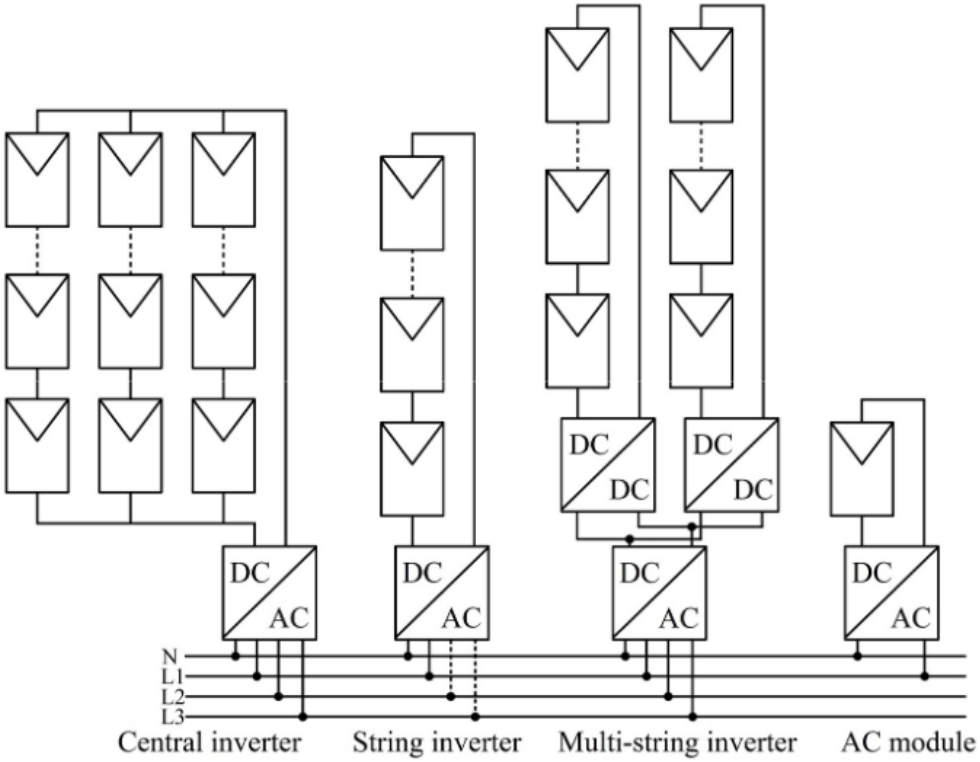

Figure 2.8. *String topologies of grid-connected PV systems [35].*

3 ELECTRIC POWER GRID

An electric power grid is the backbone of a functioning and developing society. The high level of living today is dependent on trustworthy and instant power distribution enabled by the modern power grid. National grids are divided into different sections depending on the main purpose of that particular grid part. Two general electric power grid types are transmission and distribution grids [3], [51]. The overall function is to transfer electric power from power production plants to consumption points. AC is the main form of electrical distribution and transmission grids [51]. AC has a sinusoidal waveform with single or multiple phases. Two grid frequencies, 50 Hz and 60 Hz, are used globally. Grid frequency is related to the rotating speed of SGs in the grid. [23, p. 980] Grid frequency control is an important task of both DSOs and transmission system operators which can lead to severe issues if not controlled properly [3], [51]. When considering the role of household PV systems, the role of the transmission grid might not feel as important as the distribution grid at the LV level. But the transmission grid is still the main way of delivering power consumption to the distribution grid hence enabling stable and trustworthy distribution to load points. The role of the electric power grid as a whole system is presented briefly in this chapter.

Chapter 3 discusses the theory of the electric power grid and the role and characteristics of grid-connected PV systems. Firstly, the role of the transmission grid is discussed. These include the general transmission line types and especially the N–1 criterion. The role of the distribution grid is discussed by presenting the operations of the Finnish distribution grid afterward. The general roles of grid components, like substations and power electronic components, are presented briefly. Secondly, conductors and transformers, the grid components important for the PV system operations, are presented. Their functions, main purposes and applications are discussed. In the latter part, literature about grid-connected PV systems in the distribution grid is discussed. HC is presented and discussed in the third part. Lastly, restrictive factors and tools for enhancing levels of HC in literature are discussed in the fourth and fifth parts.

3.1 Transmission and distribution grids

A transmission grid is the core of a power grid. A transmission system operator, Fingrid in Finland, is usually a public company, usually mainly owned by the government. The transmission system operator is responsible for planning, building, maintaining and operating the transmission grid [3]. The usage of higher voltages ables the economic and efficient transfer of electric power between long distances. The main operation criterion for the transmission grid is called the N–1 criterion. The N–1 criterion is the demand for transmission grid operators to accommodate the power state in the transmission grid during a contingency without causing grid safe limit violations [51]. The rising volume of REGs has forced transmission system operators to calibrate their N–1 criterion actions [53, p. 290]. The transmission grid includes high voltage (HV) lines over 100–

1000 kV main voltage values globally. High voltage AC grids are a popular form of national main grids because of their advantages. Limiting factors in an AC transmission grid is mainly the current capacity of lines and reliability issues. HVDC transmission lines are being used in the long undersea lines for the advantage of non-reactive power consumption and they are a cheaper method of transmission than AC lines in the grid with long line lengths. The advantages of HVDC are not having voltage and angle stability issues like in an AC grid. HVDC may be the only power transmission option in the long distance as AC lines need substations between about every 80 km. This and other attributes are raising public interest in replacing connections in traditional AC grids. The downside of HVDC is shorter distances between the control substations than in an AC grid. The converter stations have extensive power losses due to the high quantity of control components and their extensive usage in voltage control. The Finnish transmission grid has three HVDC connections between neighboring nations. [51, pp. 297–302] One is on land between Russia and the others are undersea to Sweden (Fenno-Ska 1&2) and Estonia (EstLink 1&2) [51, pp. 306, 307], [54]. From the point of view of PV systems, the role of the transmission grid would not seem as important as that of the distribution grid level but the role of the transmission grid cannot be ignored for enabling stabilized function and transferring power to and from the distribution grid.

A distribution grid is a platform for multiple electricity production and distribution. The role of planning, building and maintaining distribution grids is done by DSOs. Mainly consumers like business buildings, residential households, and both small- and medium-scale industries are connected to the MV and LV distribution grids. Having electricity production closer to distribution load points will decrease power losses and grid system attrition [5].

In this part, the roles and characteristics of the distribution grid in the Finnish power grid are presented and discussed. The distribution grid consists of usually two parts: MV and LV grids. The Finnish distribution grids have so-called “regional grids” that consist of single or multiple HV transmission lines that function as part of the transmission grid in the region [55]. The regional grids have both functions of transmission and distribution grid. The biggest changes in traditional power grids in the future have been projected to be in the operations of distribution grids and regional transmission. Two major tasks of distribution grids are transferring and distributing electricity as the general solution today. This solution has insufficient attributes to compensate and control power flow of REG units at distribution grid levels as the solution is based only on the traditional “downstream power flow” for compensating loads. The solution is not planned to take an account the effects of bidirectional power flow caused by the power production of REG units. The need of reinforcing both grid operations and grid-connected power production units has been noted for gaining more trustworthy and stabilized grid operations. [3, pp. 509, 510] The increasing number of PV installations in the distribution grid only highlights this issue.

The longer feeders usually use overhead lines and underground power cables are used in the shorter, city center and suburbian grid feeders. The Finnish Energy determines that the MV grid voltage levels are between 1–70 kV in Finland [56]. The large industrial loads use the 20 kV voltage level with transformers of their own located in the distribution grid [50, p. 113]. Finland is located in the far north so ice and snow cause thermal damage to the grid during winter and heat

waves during summer. Usually, ice and snow will melt away from phase conductors because of the thermal energy, due to the resistivity of the load state, leaked from overhead lines [3, p. 33]. But occasionally extreme freezing conditions cause extensive damage to the grid components or even a power line can be snapped. This happened in the extreme cold under - 50 °C in Lappland, Finland in January 1999. The line connector of the HV transmission line snapped in half and over 1000 consumers was disconnected overnight. [57]

The function of the distribution grid is to distribute power to the consumption points while maintaining nominal electric values, generally voltages levels, of the grid inside the allowed changes stated in the grid codes of a nation [3]. Electric power grids have multiple load and production types. Loads can be divided into two main types: linear and non-linear loads. Residential loads are focused on heating during the night [58, p. 141]. The present Finnish electrical grid has been built to withstand high-load states caused by residential heating [59, p. 95]. Thus, it is designed mainly for compensating loads from higher voltage grids to lower ones. European distribution grids are characterized by four-wire feeders and mostly single-phase connected loads [60, p. 2]. Power demand is low during the day when residents are away at work or for something else, like a school or a shopping mall. Demand load profiles of Finnish households are focused on heating. Newer buildings have mostly phased out oil heating and the level of wood heating is also decreasing but older Finnish households use still either of these two heating methods. The biggest power demand of households is direct electric heating especially during the coldest winter months when temperatures can drop down to freezing temperatures. The second seasonal peak demand is during summer heat waves which have forced people to think about and install electrical air-source and ground-source heat pumps. [61, pp. 4400, 4402] The usage of heat pumps and oil heating in households of the simulations is not considered in this thesis.

Figure 3.2.1. *3D substation layout [15].*

A MV grid begins from a HV/MV substation and transfers power to LV grid feeders. Substations are the main control component of the MV distribution grid. The main task of substations is to lower the voltage level from the HV transmission grid to the MV grid and eventually to the LV level in distribution transformers. The MV grid control is heavily centralized to substations for their major role in housing multiple components. The 3D layout of the substation is shown in Figure 3.2.1. Two transformers are located on the left, busbars with disconnectors and surge arrestors

in the middle, and power line structures to the high voltage or MV grid are on the right. Transformers are the main component located in substations. The electrical distribution is done by busbars of the substation that are divided into main busbars with circuit breakers and auxiliary busbars with disconnectors. Circuit breakers are designed to threshold a current caused by a disconnection during a loading state and disconnectors are only able to disconnect lines during a non-load state. The maintenance can be done with a multilayer topology of busbars without interrupting distribution. Substations also house automation and operation components. These are power electronics tools for reactive power compensation, like shunt reactors, shunt capacitors banks and series capacitors. Surge arresters are used in all voltage levels of electric power grids and are designed to lower local transient voltages, like a lightning strike on overhead phase lines. Automation enables remote control and measurement of the distribution grid. Measurement data is collected in a noise-canceled unit, like a substation closet, and can be used for designing the control operations. Data is input to the remote terminal unit and from there to the supervisory control and data acquisition system for global use. [3]

LV loads and connection points make up the most of distribution for household, small-scale industrial loads and generators. The voltage level of the LV grid in the Finnish grid is 400/230V (main/phase), respectively. The LV connections have measurement, protection and control components, mostly located in the switchboards. Every building has a main switchboard in the PCC. Single-phase loads are balanced between the three phases inside the switchboard. Balancing is done to avoid asymmetry issues, like between phase voltages. Three-phase loads follow the installation instructions. Fuses are the primary protection method for protecting equipment from overvoltages and -currents. Other typical protection components in the switchboard are circuit breakers and miniature circuit breakers. The main switch is for disconnecting the PCC due to maintenance or an emergency. Major commercial buildings, like malls, restaurants and hotels, must have an energy storage solution to illuminate the exit signs during a blackout. [50, pp. 113–116]

The Finnish LV grid has four main grid-connection system types: TN-S, TN-C, TN-C-S and IT. IT system is more regular in the industrial grids and other systems are more regular in residential circuits with only-load states. The TN-S system uses a separate grounding wire that helps in keeping the load currents in the neutral wire. This topology diminishes the issues caused by interference currents and electric fields. The supervision of fault currents is essential in keeping away currents of neutral and grounding wires from each other. [50, p. 112] The TN-C system has the shared neutral-grounding wire connected to the ground in the installation. Standard IEC 60364 also states the fault current protection cannot be used in the TN-C system. The TN-C-S system is the combination of the TN-S and TN-C systems that enables the benefits of both systems. Depending on the grid code of a nation, PV systems should be installed as generators to the LV grid with the following grounding of the particular system. With the TN-C-S system, the grounding of PV systems to the main grounding of the switchboard should fill the grid code demands. [62]

Voltage control is keeping the voltage points inside the stated values in grid codes, like EN-50610 in Europe [3] and ANSI84.1 in North America [63]. Lower values than the lowest standard values are called undervoltages and over the highest standard values are overvoltages. Overvoltages are caused usually by lighting and switching transients, resonance and ground faults between feeder line phases [46]. The voltage control of the MV grid is more sensitive than that of the LV grid [7]. The MV grid voltage control components, voltage regulators and capacitor banks, id est, affect densely the LV grid operations. Favorable factors can increase the level of HC. The nominal voltage value of the MV grid (U_{MV}) can affect greatly the nature and number of LV grid problems, as shown in Figure 3.2.2. Naturally, raising U_{MV} decreases level of HC in the LV grid. Decreasing U_{MV} does increase HC, but undervoltage buses in the LV grid will be more frequent. [10, pp. 1007, 1009] The LV grid has mainly overvoltage issues when the voltage of the MV grid is higher than nominal voltage value. LV feeders are also capable of causing voltage fluctuations in PCCs of PV systems [45, p. 6].

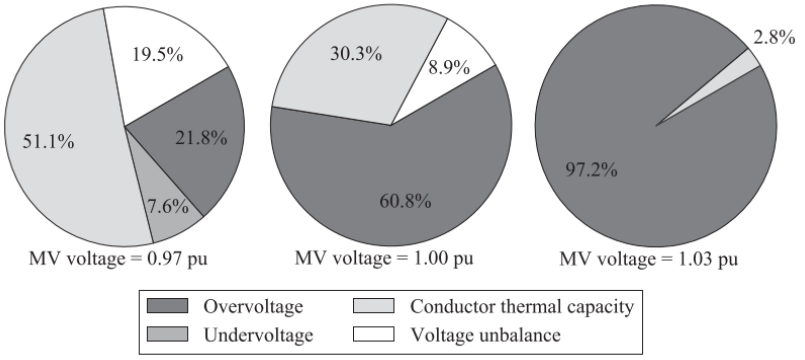

Figure 3.2.2. *Effects of voltage values of the MV grid to the portions of issue types in the LV grid [10].*

Another major grid code limit concerns RPC in the grid-connected production units. The distribution grid has a low reactance/resistance (X/R) ratio, opposite to the transmission grid with 5–7 [51]. A weak distribution grid has an X/R ratio as low as 0.5 [24, p. 415]. Traditionally, an additional parallel transformer is added to a distribution transformer to balance voltage fluctuations and improve PQ values but mainly to avoid overloading a singular distribution transformer [3, p. 150]. Installing higher-capacity conductors in the feeder is a popular grid investment method. Feeding reactive power from a transmission grid causes power losses and increases the grid operation expenses for DSOs. A local reactive power supply is better for a RPC solution. [22, p. 69] When considering PV systems, RPC can and sometimes must be able to attribute to voltage control of grids. In Puerto Rico, the weak grid causes to have stricter grid codes globally. RPC of PV systems must be able to operate with PF between 0.85 capacitive and 0.85 inductive under dynamic and steady conditions. [23, p. 978] RPC is discussed more in Chapter 3.5.2.

The increasing number of household PV installations has given a need for more complex and hybrid voltage control in MV and LV grids. Voltage dips are the main problem of REGs, like PV systems, caused to distribution grids [53]. This is due to the asynchronous nature of REGs. The voltage dip may be caused by simple cloud shading over an extensive scale on PV modules.

The grid is unable to compensate for power difference fast enough and lack of power causes a voltage dip. If the present voltage control solution cannot maintain voltage fluctuations outside of the violation limits, the last option is the disconnection of PV systems from the distribution grid [64]. The possibility of failures can also happen in a MV grid due to high PV penetration levels in a LV grid [8], [65, p. 2].

3.2 Grid components

Grid components are the key factors in maintaining electrical values in the grid inside the allowed range, as stated in grid codes of national power grids. The more complex and irregular load demands today have caused DSOs and transmission system operators to make grid investments for better control and to increase the stability and reliability of electric power grids. Multiple power electronics tools are used to achieve the operation values inside the standardized grid limits. Usual voltage control components are voltage regulators, capacitor banks and OLTC in distribution grids [3], [63, p. 4757]. Another tool is a distribution static synchronous compensator which can help improve grid values. A distribution static synchronous compensator and PV systems with the algorithm can have a positive effect on power losses, voltage profiles and balancing of loads. [21] These are modern solutions but this thesis focuses on more traditional solutions, investing in components like higher current capacity conductors and transformers with larger ratings.

Next, grid components mainly affected by PV systems are presented. Overhead lines and underground cables are discussed in the first part. Secondly, transformers and their role in voltage conversion are presented. Lastly, the grid operation factors, PF and VUF are presented and discussed.

3.2.1 Conductors

Transmission of electricity between grid points is enabled by conductors. Conductor lines are overhead lines hanging from structures and underground cables dug into the ground. This part presents and discusses the differences of these two general conductor types. Overhead lines are usually made of copper, aluminum, aluminum mix or iron. The main benefits of overhead lines are easy installations, cheaper investment cost by length, easier maintenance and fault detection than underground power cables. Overhead lines can be seen around the suburb and the countryside. These are placed close to roads to shorten fault detection and enable faster fixing time by a maintenance crew. Easier fault detection shortens the repair time and to-normal-state return time significantly. The thermal limit is the maximum temperature value of the line that can withstand without causing thermal damage to the line or other components connected to the grid. Overhead lines usually have overhead protection conductors over phase conductors to protect from lightning strikes. This increases a cost of overhead lines when compared to underground cables which are not in a need of protection from lightning. Overhead lines without overhead protection conductors are more likely to be stricken, up to seven times in the Finnish 110 kV grid lines. [3, pp. 32, 33, 278, 285, 304–306]

The second major grid line type is underground power cables. The line structure of the power cable is more complex than the structure of an overhead line. The cable consists of phase conductors, jacket or conductor screen, insulation, insulation screen and concentric neutral strand. This will make the cost higher compared to overhead lines. The parts of underground cables are designed to protect phase conductors from external factors, like heat, water, moist and magnetic fields, and enhance capacity for a longer lifetime. Phase conductors are made of copper or aluminum. Underground cables are generally the only option in city centers due to a lack of space for overhead lines and underwater lines, like crossing seas between grids of separate nations, like HVDC lines. The underground solution may save a need for space and enable safer use and distribution of electricity but both maintenance and fault detection operations are belonged and finding a fault becomes more difficult. Mainly fault detection of underground cables becomes harder, even when the feeder of the fault point is located. If the feeder is extensive, it can be difficult to locate the fault and return to the nominal distribution state in a reasonable time. And underground cables are more vulnerable to incidents due to excavation operations. Underground cables have a large capacitance opposite to the ground. Generally, overhead lines are more inductive in the AC system. [3, pp. 303–312] Underground cables of distribution grids have capacitance values similar to long overhead lines. Cables function as capacitive loads under power flow conditions. During the non-load situations of cables, overvoltages at the end of feeders can be up to 200% of the nominal voltage. This is caused by the Ferranti effect where the capacitive reactive power of cables raises the voltage. This is depending on the load levels of the grid and the capacitive charging power of the underground cable. [46, pp. 2501, 2502, 2505]

3.2.2 Transformers

In a simple definition, transformers are static grid components that form an electromagnetic field between two windings with different voltage levels to enable power transfer without changing the frequency. Power losses of the transformer are divided between 1. the core loss (hysteresis and eddy current loss) is the major loss during a non-load state and 2. the copper loss (iron windings) during a loading state. [66] Power losses in transformers mostly form as thermal energy reflecting towards the outside of the transformer box. Thermal energy flows through the transformer as thermal conduction, thermal convection, thermal radiation and a combination of all three. [12, p. 339] Distribution transformers are located close to consumption. The capacity of transformer (transformer rating), measured by apparent power S (VA), is a good approach in a planning of a PV production in avoiding excess power flow from a LV grid side with a rich-concentration of PV systems. Exceeding the threshold of the grid will cause thermal damage to the transformer, conductors, and other grid components [7, p. 16786]. The sketch of an oil-filled transformer is shown in Figure 3.3.1. Grounding of the MV/LV transformer can be an effective solution to decrease overvoltages in the LV grid during unbalanced conditions. The grounding of the transformer has none of a major impact to normal operation states but it provides a low-impedance path to the ground. This reduces overvoltages in the LV grid. [46]

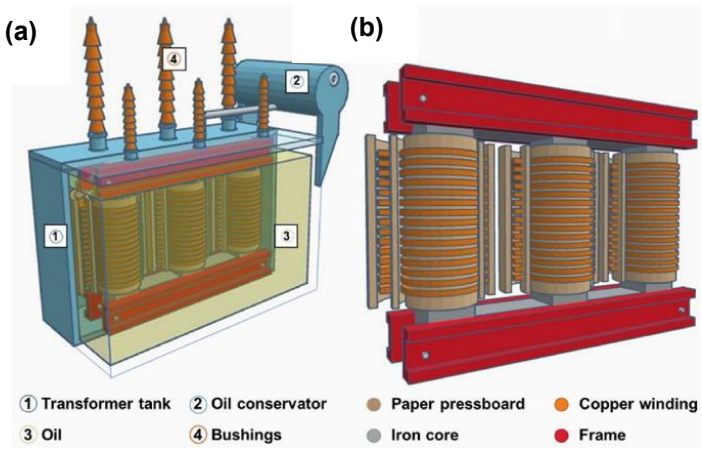

Figure 3.3.1. *Sketch of (a) a 3-phase oil-filled electrical transformer and (b) core structure [68].*

The transformer structure has two sides: primary and secondary windings. The windings are closed inside the transformer core. The windings must be able to operate under both the planned normal use and fault situations. The windings must withstand overvoltages and transient surges while keeping them from forming high temperatures. [66] Copper is a traditional material in building the windings of distribution transformers but aluminum is used occasionally [3, p. 142]. Windings are installed in the core which is made of either non-magnetic (air-core) or high-value ferromagnetic (iron-core) materials. The transformer core is kept in a container that is filled with either oil, sulfur hexafluoride (SF_6) gas or non-flammable liquid [3, p. 141]. Oil functions as a cooler liquid [66] and has a higher ignition temperature than most liquids and gasses. The transformer oils are generally non-toxic to the environment and people. [51, p. 463] The iron core is covered with paper (Kraft Paper), cardboard or other insulation material while the core is dipped in the transformer container. Power supply quality and reliability of oil-filled transformers depend on an insulation material wrapped around the windings. [67, p. 203] Insulation materials degrade with time and need to be changed. The paper and cardboard insulations last for years, even over a decade. [68] Voltage unbalances in the grid cause to a transformer overheat and accelerate thermal aging. Harmonic currents have accelerating aging and decreasing effects on the lifetime of the transformer. [52, pp. 5, 9] This can be crucial with multiple PV inverters located in a distribution feeder of a transformer. More about harmonics injected and canceled by PV inverters is mentioned in Chapter 3.4.

3.3 Hosting capacity of photovoltaic systems

This thesis discusses the next phase of the PV system development in LV grids when PV module prices have gone down with larger available quantities and are fitted according to the grid connection requirements [7, p. 16785]. This has led to a new trend where residential households are interested in installing PV modules on their rooftops for satisfying their power demand. Consumers maybe even consider selling surplus electricity when their demand is met. PV systems can have significant effects on grid operations and values.

The general belief before was that PV modules were considered to be suitable only as the main power generator of isolated grids operating on island mode located in remote areas [7, p. 16785]. These are located on islands and over long distances like in deserts and the wilderness. This type of power generation unit needs a storage system for an island mode to provide energy during a low production state of a PV system [33]. REGs without ESS applications have only the capacity to respond to 15–20% of the overall consumption in an isolated electric power system [69, p. 297]. It can be possible to install a high quantity of PV modules in an LV grid when sizing, location and concentration of PV systems are carefully considered to gain the stable operating conditions of the LV grid [7]. Firstly, to better understand PV production in the grid, we need to discuss HC to define the safe PV production level in the distribution grid.

High PV penetration levels of PV systems have brought new effects and problems to LV grids. The surplus power of PV systems can be used to partially supply the power demand of the feeder but grid violations occur if the surplus is not either consumed or stored somewhere. HC is determined as the maximum production of a grid-connected power generation unit, like a PV system, that does not cause grid issues in the connected grid [11, p. 467], [18]. Determining a HC level is affected by multiple internal factors of a PV system and external values of the connected grid, as mentioned in Chapter 2. HC is affected by multiple grid components, like several voltage regulators and capacitor banks. A topology and a profile of a LV feeder also affect the HC value, mostly the length of a grid feeder, the number of and how loads are concentrated in the feeder. [10, p. 1007]

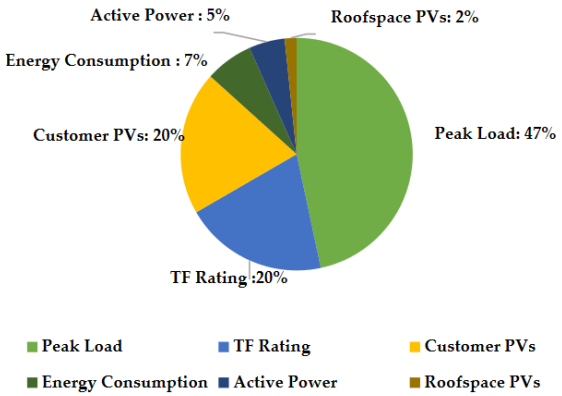

Figure 3.4.1. *Hosting capacity definition summary in literature [63].*

Studies show that the value of HC is individual to every grid feeder or region and depends on the characteristics of the grid in question [8], [49]. Determining the HC level by a single absolute reference value can be a forceful task and there has not been found a universal or absolute definition for it [7]. Literature uses multiple parameters in determining HC. The summary of literature definitions for HC by Fatima et al. [63] is shown in Figure 3.4.1. The most used reference is peak load (47%) as the maximum capacity of the grid line, the transformer rating (20%, TF rating in Figure 3.4.1), a ratio of households with PV installations (20%), the annual energy consumption (7%), the ratio of active power output of the PV installations (5%), the available roof-space for PV modules (2%) in the grid area in question. [63] Using the transformer rating might not be an optimal option because it only tells the load value of apparent power without causing permanent

damage which is meant to avoid overheating the transformer. Other studies went as far as determining the HC level according to the annual energy of total or singular load points in the grid [7, p. 16785].

This thesis uses the peak load in determining HC during the simulations. The peak load of 180 kW was measured as the highest load of the LV feeder during two simulation dates. Knowing the load profiles of the LV feeder is preferable because it can be used to tell what loads are constant and how great is a possible peak load. This information can be used for better design and planning of PV production in the distribution grid. Depending on the topology of the grid and the rating of the transformer, other definitions of HC can be ineffective, even misleading, in the planning of PV production in the LV grid. The transformer rating has been based on the total consumption of the feeder which is more downstream distribution [3] than bidirectional transmission. Longer feeder distances should be also taken into account when considering the capacity of line types.

The main problem due to high PV penetration levels in the distribution grid is overvoltages. General research has determined that under 15% HC values don't cause any major voltage problems to the distribution grid [7], [13], [44]. Studies have noted that the effectiveness and profitability of SGs as part of grid stability come in naught with 50–60% power penetration of DG units [24, pp. 414, 415]. They also note that overvoltages and power losses in the LV grid increase with 30–50% PV penetration levels depending on operations and the variety of components of the selected grid [8], [12], [60, p. 6]. Note that grid topology factors are vital and affect the capacity of PV production on the chosen grid feeder. Weak distribution grids with long line spans and lowering loads towards the end of grid feeders have generally lower HC values. Voltage fluctuations can be caused by rapid shading changes on PV modules, worse being under a response time of grid operations, in a grid region with a highly concentrated PV production. [63, p. 4768] Voltage fluctuations are caused mainly due to slower response time in the transmission grid to rapid shading changes on the PV systems located in the MV grid. Overvoltages in the LV feeder can be detected as low as 2.5% of the minimum load value of the feeder with a single, large-scale DG unit connected to the feeder. [7] The issues are highlighted by the fact that DSOs have little or no control over deciding the integration locations and sizes of privately owned PV systems in LV feeders [52, p. 2]. In Japan, the rising level of PV production has raised concerns to upgrade 6.6 kV distribution feeders to 22 kV or 33 kV to better control the PV capacity in the distribution grids. This may be a severely reasonable grid-enforcing option in the future. [70]

The main effect of RPF is causing overvoltages in a feeder. The RPF effect causes to the grid have a bidirectional power flow. RPF can be measured in a distribution grid with DG units with 30% HC, like in the LV grid in the UK [71]. RPF may occur even when the overloading of a transformer is not detected on a sunny day [12, p. 338]. RPF can cause issues with grid protection coordination and voltage regulator operations. If these aren't taken into an account, RPF can lead to voltage violations. [22, p. 68] The increasing PV penetration levels of PV systems in a distribution grid can have also a positive effect on decreasing power losses by mitigating the need for power supply from upper feeders [27], [41], [72]. It can also occur that raising the PV penetration

level to 40% would decrease the level of active power losses down to 0.85% from 3.45% in the distribution feeder in the study by Azab [27]. But the location of PV systems in the LV grid is important, as a wrong placement can increase power losses [27] and voltage instability compared to more optimal points in the same feeder [23, p. 979].

Next, different study results in the literature are presented. These are compared to the simulation results in Chapter 6.4. to better reflect the simulation results. More problematic cases are PV systems with medium or even large capacities located in the end long feeders with low consumptions [22, p. 68]. The study of Aziz and Ketjoy [7] reclaims that typical European LV grids have a general 70% HC based on the transformer rating. The simulations done by Watson et al. [13] show that over 45% HC of PV systems overloads the conductors in the LV grid. The need for grid investment becomes the necessity for over 50% HC as shown in the study by Gandhi et al. [44]. The number of overvoltage buses and the transformer overloading in the LV grid will increase rapidly with a raising HC level close to the production capacity of PV systems [8, p. 7], [12]. Alternatively, a LV grid can have a large number of PV systems, with the HC up to 110%, when evenly distributed over feeders with short lengths. However, distribution grids have no “rules of thumb” for safe PV penetration limits, as mentioned earlier. PF is a major factor in determining maximal HC. An efficient PF value increases HC of PV systems and will help to decrease power losses in both PV systems and the grid. [8, p. 9], [49, p. 2689]

3.4 Restrictive factors of hosting capacity

Earlier in Chapter 2, it was discussed how solar irradiance and cell temperature heavily affect the power production of PV modules. And how both factors are determined by weather conditions. PV systems in LV grids are small- and medium-scaled power generation units that have both AC and DC components. The PV system will cause issues in the connected AC grid if the operation states and the quality of injected power are not controlled accordingly. The irregular PV penetrations levels cause issues with the LV grid operations and control. The sudden changes in PV production affect the voltage levels of the LV grid and DSO must keep changes inside the allowed values stated by a national grid code. Different grid values and factors limit the available PV production fed to the grid. Hence leading to poorer HC levels in PV systems. These decreasing factors are poorer PF and VUF values and harmonics injected by PV inverters and non-linear loads to the grid.

PF is not a grid component but the measurement value used to determine the state of an AC circuit or system. PF is the cosine of the phase difference between voltage U and current I that is caused generally due to magnetization of an AC circuit [45, p. 8].

$$\mathrm{PF} = \frac{P}{S} = \frac{UI\cos(\phi)}{UI} = \cos(\phi) \tag{3.1}$$

Equation 3.1 defies PF as the cosine function of the angle difference ϕ between voltage and current or the ratio of active power P and apparent power S in the circuit. [73, p. 465] The relation between apparent S, active P and reactive power Q is shown in Figure 3.1.1.

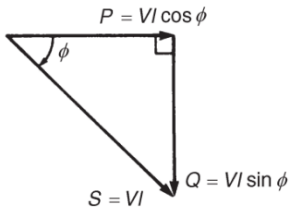

Figure 3.1.1. *Power triangle of capacitive circuit [73].*

The relation between active and reactive power can be determined by using phase angle ϕ in Figure 3.1.1. as

$$\tan(\phi) = \frac{Q}{P}. \tag{3.2}$$

And the reactive power Q can be calculated by

$$Q = \tan(\phi)P. \tag{3.3}$$

This is used to determine the reactive power values of household loads in the simulation model. More about this is mentioned in Chapter 5.2.2. PF is an essential grid and electric system value in optimizing PV production and eliminating unwanted phenomena and effects on other components in the same circuit. Having a high PF value of the grid reduces the current flowing in power generators and decreases the need for grid investments like conductors, switches, transformers and generators. PF value scales between 0–1. 0 value means that there is only purely reactive power, inductive or capacitive, and only active power in the AC system with the PF value of 1. [73] PF can be divided between values of over 0 and under 1 into capacitive and inductive. A grid part or component with an inductive PF draws and with a capacitive PF value injects reactive power into the AC circuit. Naturally, a PF value should be kept at 1 or as close to 1 as possible to maximize the use of components and the transmission capacity of the conductor. Studies and the grid guidelines identify the ideal PF value as between 0.95–1 [45, p. 8], [49, p. 2685].

A PV system functioning with inductive PF value decreases PV impact on voltage rises and enables greater HC of PV systems in the grid. The overload of conductors is the critical factor with an inductive PF. Capacitive PF increases current values and the magnitude of voltages becomes less restrictive. [10, pp. 1008, 1009] PF is the essential feature in determining the efficiency and economic profitability of PV systems. The PF control of the distribution grid can lower voltages and increase HC effectively. [70] PF also heavily affects the operations of PV inverters. The possible reactive power compensation with the capacity of the inverter can be operated only with a proper PF value. Traditional PF improvements are adding parallel capacitor banks in load points or changing the operation state of SGs in the AC power system. The main focus of solutions is to

decrease reactive power loads without changing active power values in the AC system. [73, pp. 470, 471] It should be also considered to change the PF of a PCC from inductive to capacitive, as was done in the study by Oliveira et al. [11]. When the PF was changed from 0.8 inductive to 0.8 capacitive, the level of HC was almost increased 7 times when compared to the RPC solution in the same grid case. [11]

Another critical grid value is the unbalance between phase voltages. With the most of power appliances in LV grids being single-phase grid-connected, the phase unbalance becomes an issue without balancing of single-phase grid connections between phases. The main parameter for measuring unbalance between the phases is VUF. The Equation for VUF is

$$\mathrm{VUF} = \left|\frac{U^-}{U^+}\right| \times 100\ (\%), \tag{3.4}$$

where U^- is negative and $U^+$is positive sequence voltage magnitude [9]. Standard EN-50160 states that VUF can not violate the 2% limit in 95% time of a week [6, p. 87].

PV installations with single-phase grid connections have usually the impact of increasing the value of VUF in distribution grids. But this is not certain in every situation. The study by Kitworawut et al.[71] simulated PV production in the LV grid with 4 parallel feeders connected to the common transformer. Overvoltages in the buses, RPF and cable overloading were recorded but the VUF value was under the recommended limit of 1.3% with over 200% HC. [71] Different solutions can be installed to better adjust and control the effects of the rising level of power electronics components in distribution grids.

Another characteristic of PV systems is harmonic currents and voltages injected from the power electronics of PV systems, mostly PV inverters, to the grid [5], [11], [65]. Harmonics are caused by the high-frequency switches [63, p. 4767] and non-linear loads connected to the grid which lead to PQ issues [74, p. 1135]. Generally, non-linear loads in the grid are the main cause of harmonic voltages and currents [45, p. 7], [72]. The key factor of harmonics is that they are non-linear, other than perfect sinusoidal loads that form a resonance circuit with other reactive power nature elements [59], [74]. These are caused mostly by simple parallel-connected capacitor banks, capacitive line cables and PV inverters. [44, p. 190] Harmonic values are measured using the Total Harmonic Distortion (THD) value. The level of HC can be reduced because of a high THD value under the non-favorable circumstances of the grid [11]. The standards IEEE 1547 and IEC 61727 determine the top allowed value of THD in the grid to be 5% [45]. In Croatia, the THD value caused by a single power generation unit in the distribution grid cannot exceed 2.5% [4]. THD of the grid can violate the 5% safety limit even when there were none of the non-linear loads, other than PV inverters, with 100% HC in the LV grid confirmed in the study by Gandhi et al. [44, pp. 190, 193]. The increasing number of grid-connected PV systems means also increasing THD values in the grid [5], [27], [44], [45], [72] which is causing issues, like component heating, for both customers and distribution grid [74]. Major issues of harmonic currents are overloading of consumer electrical applications, overheating of transformer windings and neutral wiring that can lead to a burst of fire. The 3rd harmonics current causes most fires started by overheating of the neutral wire. [4, p. 141] Small-scale variations of non-linear loads have been simulated and

studied but larger-scaled variations and their current draws are harder to model [59]. This has become a vital issue with the rising number of PV installations in distribution grids where harmonics cause severe long-term issues.

Harmonics are not simulated or discussed in the simulations of this thesis. But keeping the THD value under the standard limit stated by the grid codes becomes an issue as has been shown in literature with the rising number of PV installations in distribution grids. This should be considered in the planning and sizing of new PV installations. The level of power electronics in the LV grid is usually low but the increasing level of PV production raises concern about rising THD values in distribution grids. For further study, harmonics injected by PV systems could be simulated and tested more, like in a Master of Science thesis majoring in power electronics.

3.5 Solutions for enhancing hosting capacity

The purpose of this chapter is present different methods of increasing PV production, or HC, of PV systems located in the distribution grid. Generally, LV grids with larger loads during midday allow higher HC levels [10, p. 1007]. The literature revealed that a soaring HC level in LV grids can be achieved easier when compared with MV grids. However, MV control problems impose a limit on HC in LV networks. PV systems in distribution grids have caused the need for more robust voltage strategies at the MV level and developing “rules of thumb” for HC at the LV level which will increase HC levels ultimately. [7] DSOs should determine the knowledge of the HC levels in their grids and favor shorter feeders [7], [11, p. 467] that will not cause a need for additional grid investments [75]. The general rule should be testing HC levels in multiple and varying conditions. This will help better to adapt and keep the grid stability values constant under the sudden changes, like voltage fluctuations due to shading, of PV systems. [7, p. 16790] DSOs could encourage private PV system owners to keep injecting active power into LV grids in a period less than the nominal current capacity of the feeder. The limit can be calculated, simulated, or tested by increasing active power to the grid feeder. When the voltage of the feeder rises over the allowed upper limit, the injected power of that moment is the threshold value of the feeder or the transformer. [76, pp. 1600, 1601] DSOs should also consider adding protection solutions in preventing situations where a PV system feeds power to a fault point [77].

Grid reinforcement is the traditional solution for better voltage control but is undesirable due to a need for high investments. Raising the capacity of lines by replacing the existing conductors with a larger nominal current value balances voltages in the distribution grid. But higher capacity conductors have a limited effect in the terms of increasing HC. In Monte Carlo simulations of the real-life 50,000 LV grids by Torquato et al. [10], the higher capacity conductors only increased the HC level by 16.6% which is similar to the increment of the current threshold of 17% between the two conductor types. The average HC was raised by only 6.1%. It was found that the value of HC is more sensitive to impedance reduction than increasing the thermal current capacity of conductor types. [10, p. 1010] Other factors of PV systems can alter planning, building and controlling the distribution grid. One is the question of power balance. Grid investments can be caused to keep the value of so-called “spare power capacity” for sudden load changes in the

grid with a round-the-clock availability. Ultimately, increased grid investments will lead to increased electricity bills for customers. [64]

For better adjustment and control of grid issues caused by PV systems, different grid control tools are discussed in this part. The role of hybrid solutions is mentioned as well. The literature discusses different ways and methods that can be used to stabilize and balance the operation state of distribution grids with a high quantity of PV systems. Firstly, the advantages of voltage control are discussed. Voltage regulation solutions can be more economic than grid reinforcement investments [49, p. 2684]. Secondly, active power curtailment (APC) and RPC are presented and discussed. These are popular methods for avoiding power and voltage fluctuations in the grid [45], [78]. These solutions can have the wanted impact of maximizing PV production and decreasing power losses and avoiding grid violations. Lastly, we discuss the role of distribution transformers under high PV penetration levels. The transformer can be a passive grid component that merely functions voltage level component but modern distribution transformers have traditional voltage control solutions, like Off-Load Tap Changer (OfLTC) and OLTC. The OfLTC is known as "a fixed tap changer" in which the tap position can be changed only when the feeder is in a non-load state [79]. OLTC is the automated tap changer that will change accordingly the feeder situation or remotely. Due to the limited use range of OfLTC applications, this part focuses more on the study of OLTC transformer applications used in literature.

3.5.1 Voltage control

The voltage control of LV grid is a responsibility of DSOs who face voltage balancing challenges daily. The voltage control is done by balancing consumption and production in the grid [45], [65]. DSOs are tasked with keeping grid values inside the limit stated in grid codes. This affects on the maximum PV production in the distribution grid based on the safety limit values [48]. The grid violations caused by high PV penetration levels will cause disconnecting PV systems from a feeder as the last resort [64, p. 540]. The Finnish electric power grid uses the voltage limit according to European Standard EN-50160 which states overvoltages measured in the grid cannot violate ±10% of the nominal voltage U_N. But several studies have been considering on the voltage fluctations caused by PV penetrations of steady-state grid operations. For better respond to voltage fluctuations, many grid codes use the overvoltage limit +5% U_N, as in American Standard ANSI C84.1. The voltage level and the length of the feeder are major factors in determining the limit of voltage violations and HC level. The study by Fatima et al. [63] shows that a higher impedance of the grid lowers HC. But grids with higher voltage levels and more loads can threshold higher HC levels. [63, pp. 4761, 4762, 4771] For example, the short 150 m feeder can have an HC level up to 500% of the minimum load value of the conductor [5].

The increasing number of household load sizes, like heat pumps and charging modes of electric vehicles restrict HC due to undesirable grid voltage conditions [78]. Electric vehicles used as a power storage between the vehicle and the grid has been regarded having more economic potential than general storage technology [64, p. 541]. Also, the coordination among electric vehicles and PV systems can reduce power losses and decrease voltage fluctuations in the grid.

The key factor of coordination is the flexible consumption of electric vehicles from PV production in the grid. [80]

3.5.2 Active power curtailment and reactive power control

APC is active control of grid-connected production components for the sake of grid stability. APC curtails surplus PV production not consumed locally which hence can be lost. An APC application can be operated by a PV inverter. [12, p. 339] The APC method is the non-favorable option when considering the maximization of PV production [12] but an attractive option due to the smaller need for grid modifications [58]. APC decreases the MPPT operation time and can cause the disconnection of multiple PV systems due to unwanted grid conditions [8, p. 2], mostly to avoid overheating the transformer. It was determined in the review by Cabrera-Tobar et al. [23] that grid-connected PV systems need both the APC solution and the RR control in an active power control solution. The nature of weak grids has caused a demand for reserve capacity in South America and Puerto Rico. The grid codes of these nations demand that the MPPT of PV systems is mitigated under the optimal maximum value. It was concluded that the maximum value of MPPT should be kept under the capacity of the connected feeder or an installed ESS application for avoiding grid violations. [23, p. 981] An APC solution can lead to power losses over 20% in the annual PV production in the LV feeder. The application of the APC controller avoided the overloading state of the transformer in the feeder in the Swiss distribution grid and only overloading occurred during consumption distribution on winter nights. [12, p. 339] In Canada, the suburban LV feeder with PV production could decrease their need for power import from the MV grid from 50% to 20% with an APC application in PV inverters [81]. This would also decrease power losses caused by the power transfer from the MV grid to the LV grid.

RPC is the conventional tool in voltage control which can be used in all voltage level types. Multiple power electronic components, like static voltage controllers, static synchronous compensators and capacitor banks, are used to inject reactive power into power grids to control grid bus voltages. PV inverters can function as the RPC tool with small adjustments while completing their original tasks simultaneously. This helps to stabilize the grid and also boosts the production of other power generation units connected to the same grid [23, p. 984]. The inverter can alter the injected current from PV modules so that it can change the voltage level of a feeder to a more nominal value. But even inverters are capable to inject reactive power, the function is not demanded in grid codes, like in IEEE 1547 [23, p. 981]. The PV inverter can work as a RPC tool but due to the low X/R ratio of the LV grid, it does not have as great an impact at the transmission grid level [5], [24, p. 415], [45], [63]. The high resistive characteristics of LV grids can also cause higher currents and power losses when reactive power is injected. The amount of injected reactive power for balancing voltages rises if the R/X ratio of a LV grid increases. [58, pp. 139, 140]. When the value of injected active power is under the capacity of the PV inverter, the remaining capacity can be used for injecting inductive or capacitive reactive power [5]. Reactive power injection of the PV inverter located in the LV grid can mitigate voltage rises in both LV and MV grids [70]. This helps to keep the PF of the LV feeder almost constant [42, p. 121]. The ability to inject reactive

power is limited by the balancing rating with the sizing of the PV inverter. The balancing can be done by oversizing the PV inverter when the level of injected reactive power is increased. This is done so that the active and reactive power controls of the PV inverter are maintained. [43], [63, p. 4775] The main concern with oversizing PV inverters is the investment cost. Firstly, DSOs should consider other options, like reducing the loading state of transformers, and choose accordingly. [63, p. 4775]

There are several factors in defining the efficiency of a RPC solution. The capacity of RPC solution in PV inverters is limited by the current-carrying capacity of the semiconductor switch [5, p. 2071], the rating of the inverter and the THD value of the grid [45, p. 19]. DSOs are keen on consumers installing PV systems with multifunctional inverters. The reactive power control does increase PV capacity in the feeder but PF must be over 0.80 to have a significant effect on the grid voltages [5], [13]. The calibration of PV inverters must be done carefully because the reactive power compensation mode increases power losses [82]. The study by Wang and Yang shows that any PV system with over 11 kW active power injection should be capable of operating dynamic RPC [8, p. 2]. The single-phase reactive power injection is also an option and can solve overvoltage problems in both connected phase and parallel phases [44].

3.5.3 Transformer control solutions

The increasing number of household PV systems has gained more interest in investing in OLTC adaptations of transformers in LV grids [60]. The conventional tap changes of the transformer are not always fast enough to react to changes in PV production due to rapid shading conditions on PV modules. Voltage fluctuations caused by rapid power changes of PV systems may not always be maintained inside safe limits. [23, p. 979] An OLTC application is installed on the transformer at the start of a LV feeder and the control can be based on single or multiple grid values, like voltages of PCCs in Figure 3.6.1.

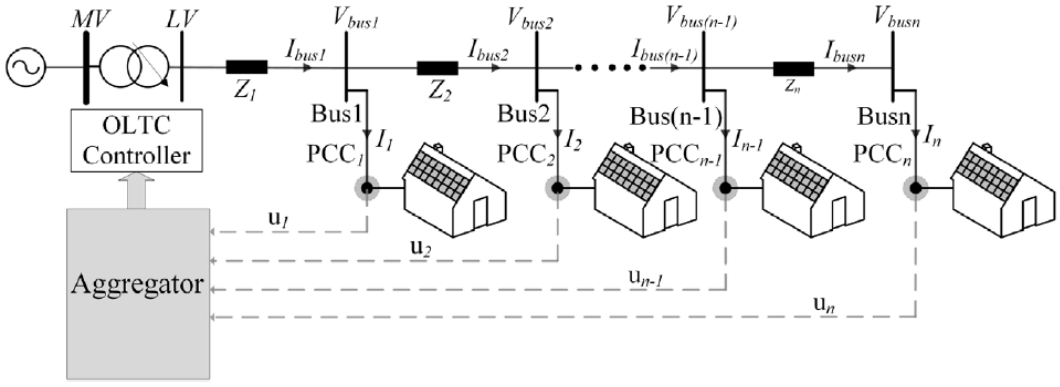

Figure 3.6.1. *OLTC control methology based on the voltages of PCCs in the LV feeder [6].*

The voltage values of all PCCs in the feeder are collected by the aggregator and the OLTC controller changes the tap position accordingly to avoid grid violations [6, p. 87]. Using the OLTC application avoids violating voltage limits due to PV penetrations that occur alongside the feeder

buses with an OfLTC application or without a transformer control solution [49, p. 2684]. The OLTC application was found to be a better voltage control solution than RPC solutions in the study by Uzum et al. [45]. With higher nominal current capacity conductors and the OLTC application in the transformer, the HC of feeder was increased from 50% to 90%. [45, pp. 13, 15]

A solid-state OLTC application with modern devices has fast response times while operating in higher frequencies. These are preferable to the conventional OLTC applications with a longer response time of between 100 ms to seconds. [63, p. 4773] The OLTCs function with physical tap position changes of primary or secondary windings of a transformer [3, p. 146]. The function range of an OLTC is ±10% to U_N of a connected grid [75, pp. 265–266]. This is done due to the voltage regulations, like standard EN 50160, with the largest voltage changes can be ±15% of U_N at least the 95% time of a week [3], [75]. OLTC applications are usually set in the tap change range of ±0.8–2.5% U_N [78, p. 2] but the longer range of over ±8% U_N with 9 (± 2% U_N) steps is used in the LV grids in the UK [60, p. 4]. For example, the range of ±10% U_N tap changes can be divided to the number of steps: 16 (±1.25% U_N) and 32 (±0.625% U_N), respectively [75]. OLTCs have, like any other applications or machine, a lifespan that can be decreased with multiple short-term and extensive tap changes. A longer lifespan can be achieved by eliminating unnecessary tap changes and limiting the number of tap changes. The tap changing of the secondary voltages of the transformer increases the HC in the feeder but with the condition of not violating the voltage limitations of the LV grid [13]. The study by Uzum et al. [45] showed the terrific promise by limiting 95% the number of tap changes with optimization and the full observability of the feeder.

OLTC applications can be operating in single or multiple phases of a transformer. The differences between applications based on the number of phases are discussed and their effects on grid values, like VUF and HC, are noted and discussed in the literature. Both single-phase and 3-phase OLTC applications can increase HC from 40% to 70% in LV grids [49], [75]. It is shown that the 3-phase applications have higher HC values and they were limited by overvoltage and transformer rating violations. HC of the single-phase PV grid connection cases was raised as well with the OLTC but lower than in the 3-phase case. The limiting factors of HC are high negative sequence unbalances and neutral wire current limit violations in the single-phase connection cases. It was highlighted that DSOs should measure the effectiveness of an OLTC application to the investment cost and consider other methods, like reinforcing a secondary substation. [18, pp. 1704, 1706, 1713] VUF values are also increased with the single-phase OLTC applications [75].

OLTC applications can be combined with additional voltage regulator solutions, like a RPC tool. Hu et al. [75, p. 270] found in their study that the combined solution of single-phase OLTC and reactive power regulation was the best strategy for voltage regulation of the LV grid. Aziz and Ketjoy [49] also mention the beneficial effects of hybrid solutions, especially the coordination between the RPC solution and the OfLCT application during high HC situations. The hybrid solution of OLTC and parallel capacitors at the LV grid level in the UK was discussed by Long and Ochoa [60]. They have stated that the coordination between capacitors and an OLTC application should be defined due to the capacitor voltage boost in the LV grid. The same paper found that the

number of tap changes was decreased by capacitors having a shorter response time than the OLTC. [60]

4 ENERGY STORAGE SYSTEMS

The purpose of ESS technology is to give a storage solution that will best match the demanded attributes of an energy production method in question. These attributes are enough storage capacity, discharge time and power rate between discharge and charge states [83]. An ESS consists of different parts: storage, control and power conditioning system [84, p. 512]. The major factor in choosing an ESS application is the capital cost. This can be based on delivered power (€/kW) and per capacity (€/kWh) of energy storage [85, p. 21]. The practicable factor in choosing an ESS technology for a PV system is the lifetime cost which includes cycle life and round-trip efficiency. Cycle life is the number of charge and discharge cycles an ESS application can do without critically decreasing the performance. [83] The round-trip efficiency is the ratio, usually %, between input energy during charging and what is retrieved as output energy during discharging of ESS. The rest of the energy is lost due to thermal losses, conversion losses during charging batteries and self-discharge losses during stand-by and off-duty modes [69, p. 299]. This is the reason why the round-trip efficiency is never 100% but all ESS applications should have a round-trip efficiency as close as possible to it.

Two main areas of usage for ESSs are daily and seasonal demand. Daily demand enables all-day-around energy distribution and seasonal demand focuses on storing large-scale production ESSs, like pumped or pumped-hydro storages (PHSs), during seasonal periods. [86] ESS technology is used in both isolated power systems, like in mines or ships, and distribution solutions, mostly in isolated grids with island mode and distribution grids. The need for ESS solutions in PV systems has become a necessity due to asynchronous PV production not being capable of injecting constant power to the power system or the connected grid. Both transmission and distribution grids use ESS solutions to enable continuous power distribution. Disconnection states of grid feeders and regions are caused partly due to unwanted tripping, a fault or an incident, caused by weather conditions and wildfires. [87], [88] ESS technologies can provide better PQ value and reliability in the connected grid. They can also provide spinning reserve, voltage and frequency regulation and energy management solutions. [85, pp. 65, 66] The need for ESS technologies in the electric power grid is magnified by longer lengths of distribution feeders between substations and load points and separate environmental conditions. Longer feeder lengths are more vulnerable to grid faults and harsh weather conditions cause a feeder to be disconnected from the main grid. ESS solutions are needed to ensure continuous electrical distribution in the feeder during the disconnected state. [88] Large-scale ESSs can be used for the stand-by reserve of transmission grid operations [85, p. 77]. Violations caused by high and rapid changes in active power injection of PV systems have been acknowledged and added to the grid codes in Puerto Rico and nations of Europe and South America. The grid codes of these nations demand a power reserve in DG units for stabilizing the grid frequency fluctuations. [23]

ESS integrated PV systems reduce overvoltages and the need for RPF solutions by storing peak PV production in ESS storages and injecting it back during the higher consumption state

of the grid feeder [45, pp. 4, 5]. Other key factors are load response and reliability from the point of view of DSOs [83]. The physical size is most likely to be a major limiting factor with the capital cost for choosing ESS applications in household PV systems. Having larger PV capacities usually means bigger storage sizes.

The primary operation factor of ESS applications is the RR control discussed in this thesis. The ESS unit RR limit must be defined to the safe maximal PV penetration level, HC, injected in the LV feeder [89]. The grid operations response times can be too long to compensate for power flow changes which can lead to grid violations [17]. A violation of a RR limit of PV systems can cause rapid voltage and power fluctuations in distribution grids [23]. RR can be measured by power (W/t), like in Denmark at 100 kW/s and Ireland at 30 MW/min, or by a capacity of PV system (%/t), like in Germany and Puerto Rico with the 10 %/min [17]. The need for adding a similar power reserve demand in national grid codes with rising PV capacities in distribution grids may become a necessity and a demand by DSOs in the future. [23] This thesis uses ESS integrated PV systems for the daily demand of PV production located on residential rooftops of the LV feeder. There was no chosen ESS technology for the simulations and the use of ESS integrated PV systems was simulated by using the RR control strategy. Mostly likely option for ESS technology in household PV systems would be a battery energy storage system (BESS) due to low investment cost and small physical size. Two RR limit values ($\mathrm{RR_{limit}}$) of ESSs are 2 %/min and 10 %/min. ESSs store PV production which will lower injected power to the grid that helps in avoiding higher voltage and current values in the LV feeder.

Different ESS technologies, control algorithms and topologies are presented and discussed in this chapter. Firstly, ESS technologies in general and their commercial use are presented briefly. ESS control algorithms and their characteristics are presented in the second part. The main focus is on the RR control strategy used in the simulations. Also, two topologies: decentralized and centralized are discussed. Lastly, different ESS-integrated PV systems in commercial use are presented and discussed.

4.1 Technologies

ESSs can be divided into four categories: physical, electrochemical, electromagnetic and thermal. Physical energy storages include PHS, compressed air energy storage (CAES) and flywheel energy storage. Electromagnetic energy storage systems can build from power electronic components, like supercapacitors and superconducting magnetic energy storage. Electrochemical energy storage can be lead-acid, lithium-ion (Li-ion), nickel-based (Ni), sodium-sulfur (NaS) and redox flow battery (RFB) just to mention a few popular technologies. [83], [89, pp. 163, 164,168] Electrochemical energy storage systems, like BESS, are the second most popular, after the physical, energy storage technology with the global capacity of 6625.4 MW in 2018. The annual increase was 45%. [89] BESS applications are the popular option for small-scaled ESS-integrated PV systems as they have fast response time and high round-trip efficiencies. The major downside of BESSs is the high capital cost. Thermal energy storages include cold and cryogenic energy storage (CES), heat storage and thermochemical and combined thermal energy storage

(TES) [83]. Li-ion, NaS and NiCd are seen as the leading ESS technologies for having high power-density characteristics [84, p. 513]. Figure 4.1 shows the performances of different ESS applications based on power and time.

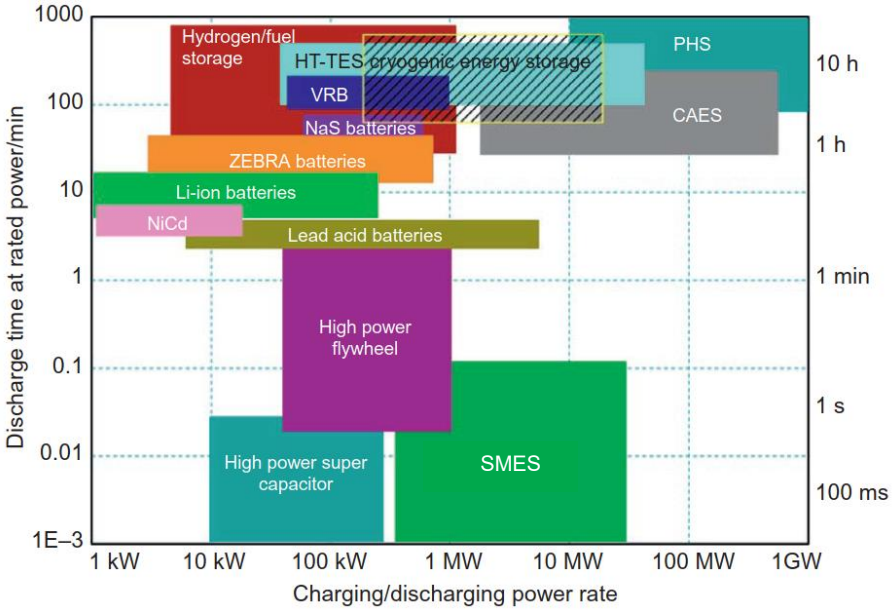

Figure 4.1. *The map of ESS applications categorized by the performance [83].*

As a single ESS technology usually has limits in meeting the requirements of the grid [83], [85], integrating a hybrid ESS solution to REGs is the popular method. Hybrid ESSs have an improved economy due to the reduced charge and discharge cycle depth and level of usage frequency compared to a single ESS technology. Battery technologies of hybrid ESSs can be divided between the high and low frequencies or the fast and slow power fluctuations depending on a chosen algorithm or strategy. [89] CAES, PHS, RFB and TES technologies are optimal for the industry- and utility-scaled ESS solutions due to their ability to provide enough capacity in smoothing electric fluctuations of medium- and large-scale PV systems. Supercapacitors and flywheel storages have a rapid response time, a few milliseconds, to grid fluctuations and are an optimal solution for smoothing distribution during line fault situations [83, p. 11]. Super magnetic energy storage technology is still in the development phase, has a high capital cost and lacks commercial maturity [85]. For these reasons, this technology is not discussed in this thesis.

BESSs are the more popular and well-known ESS technology. In the electric power grid, BESSs are an important method for smoothing residential demands and a popular choice for DG system storage. [83] The major advantages of BESS are more stability, reliability and security in grid operations. ESS enables storing power production of microgeneration units and used for own consumption later on [90]. BESSs are an efficient method to control the active power and improve the HC of PV systems by decreasing RPF in the connected grid [63, p. 4757]. BESS applications of DG systems in distribution grids have improved factors in the grid stability and economic efficiency of DGs, like PV systems [72]. But some factors, like the efficiency of PV inverters, may decrease due to separate and increased charging states of batteries during PV production [91, p.

15]. A BESS usually consists of battery storage, like lead-acid, Li-ion batteries and supercapacitors banks [45].

The lead-acid battery is the oldest electrochemical battery technology being the original car battery since the late 19th century. Lead-acid batteries have a high round-trip efficiency, cheap prices and easy installation. The disadvantages of lead-acid batteries are the low energy density, the short cycle life, hazardous to the environment and toxicity to people and animals. The lifetime of acid-lead batteries is the shortest of existing ESS applications but it has the smallest capital cost. [83, pp. 18, 19, 21] Generally, small-scale PV systems use lead-acid batteries for low investment costs but lead-acid technology has a short lifetime when compared to other ESS technologies [23, p. 983]. But lead-acid batteries have the large, existing market that enables easy availability with high quantity. The study of McKenna et al. [91] states that lead-acid batteries are not suitable for household PV systems due to environmental factors in the production of batteries and the negative impact on net costs. The annual losses were up to ~1000 £ for the 3.29 kWp PV system with integrated BESS with the 570 Ah battery located in the UK in 2013. [91]

The role of mobile devices and electric cars in society brought up the need for a high energy density and portable solution for a new storage technology at the end of the 20th century. Li-ion battery technology has been chosen as the general solution for this demand. Li-ion batteries have high efficiency, power and energy densities, round-trip efficiency and long cycle life. These factors are all close to 100% efficiency [23, p. 983], [83], [84, p. 513]. Li-ion batteries are a convenient storage solution for portable devices [84]. Li-ion-based BESSs have high round-trip efficiency and low self-discharge rate. Other BESS technologies include Nickel-based (Ni-Cd, Ni-MH and Ni-Zn) and NaS batteries. Nickel-based and NaS battery technologies both have a high energy density and long cycle life. Nickel-based technology has high-temperature tolerance and robustness to deep discharges. The NaS battery technology has also high round-trip efficiency. Both technologies are being researched to be integrated as BESS solutions for PV systems. [83] For future applications, the batteries of electric vehicles could be used as capacity for power system control and management [84, p. 517].

PHS is the main energy storage type with 96% of the capacity of global energy storage (175.4 GW in 2017). The annual increase was 4%. [89] PHS is based on the stored kinetic energy of large volumes of water between lower and higher water reservoirs. The PHS offers better controllability, low maintenance costs, low investment costs and ancillary services with part-load efficiency. These are enabled due to the availability of the PHS to supply both stable or by-demand power by converting the kinetic energy of water between upper and lower reservoirs. The PHS can enable steady and continuous power feeding from PV systems to the grid. The drawback of the PHS includes a need for a large water reservoir that will be difficult in placing close to residential areas. [83] Also, PHSs have high investment, and construction costs and can cause a permanent impact on the environment and the scenery. [85, pp. 82, 83]

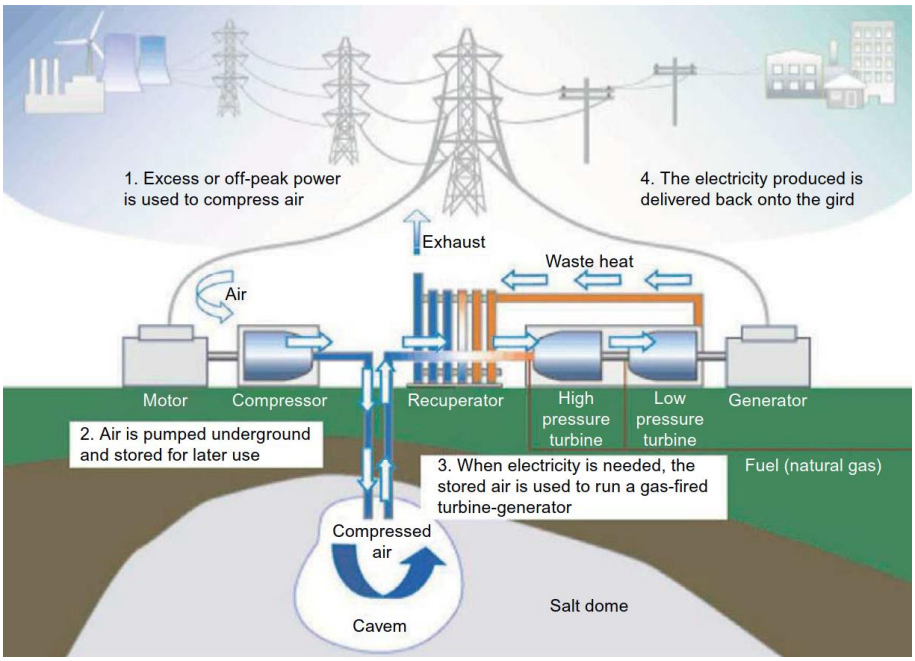

Figure 4.2. *Scheme of CAES system and the explanations of different operation states [85].*

Compressed air energy storage (CAES) is traditionally built with gas turbine technology as energy is stored by increasing pressure and discharged by releasing it. Different operations states of CAES are presented in Figure 4.2. The electricity is fed to the motor that runs a compressor. The compressor increases the pressure in the CAES tank. [83] Old mines are used as CAES tanks but when using a commercial tank, a rupture can lead to catastrophic consequences [85, p. 87]. Releasing air pressure from the tank is used to run the turbine generator to produce electricity when demanded. The CAES technology is seen as the mature technology that is designed to sustain multiple on/off cycles during load state changes. Larger CAES systems are designed to operate daily with efficient partial-load conditions, which are fast changes of swings between generation and compression modes to absorb or compensate power, with the connected grid. The long lifetime of the CAES and newer ESS technologies with faster operation times have caused a trend where the usage level of the CAES technology is decreasing and newer CAES installations have been postponed, even canceled. [83, pp. 17, 18]

Solar fuels are seen as the conventional method of storing electrical energy in a chemical form. Two major solar fuel technologies are hydrogen and hydrocarbon with three production methods by gathering hydrogen from splitting water into oxygen and hydrogen: electrolysis (by electricity), thermolysis (by heat) and photolysis (by light). Large-scaled water electrolysis units can have over 75% efficiency but other production processes have lower efficiency values in laboratory conditions. One of them is solar liquid fuel technology where carbon dioxide is turned to liquid form with higher energy densities than hydrogen. There are challenges in converting the technology from research to commercial level in the question of efficiency, capital costs and longer lifetime. [83, pp. 17, 18]

The usage of TES as an electricity management method is a more recent discovery and can be used in supply and demand side management. TES technology is divided into thermo-physical (temperature difference) or thermochemical (latent heat from phase change) forms. Thermophysical-based TES is more developed as a heating or cooling storage method. Cold and cryogenic energy storage (CES) is based on the thermochemical storage of liquid air and nitrogen. The benefits of CES as the grid operation method include the ability to store energy at low pressures and having higher volumetric storing density when compared to other ESS technologies. The CES technology has over ten times higher volumetric store density than the CAES and over 100 times more than the PHS. CES has a high efficiency due to recovering waste heat but the efficiency is just around 60% without an external heat source. Another recent TES system used is pumped thermal electricity storage (PTES). Charging of PTES includes converting electricity into cold or hot thermal energy and discharging converting another way around. The charged thermal energy is stored inside cylinders at a reasonable temperature. PTES has thermal energy losses during storing due to thermal conduction which disables long charging cycles. PTES is preferable in short charging cycles due to a higher number, usually twice an amount, of compression, expansion and heat processes. The level of global PTES technology is still small with the demonstrating 1.5 MW/ 6 MWh PTES plant planned in the primary substation in the UK in 2013. [83, pp. 17, 18]

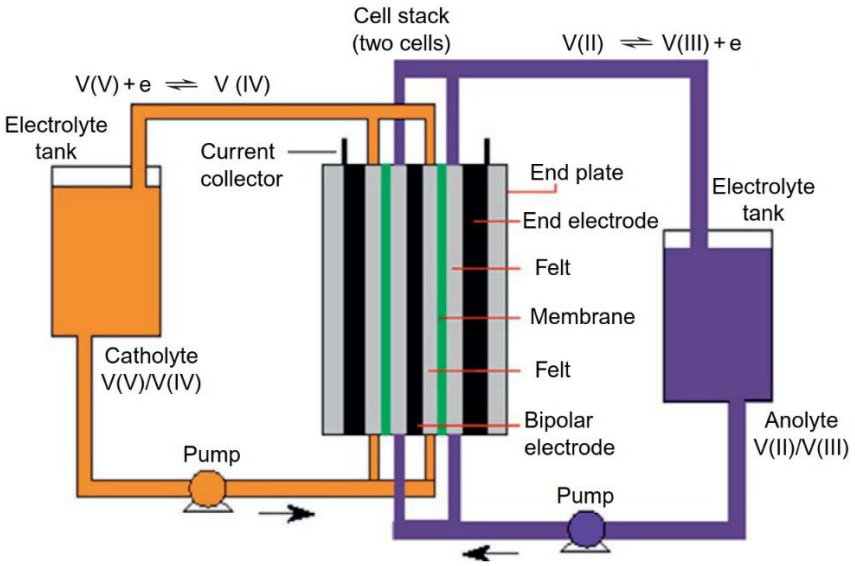

Figure 4.3. *Scheme of vanadium redox flow battery [85].*

RFB technology is based on converting electricity to electrochemical energy between two liquid electrolytes. The RFB applications are zinc-bromine (ZnBR), polysulfide bromide (PSB) and vanadium redox battery (VRB) [85, p. 78]. Electrolytes are contained inside the electrolyte tank and the conversion of energy occurs when electrolytes flow through the electrodes of a cell stack [83]. Hence the name of a flow battery. The cell has two parts: positive and negative half-cells being separated by a membrane to avoid mixing of the electrolytes as shown in Figure 4.3. By adding more electrolytes to the electrolyte tanks, the energy capacity of a flow battery can be

increased [85, p. 90]. RFBs have high round-trip efficiencies, rapid cycle inversion and a symmetrical charge and discharge process. RFBs have also a short response time to situation changes and a lifetime expectancy of 15 years. [83] The maintenance cost and need are low [85]. But the number of multiple components needed for operating flow battery applications causes to have a high capital cost [84, p. 513]. The small-scale RFB applications are being researched and developed for use in ESS applications of wind power and PV systems. [83]

4.2 Strategy and topology

When an ESS technology is selected as part of the power system or the grid, a control solution is usually needed to maintain and alter the wanted output. ESS systems installed in PV systems mostly have an algorithm for controlling injected PV power so that grid values stay inside grid code values and reduce grid problems, like overvoltages and thermal damage to the components [13], [17], [45], [76]. Different ESS control algorithms discussed in this part are smoothing algorithms. Smoothing filtering methods filter high-power fluctuations caused by power variations of a production unit. The output to the grid is under the safe reference value, like the RR limit. [17] This part discusses different ESS control solutions, mainly smoothing filtering types and the RR control solution of the ESS used in the PV system in the simulations. Two ESS topologies, centralized and de-centralized, are also presented.

The smoothing algorithms can be divided into filter type and gradient methods. This part focuses on the filtering types. The smoothing algorithms can be based on multiple parameters like voltage magnitudes, battery capacity, recorded data, et cetera. First-order low-pass filter (LPF) can be used to reduce high-frequency fluctuations in the AC system and can be defined as the smoothing algorithm as well to reduce frequency components fed by PV production to the grid. [17] The advantages of the LPF are high reliability, simple operation and easy application to ESSs. The algorithm of LPF is low-pass filtering. The low-pass filtering algorithm is preferable for suppressing output fluctuations of ESS applications to better meet the grid requirements. The high-pass filtering algorithm is also used in smoothing output fluctuations but cannot deliver real-time operation results due to time lags in the operation algorithm. [89, p. 165] Second-order low-pass filter is a similar algorithm method to LPF but the filter has a steeper filtering ability that helps to reduce the sizing of ESS.

The moving average (MA) algorithm is the most commonly used smoothing filtering type method algorithm. The MA algorithm is the smoothing algorithm based on the average PV power in a given period. This can be enhanced in the exponential MA algorithm that uses recorded data from the PV system. [17, pp. 3, 4] The MA algorithm has the issue of relying too much on the recorded data which has a high influence on affecting the smoothing results [89, p. 166]. Discrete Fourier transform (DFT) algorithm is used for measuring multi-time scale power signals. DFT analyzes the power spectrum of DGs and changes signals from the time domain to the frequency domain. DFT algorithm smooths output fluctuations according to the spectrum transformation. The disadvantage of DFT is the dependence on all-time domain information to enable a reliable and correct spectrum transformation. Incorrect time domain values means also insufficient output

fluctuations. DFT algorithm is used in hybrid ESS technologies. Kalman filter algorithm is the linear discrete system that it does not need to store a large time data, like DFT, to operate sufficiently. Kalmar algorithm advantages include smoother output fluctuations of DGs and majorly improving the lifetime of batteries due to minimizing unnecessary operations. The operation of the empirical mode decompensation (EMD) algorithm is based on diving signals from DGs to the frequency bands. Signals are divided into low- and high-frequency bands to better suppress output fluctuations of PV systems. The hybrid ESS technologies with BESSs and other ESS are preferable to use the EMD and the wavelet packet decomposition algorithm to better operate different ESS technologies of the PV system. EMD algorithm may cause issues due to different decomposition results of the same power signals that make it harder to suppress output power fluctuations. The wavelet packet decomposition algorithm is based on the wavelet decomposition algorithm that is suitable for processing non-stationary mutation signals. Wavelet packet compensation algorithm is preferable for the gradient signals and the algorithm can decompose both low- and high-frequency parts to improve the time-frequency resolution. For this reason, wavelet packet decomposition is a preferable algorithm for hybrid ESSs. The model predictive control algorithm uses the early prediction method based on the current situation that can predict output fluctuations values for a few next steps. Filtering algorithms can be used in hybrid ESSs, that use low- and high-frequency algorithms to improve the operation states of two different ESS technologies. [89, pp. 166, 167]

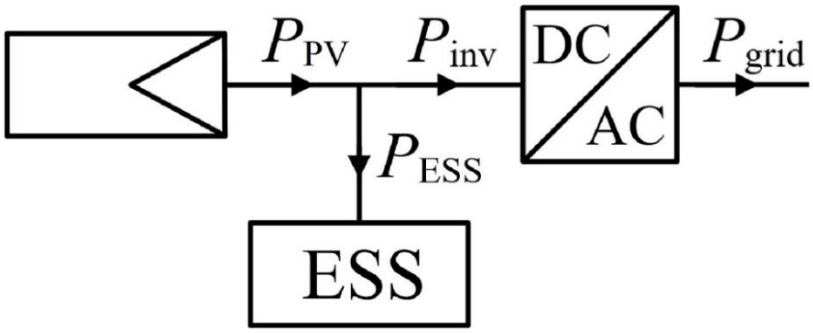

Figure 4.4. *Diagram of the PV system used in the simulations [43].*

This thesis uses the same RR control strategy of the PV system with 23 PV modules and the ESS solution used in the study of Lappalainen and Valkealahti [43]. The PV system is the same two PV strings located on the rooftop of Sähkötalo in Hervanta Campus, Tampere. More about the PV strings is mentioned in Chapter 5.2.3. The diagram of the PV system with the ESS and the inverter is shown in Figure 4.4. The active power of a PV module or system P_{PV} is the sum of the active power fed to the inverter P_{inv} and the ESS P_{ESS}. The PV inverter is assumed to have zero operation losses which means that P_{inv} has the same value as the active power fed to the grid P_{grid} . P_{PV} can be calculated by

$$P_{\mathrm{PV}} = P_{\mathrm{inv}} + P_{\mathrm{ESS}} = P_{\mathrm{grid}} + P_{\mathrm{ESS}}. \tag{4.1}$$

The maximum power fed to the grid $P_{\text{grid, max}}$ is the nominal active power of a module or system $P_{\text{PV, nom}}$ limited by the DC/AC ratio of the inverter as

$$P_{\text{grid, max}} = \frac{P_{\text{PV, nom}}}{\text{DC /AC ratio}}. \tag{4.2}$$

$P_{\text{grid, max}}$is the reference value in determining the RR limit RR_{limit}values used in this thesis. Two RR limits RR_{limit} 2 %/min and 10 %/min of $P_{\text{grid, max}}$ are used in the simulations. Having a lower RR limit means also that more power from the ESS is drawn for the smoothing. For enabling this, the ESS is not limited by the capacity to ensure that all PV power ramps are smoothened by the set RR control. The PV inverter is assumed to always operate at MPP and without any losses during the simulations. The control of the ESS can also be taken an account in an incident situation. There is always a minimum charging of the ESS $E_{\text{ESS, min}}$ depending on the situational value of P_{grid}. $E_{\text{ESS, min}}$ is shown as

$$E_{\text{ESS, min}} = \frac{P_{\text{grid}}^2}{2\text{RR}_{\text{limit}}}. \tag{4.3}$$

For this reason, the ESS is always kept charged depending on the present situation stated by Equation 4.3. But otherwise, the charging state of the ESS is kept to a minimum. [43, p. 1369]

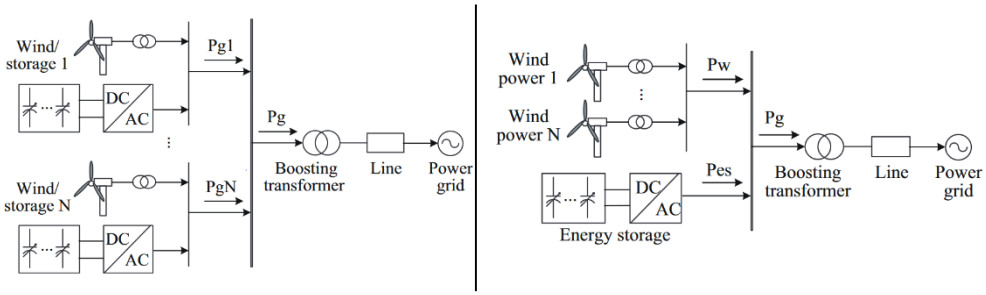

Figure 4.5. *(a) De-centralized (b) centralized topologies of a wind power park [89].*

The other choosing factor with the ESS algorithm is the topology, the physical placement, of an ESS application. The typical topologies presented in this thesis are de-centralized and centralized. The de-centralized topology includes the placement of an ESS application next to a DG unit, as seen in (a) of Figure 4.5. The centralized topology includes the placement of a single, larger capacity ESS application in the grid connection, as seen in (b) of Figure 4.5. The centralized ESS application is usually installed on the primary voltage side of the distribution transformer [72].

The study by Khatib and Sabri [72] focused on the impact of voltage control in a 33/0.4 kV distribution grid with LV PV systems done by two ESS topologies: centralized and de-centralized. De-centralized topology decreased, active 13.43% and reactive 14.49%, power losses more than in the centralized topology, active 4.43% and reactive 2.6%, when compared to the original grid state without an ESS integration to PV systems. The de-centralized topology was found to better support the voltage profile and avoid overloading of the transformer. The de-centralized topology was found to decrease PQ values, like violating the allowed harmonics in the grid, due to having

more PV inverters than in the centralized topology. [72] This thesis uses the de-centralized topology for ESSs in the simulations.

4.3 ESS integrated photovoltaic systems in use

ESS technologies have been in wide use as power control solutions for PV systems for years. ESSs can be installed in PV systems in an electric power grid or the isolated power system to better control the PV output or for other needs. In this part, different ESS-integrated PV systems in use are presented. This is done to better understand the role of ESSs as part of PV systems.

The island of Tilos, Greece has a PV-PHS system that enables continuous and reliable distribution on the island. The island has a single 20 kV undersea power cable to the mainland that is the only connection to the transmission grid. The island with 600 habitats and the peak power demand of 0.92 MW suffers multiple blackouts due to insufficient production to meet high consumption periods during summer. For this reason, the island has the PHS system with the total reservoir volume of 220,000 m^3 and 100 m elevation between the reservoirs to have better power demand response during low PV production periods. The PV-PHS system consists of the PV parks, the pump control station, the hydropower station, the reservoir pools, the auxiliary lead-acid battery storage and the central operation station, as shown in Figure 4.6. Depending on a load demand state, the PV-PHS system charges lead-acid batteries and pumps water in the reservoirs during surplus PV production. PV production is the primary method to cover the load demand of the island. When PV production is insufficient to meet load demand, the pump station draws water from the upper reservoir and the lead-acid battery system to inject power to better meet the load demand. [69, pp. 315–324]

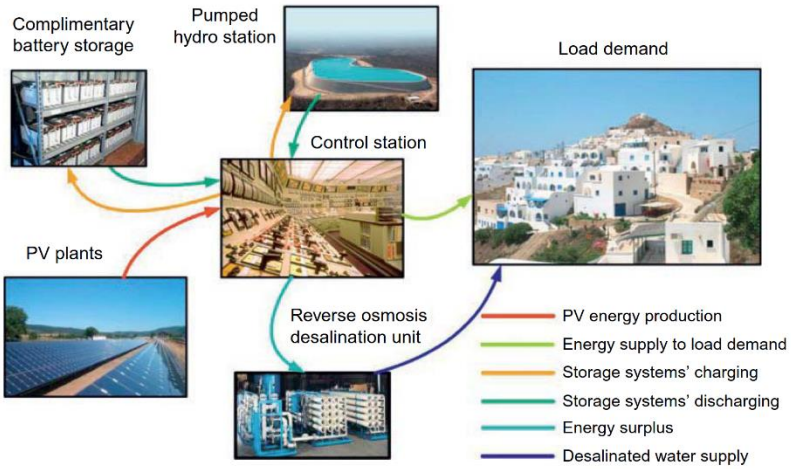

Figure 4.6. *Parts of the PV-PHS system located in the island of Tilos, Greece [69].*

The grid-connected BESS technologies have become an interesting option in the investment market. Rapid solar irradiance changes on PV modules cause extensive changes in injected PV power to the grid. ESS application modes are needed especially for two situations: clear-sky and partly-cloudy days. The ESS smoothens an injected PV power to the grid to avoid grid violations during clear-sky days and rapid power ramps during partly-cloudy days. Large quantities of

power fluctuations are needed to be smoothed when increasing the capacity of the ESS application. [43]

A BESS application located to next of transformer can help to stabilize the safe control [12]. Transformers can have a BESS application installed which helps supply power on the MV side under the full-load situation on the LV grid [88, p. 6216]. The algorithm of a BESS can maximize PV production by shaving peaks during noon with low load situations in residential areas [45, p. 5]. It should be also focused on the importance of the location of a BESS with a PV system in a grid feeder. The study by Uzum et al. [45] confirms this by founding that voltage fluctuations continued with 20% BESS integrated into the grid. This occurred under low PV penetrations and the solution was relocating the BESS downwards of the feeder. [45] The need for disconnecting PV systems during peak production can be decreased with an integrated BESS. A BESS-integrated PV system can limit reverse current flow towards the transformer in the feeder [49]. Verschueren et al. [64] confirm in their study that the PV production in the LV grid could be saved with the BESS application up to half of the otherwise lost energy due to undesirable disconnections of PV systems. The number of PV systems disconnected due to the excess production dropped from 45% to 28% by adding the 9 kWh BESS to every household PV system. [64]

5 SIMULATION METHODS AND DATA

The simulations of this thesis are done to better understand the effects of high PV penetration levels in a typical Finnish distribution grid. These are studied by a simulation model of a suburban area with a short LV feeder in this thesis. The simulation example model consists of 49 apartments between 21 residential buildings that are located in the LV feeder. An aerial view of the simulated area from the south is shown in Figure 5.1. The simulations include only the LV side of the transformer. PV systems are integrated towards the end of the feeder on the rooftops facing south. PV systems are connected to the feeder with 3-phase grid connections. Single-phase grid connections are not available due to a simulation component issue of the simulation program. The impact of PV production is simulated by first satisfying the consumption of residential buildings and injecting excess power into the feeder. This is done by the chosen simulation program of $\mathrm{Matlab}^{\mathrm{TM}}$ Simulink. PV data used in the simulation was measured in the solar PV power research plant located at the Hervanta Campus of Tampere University. ESS data was calculated based on the PV data. The goal is to determine the HC of the feeder and study the effects of ESS applications on increasing the HC. The simulations are simple. The simulations only study the effects of power injection from PV systems into the LV feeder. They do not measure other general factors, like harmonic injections from PV inverters, as mentioned in the earlier chapters.

Figure 5.1. *Aerial view of the simulated suburban area with PV modules on the rooftops facing south.*

The factors of simulation theory and background are discussed in this chapter. First, the solar PV power research plant and the weather measurement instruments in Hervanta Campus are presented. Lastly, the simulation model values are discussed. These consist of the load profiles in the LV feeder and the PV data used in the simulations. The PV data consist of both active and reactive power values during three PV production modes: the PV capacity without an ESS application, the 2 %/min and the 10 %/min $\mathrm{RR}_{\mathrm{limit}}$ of ESS applications. The measurement values

consist of voltages of distribution cabinets, currents of underground cable lines in the LV feeder and voltages of PCCs. The PV capacity was increased until either of these value limits was violated.

5.1 Components of the solar photovoltaic power station research plant

This part is for presenting the layout and the components of the solar PV power station research plant and the measurement instruments of the automated weather station are presented. The PV data used in the simulations are the measured data from the solar PV power research plant located on the rooftop of the Sähkötalo building of Tampere university in Hervanta Campus, Tampere. The research plant has a total of 69 NP190-GKg PV modules with 6 separate strings connecting between 6 to 17 modules in series connection. The total peak power of the plant is 13.1 kW. [14, pp. 2, 7] The STC irradiance is 1000 $\mathrm{W/m^2}$ in Tampere region [43]. Up to 40% of measured global irradiance is diffused irradiance reflected from snow to modules in the research plant during winter [14, p. 5]. The cloud enchantment phenomenon can be seen in affecting the mean irradiance values from the measurement data of the PV string of 23 modules exceeding 1000 $\mathrm{W/m^2}$ on both simulation dates shown in Figures 5.2.15 and 5.2.17. PV modules are placed at the fixed angle of 45° to horizontal rooftop platforms. The backs of PV modules are facing 26° to the east. [14] The PV modules fixed on rooftops facing south with this angle receive at least 80% of the annual solar radiation [63, p. 4769]. The research plant has the automatic weather station for measuring cell temperature, humidity, global and diffused irradiance, wind speed and wind direction. Figure 5.1.1 is the picture of the research plant.

Figure 5.1.1. *Part of the solar PV power research plant of Hervanta Campus at August 2022.*

The research plant has 69 NP190-GKg PV modules manufactured by Naps Systems Oy. The PV module type is a commercial product designed to be part of a grid-connected PV application. The informed power production of a single PV module in the MPP is 190 W. Each PV module has 54 polycrystalline Si-solar cells connected in series and the module is covered in

4mm iron tempered glass. The PV module has 3 bypass diodes, each connected in parallel with 18 cells. [14, p. 2] The electrical performance under STC and dimension values of the NP190-Gkg PV module are shown in Table 5.1.1 where MPP values of the PV module are active power P_{MPP}, voltage U_{MPP} and current I_{MPP}.

Table 5.1.1. *Performance and dimension values of NP190-Gkg module.*

P_{MPP}	190 W
I_{MPP}	7.33 A
U_{MPP}	25.9 V
I_{SC}	8.02 A
U_{OC}	33.1 V
Dimensions (length x width x thickness)	1475mm x 986mm x 35 mm
Weight	19.5 kg

The PV modules are placed on three rooftops as shown in Figure 5.1.2. The height difference between the lower and upper rooftops is between 1–2.6 m, respectively. Also, multiple structures of air-conditioning engine rooms, 5.8 m over to the lowest rooftop, cause partial or even complete shading of the PV modules between different seasons. This has been considered with the placement of the PV strings to decrease the possibility of complete shading. Partial shading conditions due to multiple high structures cause multiple MPPs in the PV strings. [14, p. 2]

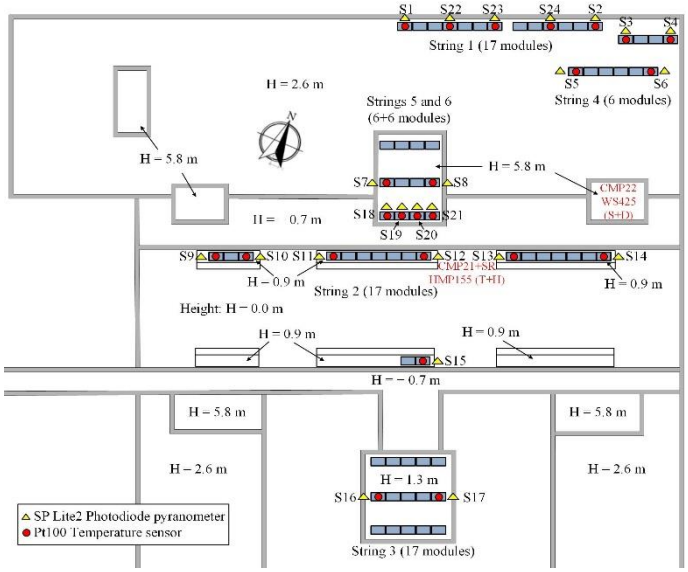

Figure 5.1.2. *Layout of the solar PV power station research plant with the measurement instruments [36].*

Generally, the first and last modules of PV string rows have photodiode-based pyranometers SP Lite 2 (marked S1–S24 in Figure 5.1.2) manufactured by Kipp&Zonen for measuring solar irradiance. The temperature sensors Pt-100-type RTDs (marked with red balls in Figure 5.1.2) are placed behind the PV modules for measuring the operating temperature of modules around the research plant. Having these individual measurement methods of the PV modules enables the possibility to interpolate between production values of strings during partial shading conditions. 4 SP lite 2 sensors are connected on the top of PV modules in Strings 1 and 6 instead on the side as shown in Figure 5.1.3. The SP Lite 2 sensors are marked as yellow triangles and the Pt-100 sensors as red dots in Figure 5.1.2. The SP Lite 2 sensors are mounted and tilted at the same angle as PV modules to gain exact irradiance measurement results. The SP Lite 2 sensors are mounted on the side or the top of PV modules, as shown in Figure 5.1.3. The Pt-100 sensors are installed on the backside of PV modules to measure the operation temperatures of PV modules, as shown in Figure 5.1.4. The sensors have a 3-way wire connection to ensure accuracy and diminish background noises. [32, p. 61]

Figure 5.1.3. *SP Lite 2 sensors mounted on side (left) and the top (right) of PV modules.*

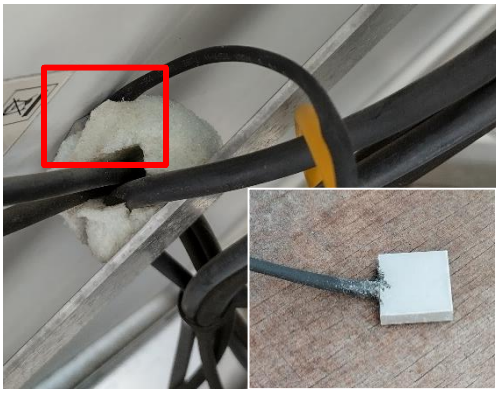

Figure 5.1.4. *Pt-100 sensor inside of the aluminum sink (down-right) and the sink installed on back of the PV module (red box).*

The solar PV power station research plant has the automatic weather station measuring and feeding results of cell temperature, relative humidity, wind speed and direction to the data-acquiring system. The wind speed and direction are measured by the WS425 ultrasonic wind sensor by Vaisala. The WS425 is mounted on top of the weather station poleThe global and diffuse radiation are measured by CMP22 and CMP21 sensors of Kipp&Zonen. The CMP 22

measuring global radiation is mounted on the weather station pole on the rooftop of an air-conditioning engine room. The cell temperature and air humidity are measured by HMP155 sensors by Vaisala. [32] The weather station is located on the rooftop under String 4 and over the right side of String 2 in Figure 5.1.2. The measurement frequency of 10 Hz has been determined to be as sufficient enough for detecting sudden changes in PV production due to shading caused by fast cloud movements [14, p. 3].

5.2 Simulation model

An area picture of buildings in the LV feeder is shown in (a) of Figure 5.2.1. The simulation model has three types of residential, single, 4 and 5 apartment, buildings located in a typical Finnish suburb. The distribution is done by connecting them to distribution cabinets in the LV feeder. The LV feeder is connected to a distribution transformer. The feeder components, cabinets and feeder lines, are shown in (b) of Figure 5.2.1.

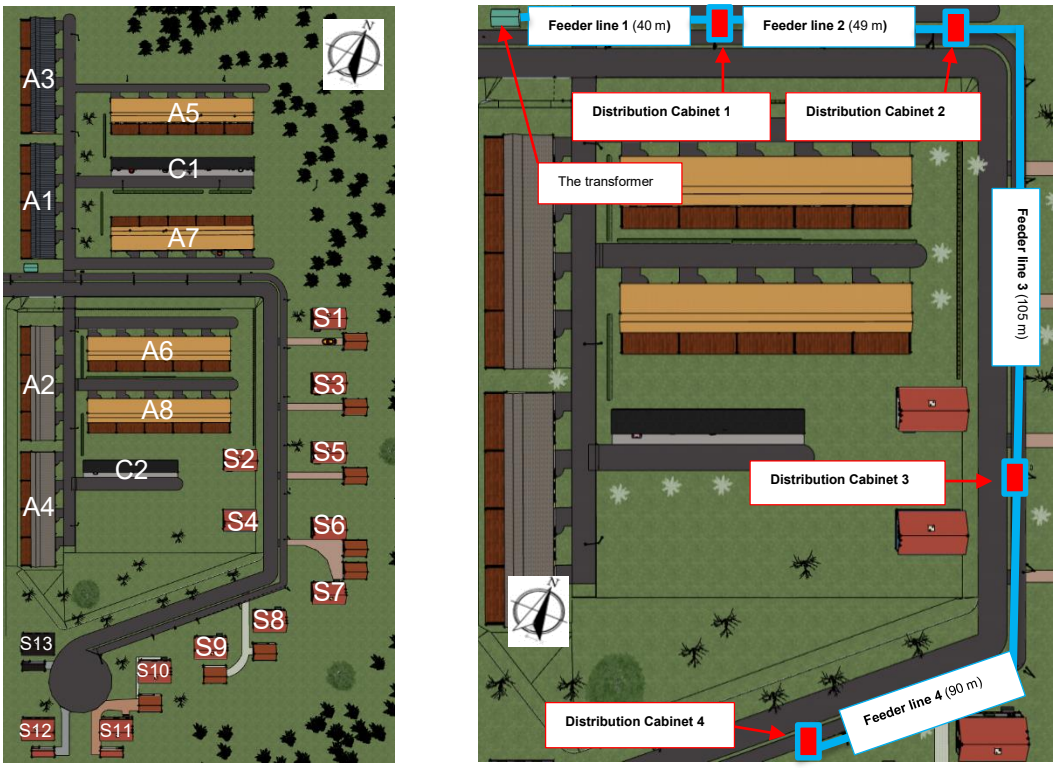

(a) **(b)**

Figure 5.2.1. *Top picture of (a) the suburbian apartments and (b) the grid components of the LV feeder.*

PV modules are placed on the rooftops facing south. The dimensions of the PV module type in the model are the same as the research plant modules listed in Table 5.1.1. Increasing the PV capacity of the feeder is done by multiplying the PV data of the PV string discussed in Chapter 5.2.3. The practical method is adding a group of 23 PV modules on a rooftop and increasing the capacity with groups of 23 PV modules until the available area of rooftops is used. The values of PV strings are just multiplied by the number of groups of 23 PV modules on a

rooftop. The values are not as realistic as possible because the layout of the buildings and the conditions differ from the research plant on the Sähkötalo building. PV modules of residential buildings are fixed on gabled rooftops with small space with the back of modules and rooftops. Only the PV modules on the carports have a similar large volume of air behind PV modules, like modules of the research plant. The apartment and single-house buildings have fixed PV modules in the same 45° angle but modules are installed with little space between modules and the rooftops. This would affect the cell temperatures of the PV modules when rooftops heated by the sunlight radiating heat on modules. Also, shading differs as there are no over 3 stories buildings or other high structures located in the LV feeder. The research plant has more shading periods due to the structures mentioned earlier. All these factors will affect the PV output values but are not taken into account in the simulations.

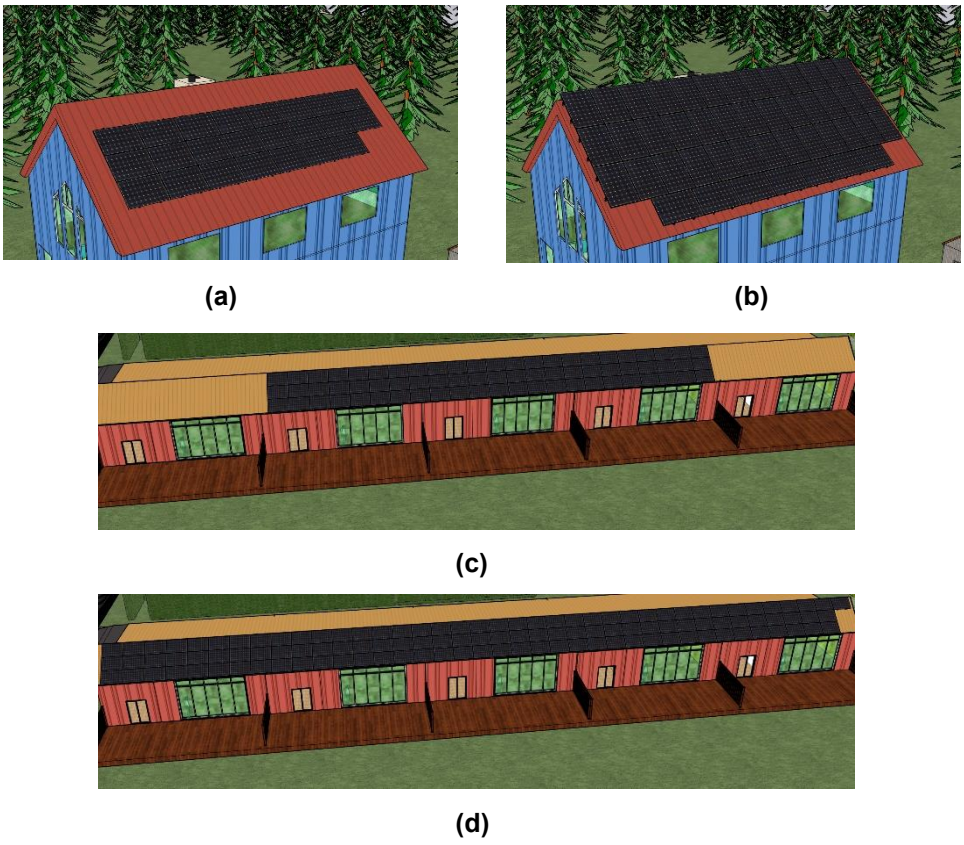

Figure 5.2.2. *Layout of PV modules on the rooftops of a single-household with (a) 23 and (b) 46 PV modules. The rooftop of apartment building with (c) 69 and (d) 115* PV *modules is also demonstrated.*

The first residential buildings in the LV feeder are 4-apartment buildings (A1–A4 in Figure 5.2.1.). These are categorized as only-load profiles without any PV production. Different rooftop layouts of PV modules of are shown in Figure 5.2.2. The households are connected to distribution cabinet 1 which is the closest cabinet to the transformer in the LV feeder. Secondly, down the LV feeder are 5-apartment buildings (A5–A8) aligned from east to west which have load profiles with the availability of PV production on the rooftop up to 115 PV modules. These are marked as buildings 5–8 and have separate carports, C1 and C2, with C1 having the rooftop area capacity for up to 115 PV modules ((b) in Figure 5.2.4.) and C2 having the rooftop area capacity for up to

46 PV modules. The PV production of C2 is connected to the switchboard of the building A8 and the PV production of C1 is shared between the switchboards of buildings A5 and A7. Power losses between a PV system on carport rooftops and grid-connected points of the apartment buildings are assumed to be zero. A5–7 are connected to distribution cabinet 2 and A8 is connected to distribution cabinet 3. Single apartment loads are added together as a load of an apartment building which is considered the total consumption of the single three-phase grid connection in the LV feeder. An individual load profile of an apartment is not as essential as those of single-household buildings.

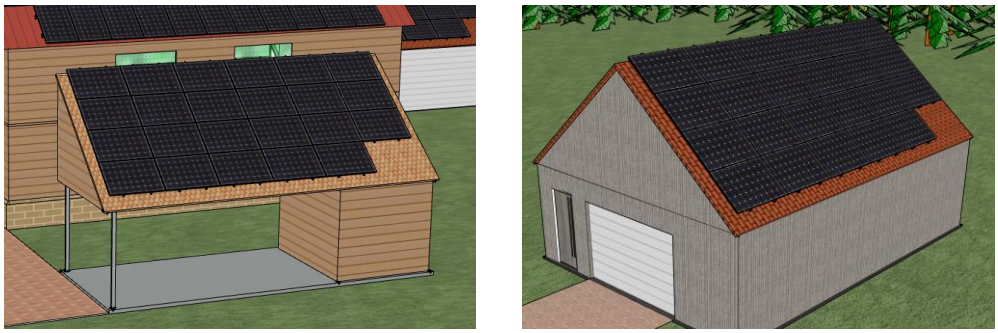

Figure 5.2.3. *Two types of single-household carages with 23 PV modules on rooftops.*

The last building type is 13 single-household buildings (S1–S13 in Figure 5.2.1) and they are located at the end of the LV feeder. These have the capacities of 23, (a) in Figure 5.2.2, and 46, (b) in Figure 5.2.2, PV modules on rooftops. S1, S3 and S5–S13 have separate garage buildings with the capacity of 23 PV modules on rooftops, as shown in the two types of garages in Figure 5.2.3. A single-household building can have up to the capacity of grid-connected PV production from 69 PV modules. S1 and S3 are connected to distribution cabinets 2. S2 and S4–S8 are connected to distribution cabinet 3 and the rest (S9–S13) to distribution cabinet 4. Layouts of carports C1 and C2 with PV module capacities are shown in Figure 5.2.4. Household buildings use two different heating solutions: direct electric and geothermal heating. Single-household buildings S1–S7 use direct electric heating. The apartment buildings (A1–A8) and the single-household buildings S8–S13 use geothermal heating as the major heating solution.

(a) (b)

Figure 5.2.4. *Carport rooftops with the capacities of (a) 46 and (b) 115 PV modules.*

In this part, the simulation methods and data are presented. First, the LV feeder simulations are done by using the model of $\mathrm{Matlab}^{\mathrm{TM}}$ Simulink program. The grid components and operations are presented and discussed. The load profiles of buildings in the LV feeder are presented in the second part. Lastly, the PV data of the research plant is presented in three modes: the PV capacity without an ESS application and with two ESS application mode limits: 2 %/min and 10 %/min $\mathrm{RR}_{\mathrm{limit}}$.

5.2.1 $\mathrm{Matlab}^{\mathrm{TM}}$ SimuLink Model

The simulations were done by the Simulink model. The simulation components are taken from the $Matlab^{TM}$ Library. These components are assumed not to have any power losses. The component used for injecting power values to the LV feeder are the Three-Phase Source-component and the Dynamic Three-Phase Load-component. The Three-Phase Source-component simulated the power flow from the MV grid and the component values were the voltage of 0.4 kV and the frequency of 50 Hz. The generator type was swing.

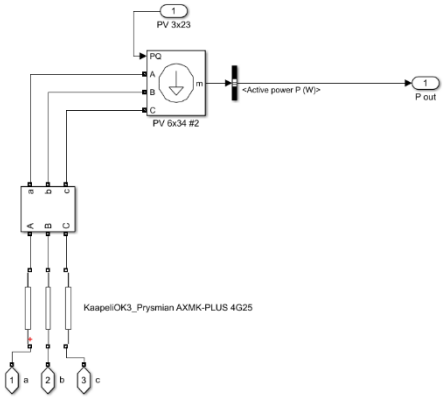

Figure 5.2.5. *Simulink model of the PCC of the single-household building 3 (S3).*

The layout of single-house components is shown in Figure 5.2.5. Residential loads and their PV production were simulated by Dynamic Three-Phase Load-components (PV 6x34 #2 in Figure 5.2.5). The load value (PV 3x23) is already subtracted the load value by a PV value. The component simulates different loads and PV production every second. PV production values subtract the load values and the solution is added as the load in the PCC. When the PV production

is higher than the load, the solution becomes a negative value. This causes the voltage to rise in the PCC. The measurements were done Three-Phase V-I measurement components (the middlebox in Figure 5.2.5).

The simulation model has 25, 4 feeder lines and 21 residential, cable lines from the distribution cabinets to the switchboards. The cable choices and lengths are listed in Table 5.2.1. The feeder line type was Prysmian AXMK-PLUS 4G185 and the residential cable type was Prysmian AXMK-PLUS 4G25. The current limit of underground cable for AXMK-PLUS 4G185 is 330 A and 100 A for AXMK-PLUS 4G25 according to the datasheet of the manufacturer [92]. The information table of the cable types is listed in Table A.1 in Attachments. The operation of the transformer is not included in the simulations and power is fed from the Three-Phase Source-component. A typical distribution transformer in the Finnish grid would have been 20/0.4 kV transformer with varying transformer ratings [3].

Table 5.2.1. *Cable types and lengths of the simulation model.*

Feeder line	Cable type	Length (m)
Feeder line 1	Prysmian AXMK-PLUS 4G185	40
Feeder line 2	Prysmian AXMK-PLUS 4G185	49
Feeder line 3	Prysmian AXMK-PLUS 4G185	105
Feeder line 4	Prysmian AXMK-PLUS 4G185	90
Apartment building cable 1	Prysmian AXMK-PLUS 4G25	30
Apartment building cable 2	Prysmian AXMK-PLUS 4G25	45
Apartment building cable 3	Prysmian AXMK-PLUS 4G25	60
Apartment building cable 4	Prysmian AXMK-PLUS 4G25	60
Apartment building cable 5	Prysmian AXMK-PLUS 4G25	65
Apartment building cable 6	Prysmian AXMK-PLUS 4G25	30
Apartment building cable 7	Prysmian AXMK-PLUS 4G25	10
Apartment building cable 8	Prysmian AXMK-PLUS 4G25	35
Single-household building cable 1	Prysmian AXMK-PLUS 4G25	30
Single-household building cable 2	Prysmian AXMK-PLUS 4G25	20
Single-household building cable 3	Prysmian AXMK-PLUS 4G25	60
Single-household building cable 4	Prysmian AXMK-PLUS 4G25	20
Single-household building cable 5	Prysmian AXMK-PLUS 4G25	20
Single-household building cable 6	Prysmian AXMK-PLUS 4G25	20
Single-household building cable 7	Prysmian AXMK-PLUS 4G25	45
Single-household building cable 8	Prysmian AXMK-PLUS 4G25	35
Single-household building cable 9	Prysmian AXMK-PLUS 4G25	10
Single-household building cable 10	Prysmian AXMK-PLUS 4G25	15
Single-household building cable 11	Prysmian AXMK-PLUS 4G25	50
Single-household building cable 12	Prysmian AXMK-PLUS 4G25	65
Single-household building cable 13	Prysmian AXMK-PLUS 4G25	55

5.2.2 Load profiles

The load profiles of the households used in the simulations are presented in this chapter. The load types were mentioned in Chapter 3.1. Possible wood heating is considered as zero electrical value in the LV feeder. Secondary load types of the simulation model are high-powered residential AC appliances, like ovens and dishwashers, that are used more toward night. Residents arrive from work and school in the afternoons and start preparing food. Occasionally people eat out which does not consume a load for making food. Another high-powered load type is saunas which most Finnish households have. People tend to use a sauna more on weekends but also occasionally during a work week. The load value of saunas is between 6–11 kW between residential households in the simulations. The load profiles consist of two simulation dates: 07.08.2021 and 27.04.2022.

A load is rarely purely resistive in an AC system. General residential and industrial loads in electric power systems are inductive loads [73, p. 470]. An inductive load is the combination of active and inductive reactive load. The relation between an active and reactive load of apartment building 6 is shown in Figure 5.2.6 which shows that the relationship is linear between the two types of household loads. Reactive loads of households are considered and simulated as inductive reactive loads during the simulations. A reactive load can be determined by Equation 3.3 when the value of the active load and PF of the AC circuit or grid are known. ϕ is determined from the PF value and added to Equation 3.3 with a value of the active load. The ideal PF value is between 0.95–1.00 as mentioned earlier. The simulation model used the PF value of 0.96 inductive.

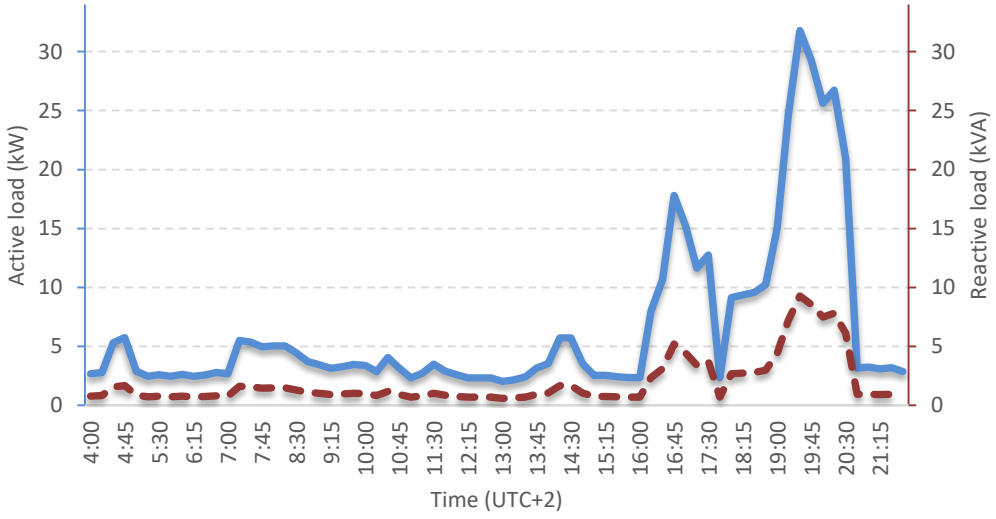

Figure 5.2.6. *Load profile of the apartment building 6 (A6) on 27th April 2022.*

Next, the load profiles of residential households in the simulation model are shown and discussed during two simulation dates. Only active power loads are shown in the following Figures to simplify the presentation of the load profiles. The loads are considered constant for every 15 minutes in the simulations. The load profiles are based on the load data of household types in Finland and values have been randomized to maximize the realistic behavior of the LV feeder

during the simulations. Loads of the 4- and the 5-apartment buildings in the first simulation date 07.08.2021 are shown in Figures 5.2.7 and 5.2.8.

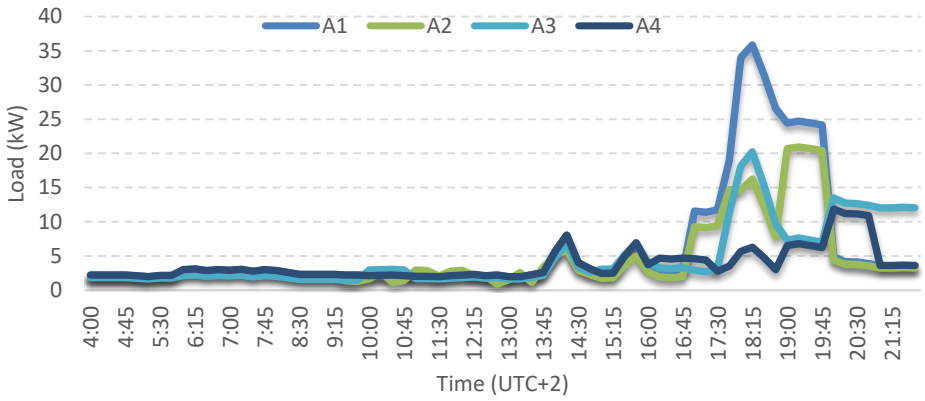

Figure 5.2.7. *Load profile of the 4-apartment buildings (A1–A4) on 7th August 2021.*

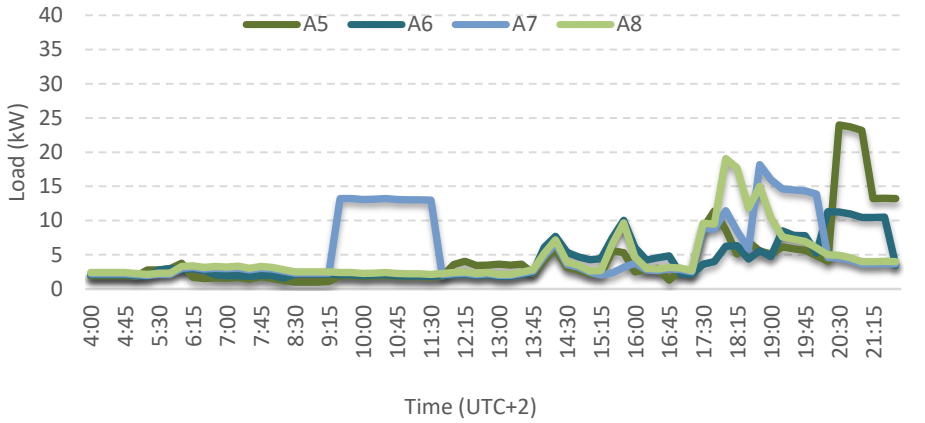

Figure 5.2.8. *Load profile of the 5-apartment buildings (A5–A8) on 7th August 2021.*

Peak loads occur during the night. Multiple apartments heated saunas on Saturday night and the single apartment (A7) decided to heat the sauna on day morning on 7th August 2021 in Figure 5.2.8. The load profiles of apartment buildings during the second stimulation date 27.04.2022 are shown in Figures 5.2.9 and 5.2.10.

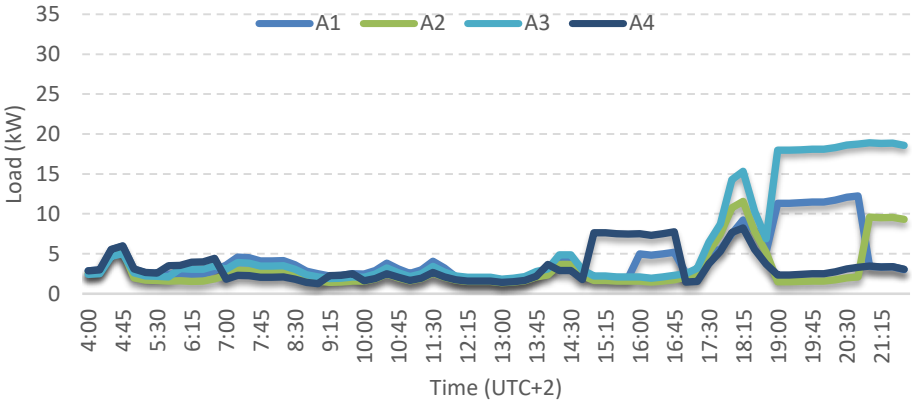

Figure 5.2.9. *Load profile of the 4-apartment buildings on 27th April 2022.*

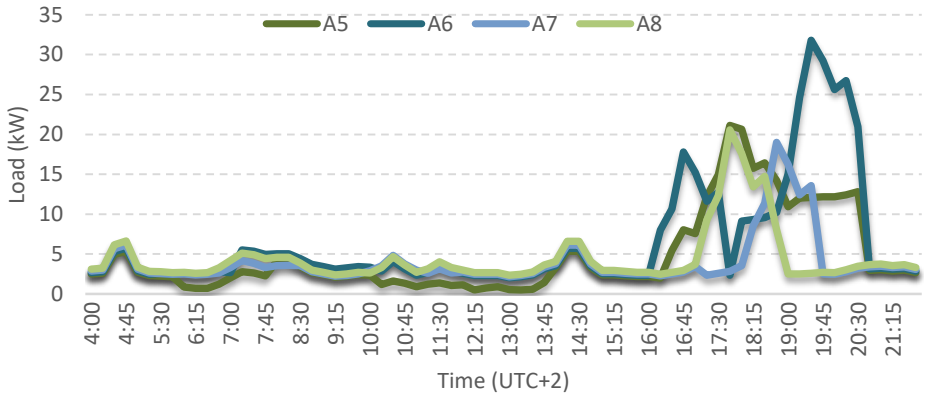

Figure 5.2.10. *Load profile of the 5-apartment buildings on 27th April 2022.*

The load profiles of the second simulation date 27.04.2022 are quite similar to the first simulation date except heating is used more frequently during the nights until the early mornings of spring. Some saunas are also heated, especially shown during the night hours in Figure 5.2.9.

The third type of residential building in the LV feeder is single-household buildings. The load profiles of single-household buildings are naturally smaller sized than apartment buildings and many use direct electric heating as the heating method. This can be seen as peak loads after 21 o'clock in Figures 5.2.11 and 5.2.12.

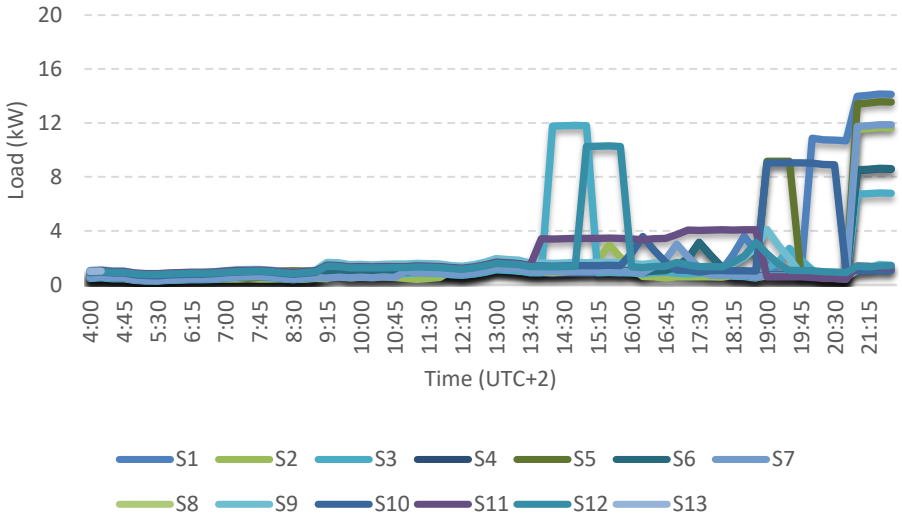

Figure 5.2.11. *Load profile of single-household buildings (S1–S13) on 7th August 2021.*

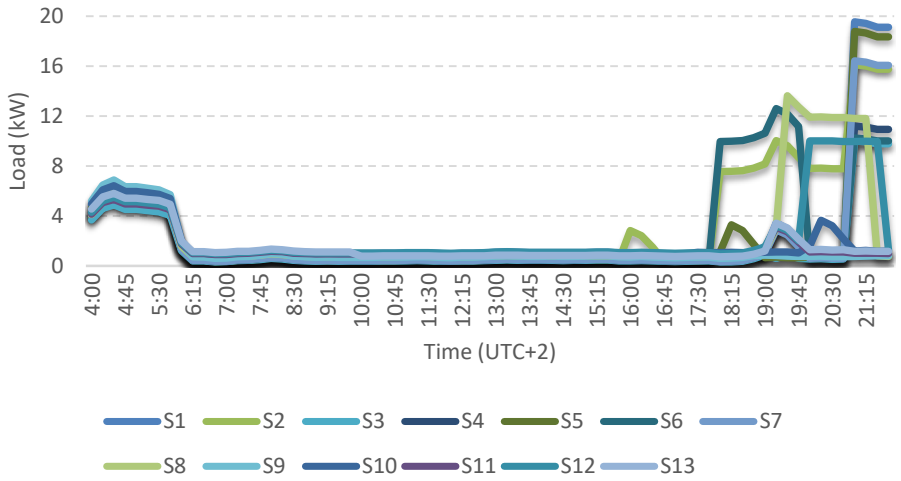

Figure 5.2.12. *Load profile of single-household buildings on 27th April 2022.*

Saunas are turned on and the loads caused by making food occur during the evenings. Two load peaks between 14 and 16 o'clock are caused by saunas in two single-households in Figure 5.2.11. The total load of the LV feeder in the simulation dates is shown in Figure 5.2.13. The load levels rise after 14 o'clock and the largest load occurs at 21 o'clock when the direct electric heating is turned on. The average load of the LV feeder is about 60 kW during the two simulation dates. The peak load under 180 kW occurs at 21 o'clock on 27th April 2022 when the direct electric heating of single-household buildings is turned on. Lower load values around 30 kW occur during the middays and turning on the electrical heating causes rapid rises of loads in the afternoons. The peak load of the feeder is used as the value in defining the value of HC in Chapter 6.3.

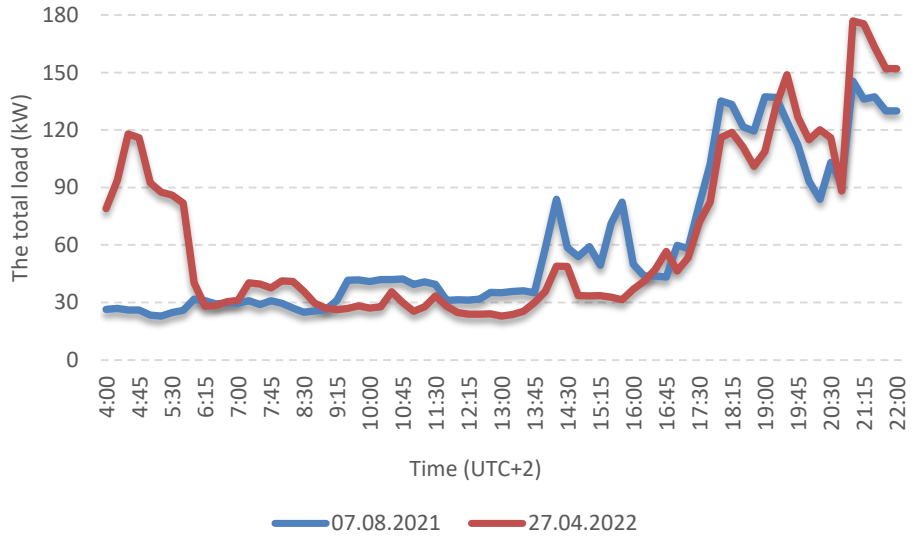

Figure 5.2.13. *Load state of the LV feeder during two simulation dates.*

5.2.3 The photovoltaic simulation data

The simulations use the data of PV production of the solar PV power research plant on the Hervanta campus. The data is measured in a PV system consisting of 23 PV modules with a single series string on the rooftop of the Sähkötalo building. The peak production of the PV string is 4.37 kW. The PV string can have up to 130% of the nominal power due to the cloud enchantment. [43, pp. 1368, 1370] The PV system of 23 PV modules is shown in Figure 5.2.14. The PV modules are located in the northeast corner of the rooftop of the Sähkötalo building as shown in the right-up corner of Figure 5.1.2.

Figure 5.2.14. *Picture and layout (down-right corner) of the 23 PV modules which the measured data is used in this thesis.*

The measured PV data consists only of active power values. To gain more realistic measurement results, the reactive power of PV systems has to be calculated and added to the simulation model. Generally, a PV inverter injects capacitive reactive power q_{PV} to the connected AC circuit or system. The injected reactive power q_{PV} from the grid filter of the PV inverter can be calculated by using

$$q_{\mathrm{PV}} = d_0 + d_1 p_{\mathrm{PV}}. \tag{5.1}$$

The parameters p_{PV} and q_{PV} are the normalized active and reactive power output of the PV inverter. Based on the PF measurements of existing PV inverters, the polynomial coefficients have been determined as $(d_0, d_1) = (7.2 \cdot 10^{-2}, 3.4 \cdot 10^{-2})$. The injected reactive power q_{PV} has scarcely any effect on the stability of the LV grid but can have a greater impact on an inductive grid with large quantities of PV systems. [93, p. 204] The reactive power q_{PV} of the PV inverters have been calculated by using Equation 5.1 and the values have been added to simulation model.

Next, the PV data values are presented and discussed in three different modes: without an ESS application, with the 10 %/min and the 2 %/min $\mathrm{RR}_{\mathrm{limit}}$ of the ESS applications installed in the PV systems. The modes are simulated on two simulation dates. The PV system data from 7th August 2021 are presented in Figures 5.2.15 and 5.2.16.

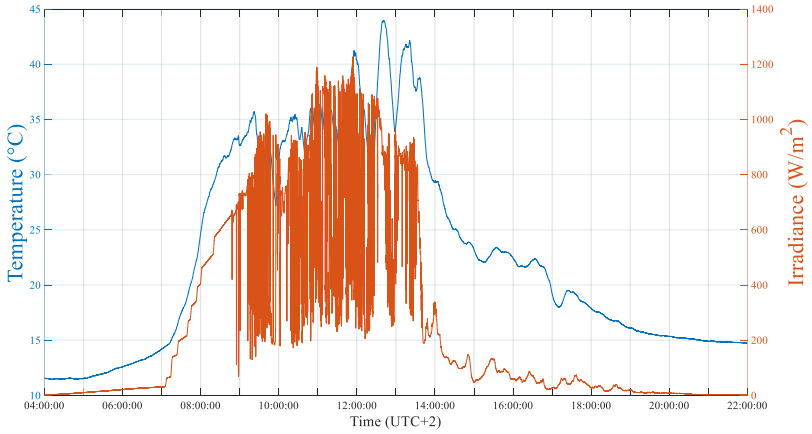

Figure 5.2.15. *Mean temperature and mean irradiance values of the 23 PV module system on 7th August 2021.*

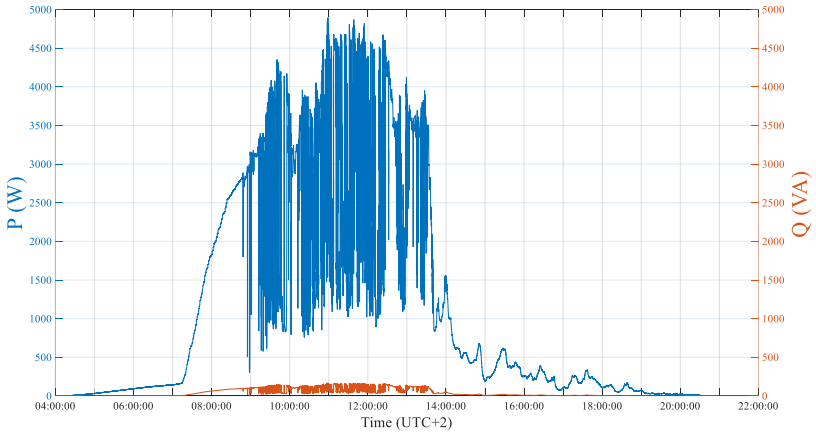

Figure 5.2.16. *PV production of the 23 PV module system on 7th August 2021.*

The mean temperature was determined from the results of the Pt-100 sensors behind the modules and the mean irradiance from the results of the 9 SP Lite 2 sensors (S1–S6 and S22–S24 in Figure 5.1.2) on the top and sides of the modules of Strings 1 and 4. Noticeable is that irradiance is the main factor in the PV production values. The cloud enchantment causes irradiance values to alter greatly between 9 and 14 o'clock.

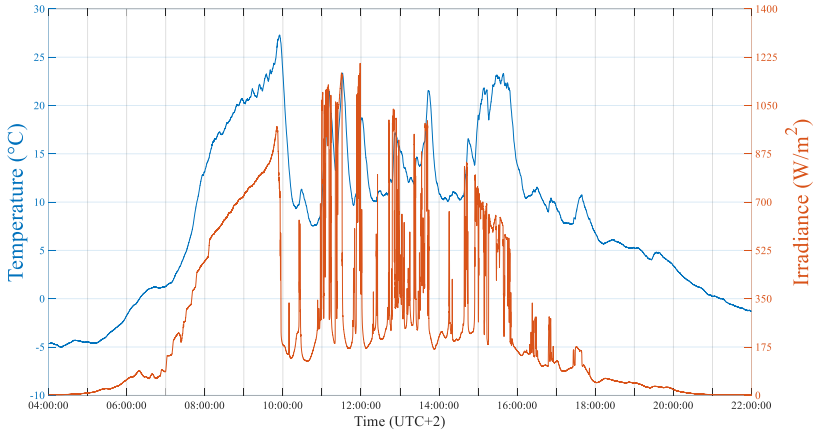

Figure 5.2.17. *Mean temperature and mean irradiance values of the 23 PV module system on 27th April 2022.*

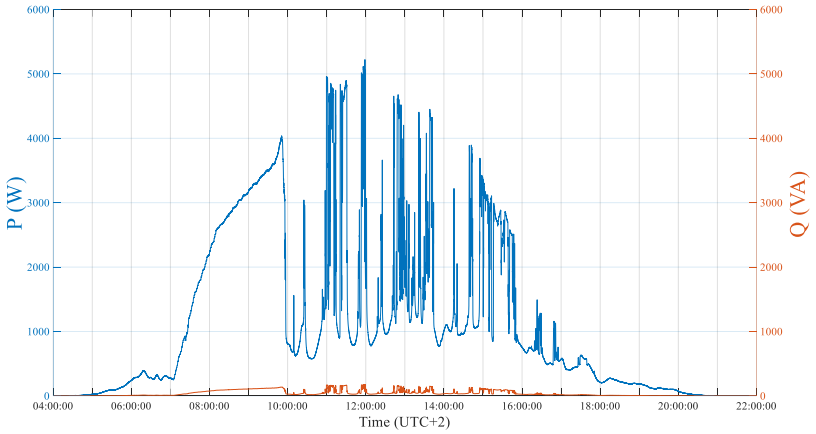

Figure 5.2.18. *PV production of the 23 PV module system on 27th April 2022.*

The PV system data from 27th April 2022 are presented in Figures 5.2.17 and 5.2.18. The PV production is greater on 27th April 2022 when the peak value $p_{\mathrm{PV,\ peak}}$ is over 5 kW and the peak value of August 2021 is only just under that. The greater values over the informed value of 4.4 kWp by the manufacturer are most likely caused due to diffused radiation reflected from clouds. The values have great and rapid changes due to moving clouds over the PV modules from 10 to 17 o'clock afternoon. The average shading period lasts around a minute between the scale from zero to 5–6 hours daily in the Tampere region [36, p. 192]. Noticeable differences in the two measured data are that there are more rapid changes on 7th August 2021 and higher values after 14 o'clock on 27th April 2022 in Figure 5.2.18. Overpassing clouds are the main reason for rapid solar radiation changes which cause fluctuations in PV production. Clouds cause high shading strength to cover the PV modules which can be seen as the low PV production starting around 13:30 o'clock and remaining low for the rest of day on 7th August 2021. The values of 27th April 2022 can be seen to be rising steadily in the morning when there is a clear sky similar to the values on 7th August 2021. Shading of PV modules occurs first after 10 o'clock when the PV production drops instantly from 4 kW to under 1 kW in Figure 5.2.18. The same pattern is seen when clouds cause rapidly changing shading of PV modules for the rest of day. The injected

reactive power of the PV inverter is shown in both figures where the peak values are $q_{\mathrm{PV,\ peak}} = 166.43$ VAr on 7th August 2021 and $q_{\mathrm{PV,\ peak}} = 177.61$ VAr on 27th April 2022.

The second operation mode of the PV system is the installed ESS application with the 10 %/min $\mathrm{RR_{limit}}$ mode. The data values of the 10 %/min $\mathrm{RR_{limit}}$ ESS mode during the two simulation dates are shown in Figures 5.2.19 and 5.2.20.

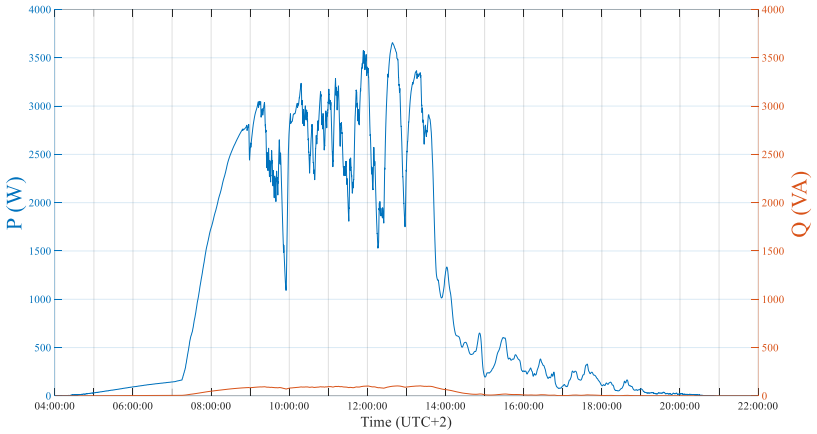

Figure 5.2.19. *Nominal PV production of the 23 PV module system with the 10 %/min RR limit of ESS application on 7th August 2021.*

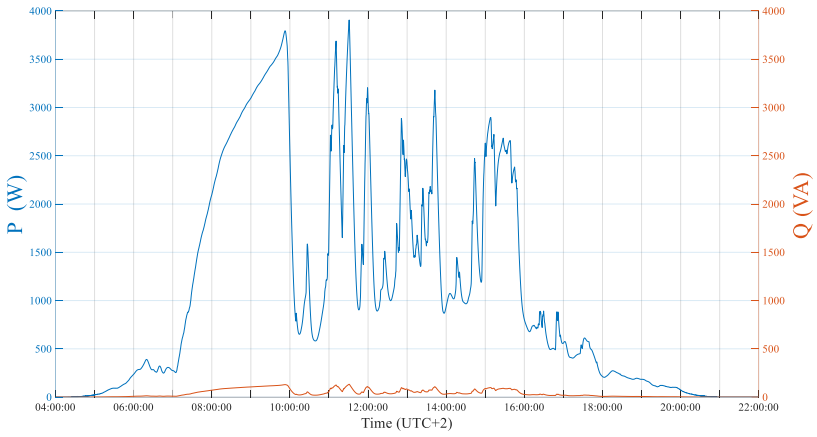

Figure 5.2.20. *Nominal PV production of the 23 PV module system with the 10 %/min RR limit of ESS application on 27th April 2022.*

The most visible changes to the values without the ESS application are rapid changes due to clouds. The data lines of the ESS figures are smoother which makes easier to read values using the gridlines. The injected PV production is also lower as the peak value is just over 3.5 kW in Figure 5.2.19 and under 4 kW in Figure 5.2.20. The injected reactive power of the PV inverter is shown in both figures where the peak values are $q_{\mathrm{PV,\ peak}} = 103.43$ VAr in August 2021 and $q_{\mathrm{PV,\ peak}} = 132.90$ VAr in April 2022.

The last operation mode of PV systems is with the 2 %/min $\mathrm{RR_{limit}}$ mode of the installed ESS application. The data values are shown in Figures 5.2.21 and 5.2.22. The lines are even smoother than in the 10 %/min mode and the peak values are smaller as 3 kW in Figure 5.2.21 and under 3.5 kW in Figure 5.2.22. The injected reactive power of PV inverter is shown in both

figures where the peak values are $q_{\mathrm{PV,\ peak}} = 103.43$ Var on 7th August 2022 and $q_{\mathrm{PV,\ peak}} = 115.97$ Var on 27th April 2022.

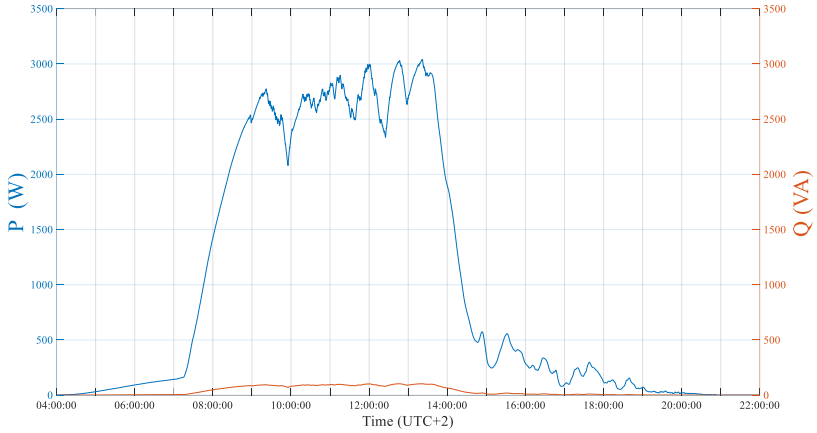

Figure 5.2.21. *Nominal PV production of the 23 PV module system with the 2 %/min RR limit of ESS application on 7th August 2021.*

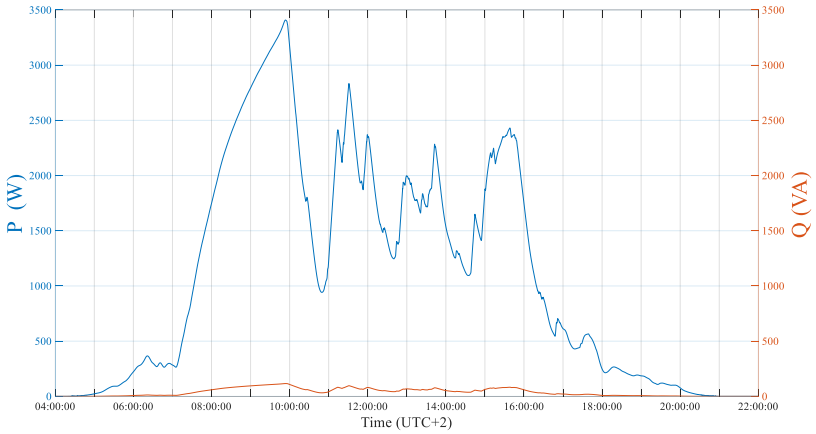

Figure 5.2.22. *Nominal PV production of the 23 PV module system with the 2 %/min RR limit of ESS application on 27th April 2022.*

The data values are added to the simulation model and multiplied depending on locations and a number of the groups of 23 PV modules on the rooftops in the LV feeder. The cloud movement causes shading on the modules to be covered a couple of seconds earlier or later than the PV modules on other buildings. The simulated shading speed is considered as the constant value of 10 m/s towards the east. The wind direction is shown in Figure 5.2.23. The PV systems will have same PV values but depending on the locations of the PV systems, the same PV value can be simulated up to 14 seconds apart when there is 140 m distance between two PV systems, located on buildings A5 and S7, when measured from west to east. A top photo of the residential buildings was taken and a guidance line was added to measure the distances of the PV systems to the line, as shown in Figure 5.2.23. The distance from the guidance line to the center of each PV system was measured. The distances to the guidance line of the PV systems are listed in Figure 5.2.23. Only the PV system on building S12 was on the line, hence their PV systems simulated the same PV data values of the 23 PV module group. Having more realistic timing

determined by locations between PV systems in the LV feeder will have a minor impact on the operation state of the LV feeder but gives more realistic results in the simulations.

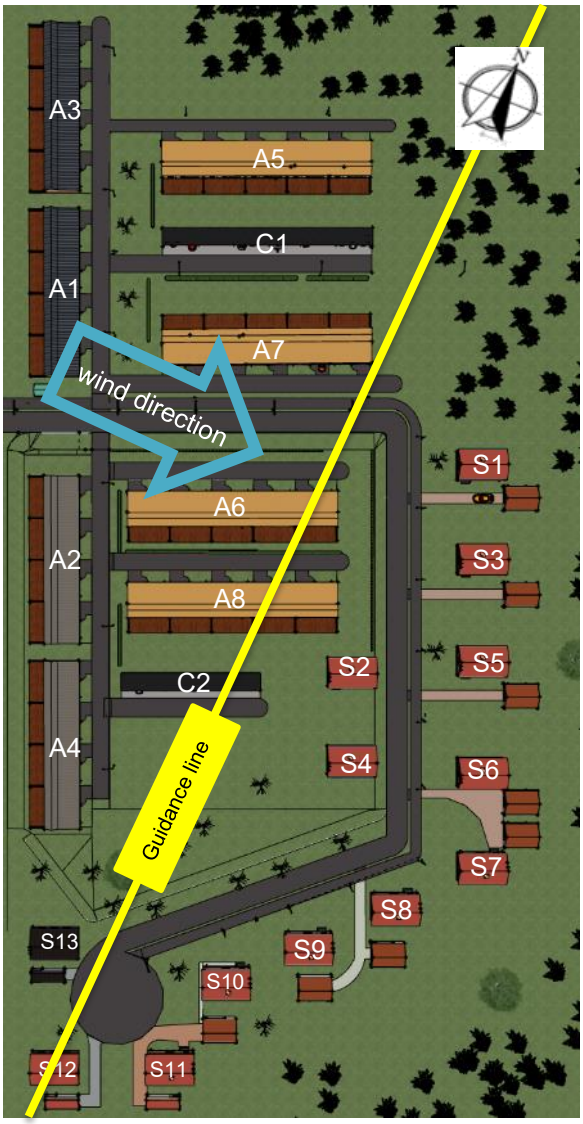

Figure 5.2.23. *Top picture of the residential buildings with the guidance line and wind direction.*

Table 5.2.2. *Distances of PV systems on building and cartop rooftops to the guidance line.*

Building	Distance (m)	Building	Distance (m)	Building	Distance (m)
A5	50	**S4**	45	**S11**	35
A6	15	**S5**	65	**S12**	0
A7	30	**S6**	80	**S13**	15
A8	5	**S7**	90	**C1**	40
S1	45	**S8**	70	**C2**	5
S2	35	**S9**	55		
S3	55	**S10**	40		

6 RESULTS

Installing household PV systems is a new trend and this thesis discusses reasonable limit values for high PV penetration levels, mainly determining HC, in the simulated LV grid. The focus was to integrate rooftop-scaled PV systems starting from the transformer in the LV feeder located in a typical Finnish suburb. The goal was to determine the HC level of the LV feeder. The LV feeder of the simulation case has apartments, single-household building loads and none of the existing power generations before integrating PV systems on the rooftops. The PV production peaks at midday which can lead to RPF as a low load state in the LV feeder. RPF can cause overvoltages in distribution cabinets and thermal damage with high currents in the feeder lines.

The raising of the PV production in the LV feeder is simulated in 17 different PV capacity cases. The first case consists of a single building with a PV system located closest to the transformer, adding a single household PV system along the feeder in the following cases and the 17th case is the PV capacity of the LV feeder. Later on, the same situation cases are simulated with two ESS application modes installed in the PV systems. This is done to study the level achieved by an ESS application as voltage control and a grid stability tool.

In the first part, the base case without any PV production in the LV feeder is discussed. This is done to discuss the normal gird operations and effects of different residential loads in the LV feeder. Next, the results of three PV capacity cases are presented and discussed. PV capacity cases are categorized depending on three different situations of residential interests with a raising number of integrated rooftop-scaled PV systems in the LV feeder. This part discusses raising PV production by adding more PV modules on the rooftops of household buildings and garages. This is done until the grid limitations are violated. The reference value of an overvoltage limit in the LV feeder is +5% U_N of American Standard ANSI C84.1 due to the expansive usage in literature. Another factor is to ensure that the current capacities of underground cables are not violated. Thirdly, the results of using the ESS modes of 2 %/min and 10 %/min RR limits are discussed. The end of Chapter 6 discusses the total HC of the PV capacity and ESS application modes.

6.1 Base case without photovoltaic production

The base case is the state of the LV feeder without PV production. There are not any power generators in the LV feeder before the simulations and power demand is accommodated by feeding power from the MV grid. This is a simple distribution feeder focusing on distributing power to the heating of households and other loads in the LV feeder. Firstly, we must understand how the load profiles of households affect the LV feeder during the two simulation dates. In general, the LV feeder has large loads at night and less demand during the daytime.

The first simulation on 7th August 2021 is a late summer day when evenings are getting colder. The voltage and current levels on the first simulation date are shown in Figure 6.1.1. The loads are considered to be constant every 15 minutes as mentioned earlier. The lowest voltage 389 V is in the distribution cabinet 4, the highest voltage 399 V is in the distribution cabinet 1 and the largest current 212 A occurs in feeder line 1. But none of the grid limits are violated.

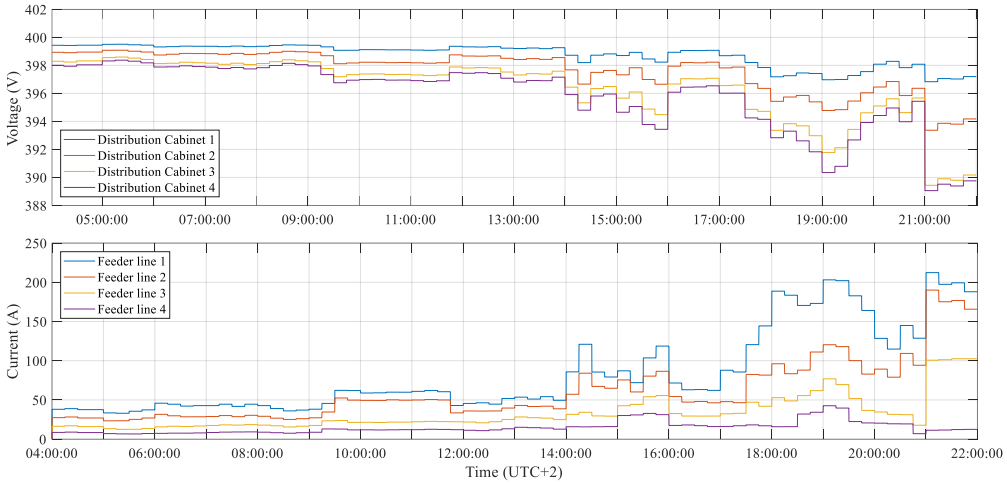

Figure 6.1.1. *Voltage and current levels of the LV feeder without PV production on 7th August 2021.*

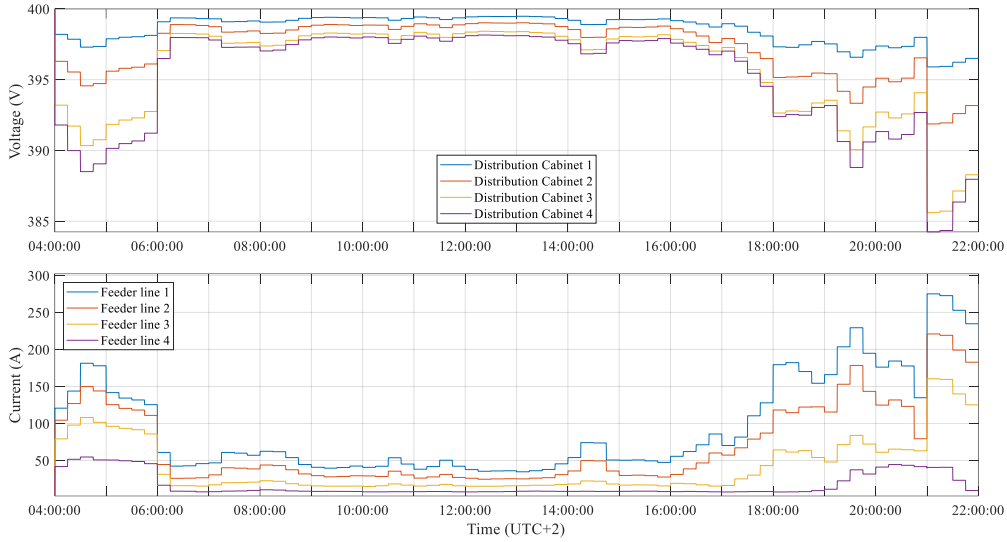

Figure 6.1.2. *Voltage and current levels of the LV feeder without PV production on 27th April 2022.*

The second simulation date 27.04.2022 is the spring day. Nights are usually cold after winter, as shown in Figure 5.2.17, and can drop under freezing temperatures. Direct electric heating is turned on for the night, kept on until the morning and is usually turned down during the day. The voltage and current values on 27th April 2022 are shown in Figure 6.1.2. Direct electric heating is turned on during the night which can be seen in lower voltages in the cabinets and higher currents in the feeder lines. The heating is turned off after 6 o'clock and the demand stays low

during the daytime. The load demand rises towards the night and direct electric heating is turned on at 21 o'clock, like on the other studied day. The demand is higher and feeder line 1 has the highest measured current value 275 A which is 83% of the rated current of the underground cable type. The lowest voltage is in the distribution cabinet 4 with 384 V and the highest voltage 399 V is in the distribution cabinet 1. But like in the other simulation date, no grid violations are recorded.

6.2 PV capacity cases

Major factors in the effects of high PV penetration levels in the distribution grid is the level of existing PV capacity and consumption of the grid. Even a few small-scale PV systems cause grid violations in the connected grid but a PV production under HC of the grid region or feeder will not cause a need for grid and control tools investment in stabilizing the grid operations as generally mentioned in the literature. But the quantity of PV modules on rooftops has only the theoretical limit of rooftop area. In the future, the demand for household PV systems in the distribution grid can explode and cause grid violations without appropriate solutions.

In this part, the level of PV capacity is raised in three simulation cases until grid violations are caused in the LV feeder. The role and effects of ESS applications and the RR control strategy are used in the later simulations to see if they can help in avoiding grid violations in the LV feeder with the PV capacity causing them in Case 3.

6.2.1 Medium-scale PV capacity in Case 1

Case 1 is a subtle simulation case where most buildings in the LV feeder have a medium-sized PV production. This case considers the situation where residents have installed a pair of dozen PV modules to test if the PV system can improve their power demand situations. The LV feeder has the total number of 575 PV modules in Case 1. Apartment buildings A5–A8 have 69 modules each on the rooftops facing south. The apartment building PV systems consist of three groups of 23 PV modules. The total capacity of apartment buildings is 276 PV modules. The single-household buildings S1–S13 have 23 PV modules on the rooftops facing south. The total PV capacity of single households is 299 PV modules. The PV production of the LV feeder during two simulation dates is shown in Figure 6.2.1. The injected reactive power of the PV inverters has been left out of Figures 6.2.1, 6.2.4, 6.2.7, 6.2.10 and 6.2.13 due to their low values when compared to the active power of the PV systems. But reactive power injected by PV inverters is used in the simulations.

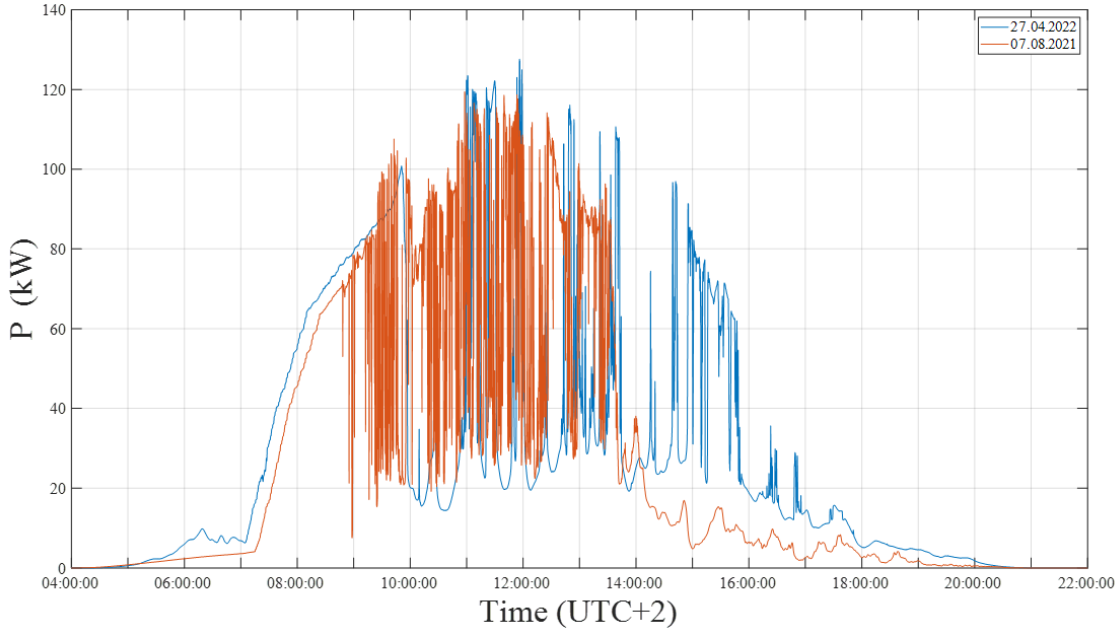

Figure 6.2.1. *PV production of the LV feeder in Case 1 during the two simulation dates.*

The total PV production of the LV feeder is over 110 kW on both dates. The peak values are 119 kW in August 2021 and 127 kW in April 2022. Notable is that the PV production is greater in the afternoon in April 2022 than in August 2021. This is due to more cloudy weather causing shading of PV modules on 7th August 2021, as mentioned earlier in Chapter 5.2.3. The voltages and current values of the LV feeder on 7th August 2021 are shown in Figure 6.2.2. The highest voltage 407 V between cabinets is in the distribution cabinet 4 and the currents due to RPF are peaking at only 41% of the rated current of the feeder lines. There are no voltage violations in the household switchboards with the highest voltage 408 V in the switchboard of S12. The residential cable currents peak during the night when the direct electric heating is turned on.

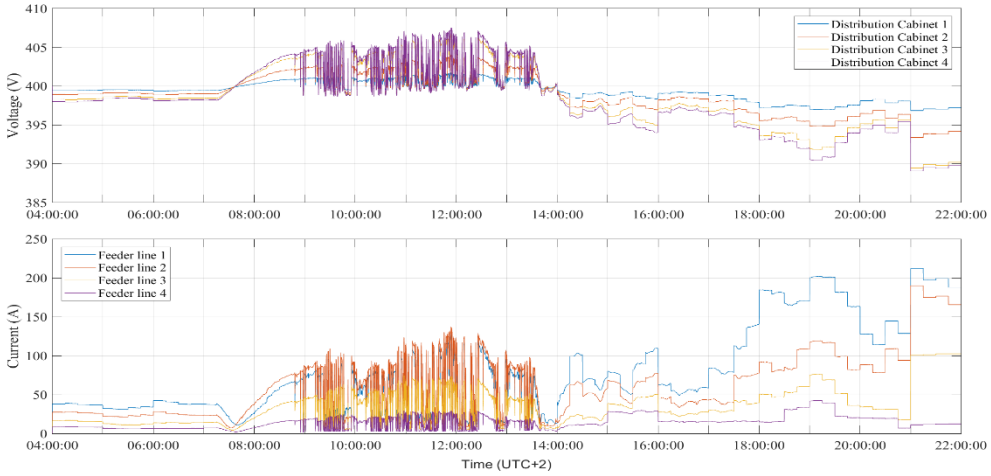

Figure 6.2.2. *Voltage and current levels of the LV feeder in Case 1 on 7th August 2021.*

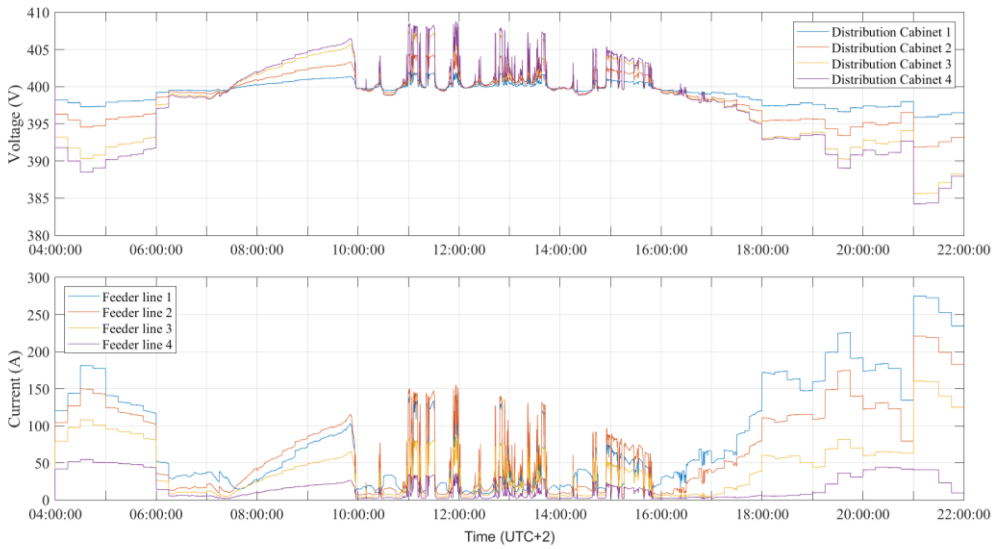

Figure 6.2.3. *Voltage and current levels of the LV feeder in Case 1 on 27th April 2022.*

The simulation results are similar on 27th April 2022 to the other simulation date as shown in Figure 6.2.3. The highest voltage 408 V between cabinets is in the distribution cabinet 4 and the currents due to RPF are peaking at only 47% of the rated current of the feeder lines. There are no grid violations. The results in Case 1 show that small-sized PV systems have not caused any grid violations or thermal damages to the grid components. The voltage levels stay under +2.5% U_N and current values of RPF are under the currents caused by direct electric heating later in the evening. There are no voltage violations in the household switchboards. The highest voltage 409 V is in the switchboard of S12. The currents of residential cables peak during the night when the direct electric heating is turned on, like during the other simulation date. Multiple household loads in the LV feeder can compensate for the high PV penetration levels that decrease the probability of grid violations. The phase voltages rise after 16 o'clock towards the end of the LV feeder but the length of the feeder is limited to cause any overvoltage violations. There are no grid violations in Case 1 during the two simulation dates.

6.2.2 Large-scale PV capacity in Case 2

Case 2 studies the increased PV production in the LV feeder after Case 1. Case 2 simulates the situation where residents have installed more PV modules in their existing PV systems to increase their PV production either to better match their load demands, sell more PV production in the electrical stock market or both. The LV feeder has the total number of 920 PV modules in Case 2. The PV system of the apartment building A5 has 161 modules on the rooftops of the building (115 PV modules) and the garage (46 PV modules). Apartment buildings A6–A8 have 115 PV modules on the rooftops facing south. The single-households S1, S3, S5 and S11–S13 have 46 PV modules on the rooftops of the building and the garage facing south. The single-households S2, S4 and S6–S10 have 23 PV modules on the rooftops facing south. The PV production of the two simulation dates is shown in Figure 6.2.4.

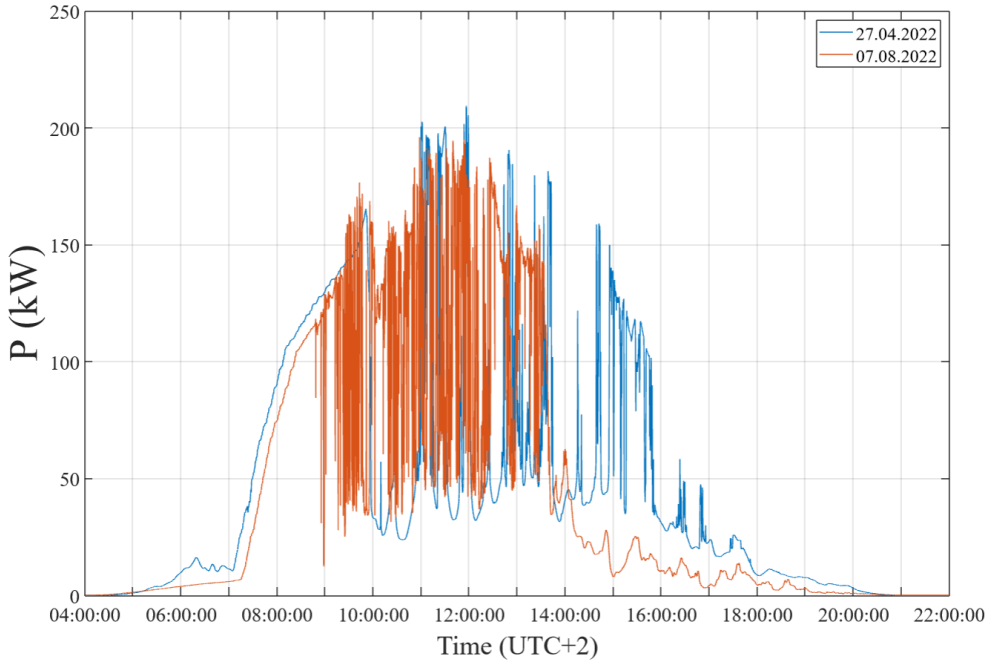

Figure 6.2.4. *PV capacity in Case 2 during the two simulations dates.*

The increased PV production has the peak values over 190 kW. The peak active power value is 195 kW on 7th August 2021 and 209 kW on 27th April 2022, respectively. This causes higher voltages and RPF in the LV feeder on 7th August 2021 as shown in Figure 6.2.5.

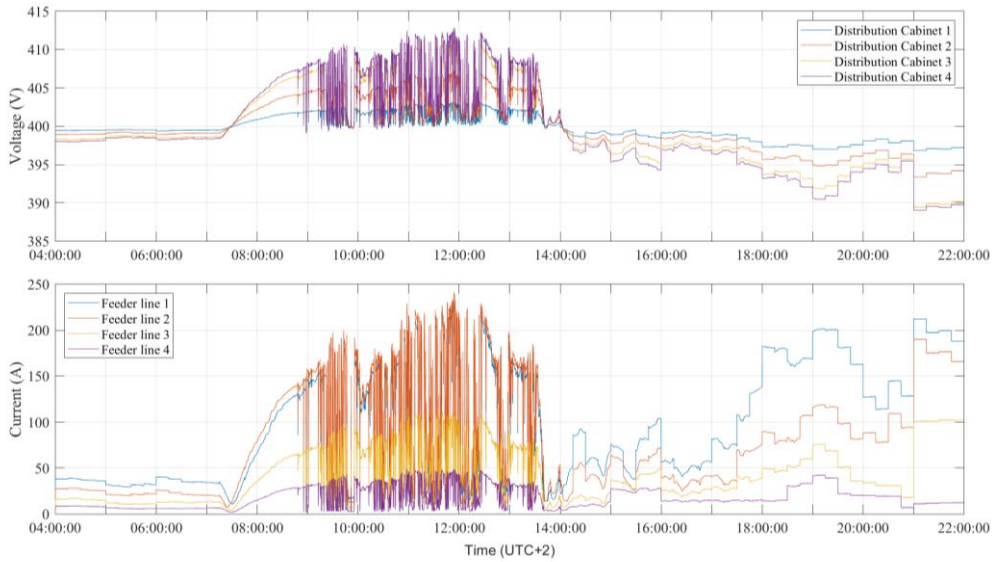

Figure 6.2.5. *Voltage and current levels of the LV feeder in Case 2 on 7th August 2021.*

The highest voltage is in distribution cabinet 4, like in earlier cases, with the peak voltage 412 V between cabinets and the peak RPF current is 73% of the rated current of the cable type in the feeder line 2. There are no voltage violations in the household switchboards with the highest voltage 414 V in the switchboard of S12. The peak RPF currents are higher than the current flow of direct electric heating on the same day. But there are no grid violations.

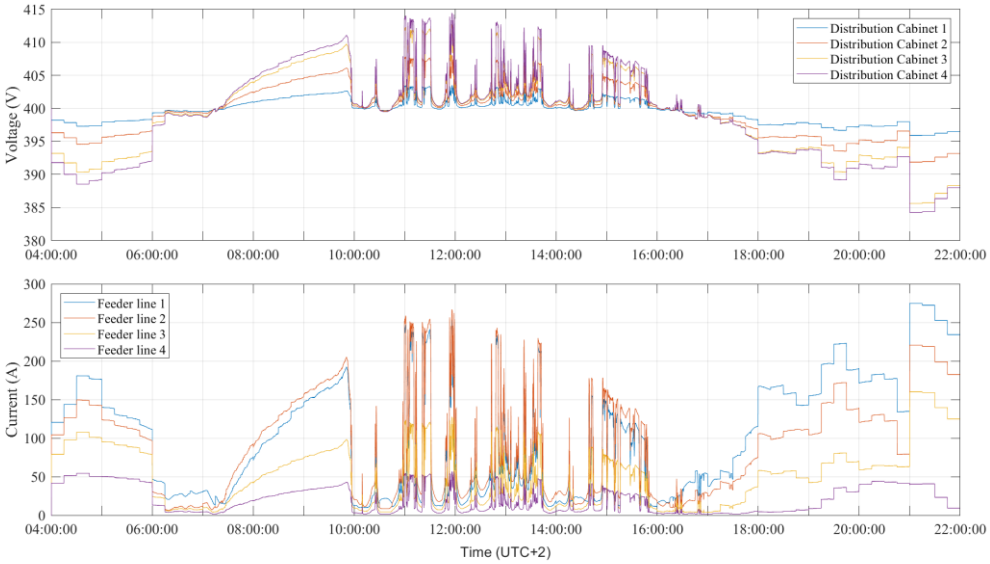

Figure 6.2.6. *Voltage and current levels of the LV feeder in Case 2 on 27th April 2022.*

The increased PV production has similar effects on the grid values on 27th April 2022 when compared to the other simulation day. The voltage and current values are shown in Figure 6.2.6. The peak voltage 414 V between cabinets is measured in distribution cabinet 4 and the peak RPF currents are 81% of the rated current of the cable type. There are no voltage violations in the household switchboards with the highest voltage 416 V in the switchboard of S12. The currents of residential cables peak during the night when the direct electric heating is turned on, like in Case 1. The peak RPF current values are similar to current values caused by direct electrical heating in the evening but higher than in the morning.

Having higher PV production in Case 2 did not cause any grid code violations in the two simulation dates. There are still multiple loads in the LV feeder to consume PV production. But the level of PV capacity has been increased closely under the level of HC which above RPF will cause grid violations.

6.2.3 Grid violations caused by high PV penetrations in Case 3

Case 3 is the situation where the PV production in the LV feeder is increased surpassing the HC level. Case 3 simulates a situation where the owners of PV systems and the DSO ignore the effects of high PV penetration levels in the LV feeder during midday while the consumption is low. This causes damage to the grid components. The LV feeder has the total number of 1357 PV modules in Case 3. Apartment building A6 has 115 PV modules on the rooftop facing south. The PV system consists of five groups of 23 PV modules. PV systems of apartment buildings A5 and A8 have 161 PV modules on the rooftops of buildings (115 PV modules) and garages (46 PV modules). Both PV systems consist of seven groups of 23 PV modules. Apartment building A7 has 184 PV modules on the rooftops of the building (115 PV modules) and the garage (69 PV modules) facing south. The PV system consists of eight groups of 23 PV modules. The single-household buildings S1, S3, S5, S6 and S10–S13 have 69 PV modules on the rooftops of the building (46 PV modules) and the garage (23 PV modules). The PV systems have three groups

of 23 PV modules. The single-household buildings S2, S4, S8 and S9 have 46 PV modules on the rooftops facing south. These PV systems have two groups of 23 PV modules. The PV production of the two simulation dates is shown in Figure 6.2.7. The peak value is 296 kW on 7th August 2021 and 315 kW on 27th April 2022. The grid violations caused by high PV penetrations on 7th August 2021 are shown in Figure 6.2.8.

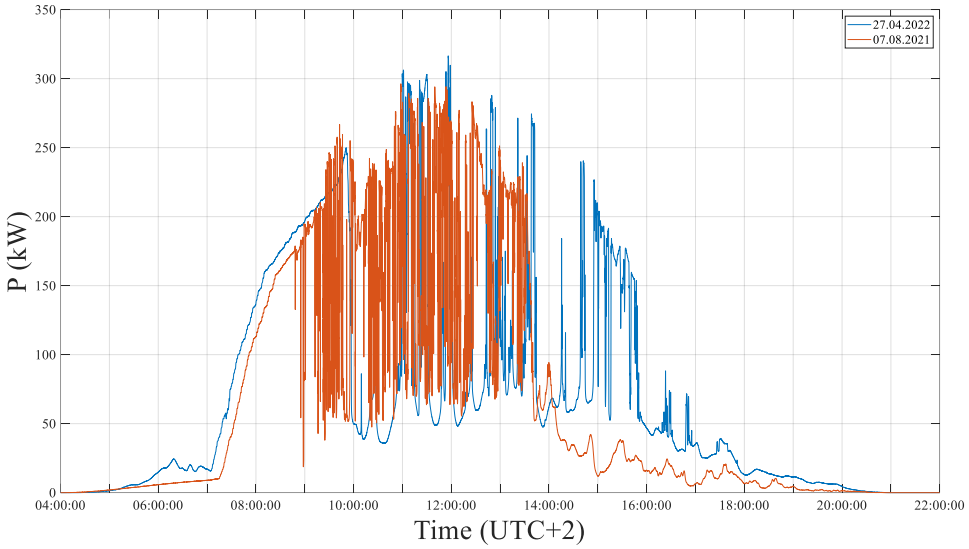

Figure 6.2.7. *PV production of Case 3 in the LV feeder during the two simulation dates.*

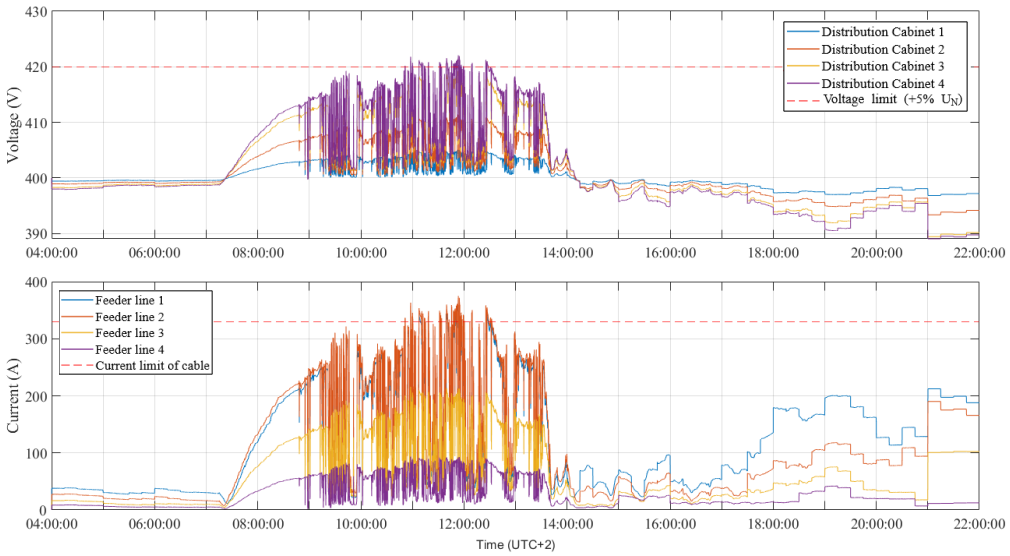

Figure 6.2.8. *Voltage and current levels of the LV feeder in Case 3 on 7th August 2021.*

The voltage limit of +5% U_N (420 V) and the current limit of underground cables is violated multiple times on 7th August 2021. The grid violation lines are marked as the dotted red lines in Figures 6.2.8 and 6.2.9. There are also multiple voltage violations in the household switchboards. Over 420 V voltages occur in the switchboards of residential buildings S5–S13 with the highest voltage of 425 V in the switchboard of S12. There are no current limit violations of residential cables during peak PV production on either of the simulation dates. The RPF currents are violating the current rating of feeder lines 1 and 2 with a peak of 113% of the rated current of the cables. The voltage of distribution cabinet 4 exceeds the voltage limit multiple times. A voltage control solution is needed to avoid grid violations and thermal damage in the feeder cables.

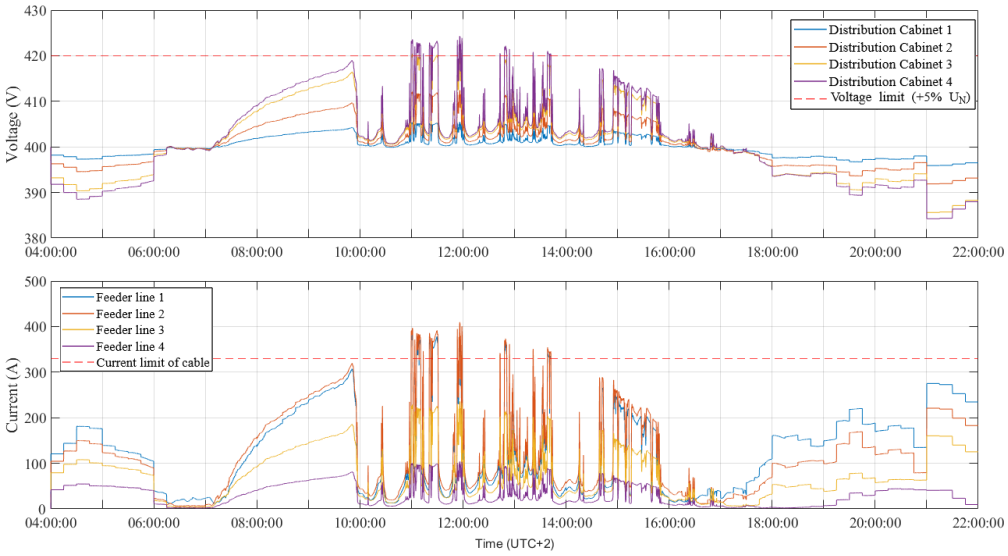

Figure 6.2.9. *Voltage and current levels of the LV feeder in Case 3 on 27th April 2022.*

The results of Case 3 show that grid violations occurred also on 27th April 2022, as shown in Figure 6.2.9. The overvoltages and the peak RPF currents violate grid codes multiple times between 11–14 o'clock. There is also multiple voltage violations in the household switchboards. Over 420 V voltages occur in the switchboards of residential buildings A5, S2 and S4–S13 with the highest voltage 427 V in the switchboards of S12 and S13. There are no current limit violations of residential cables during the peak PV production, like the other simulation date. The overvoltages occur in the distribution cabinets 3 and 4. The peak RPF current is 124% of the rated current of cables. Case 3 shows that grid violations occur during high PV penetration levels and balancing in injecting PV production to the grid is needed. The LV feeder cannot sustain RPF values without grid violations. Using APC solutions is not profitable from the point of view of PV production because a portion of peak PV production is lost. The ESS application can be an alternative solution for stabilizing the grid operations and maximizing PV production simultaneously.

One solution for avoiding grid violations due to RPF in the LV feeder is installing ESS applications in the PV systems. The main task of ESS is to store PV production. This effectively helps to avoid grid violations. The ESSs will keep P_{grid} of the PV systems injected into the feeder under the safe limit by the $\mathrm{RR}_{\mathrm{limit}}$ values. The ESSs are mostly at a minimal charge during the morning and the night. The PV systems have two ESS modes: the 2 %/min and the 10 %/min

$\mathrm{RR}_{\mathrm{limit}}$ of $P_{\mathrm{grid,\ max}}$. The function of ESS has been simulated as lowering injected PV production to the LV feeder on the two simulation dates of Case 3 from the earlier simulations. The PV production of the LV feeder without an ESS application and with two ESS RR limit modes is shown in Figure 6.2.10. The HC levels are smaller when PV systems with ESSs. The 2 %/min $\mathrm{RR}_{\mathrm{limit}}$ mode is more effective in storing PV production as the peak PV production is 191 kW when compared to 226 kW in the 10 %/min $\mathrm{RR}_{\mathrm{limit}}$ mode.

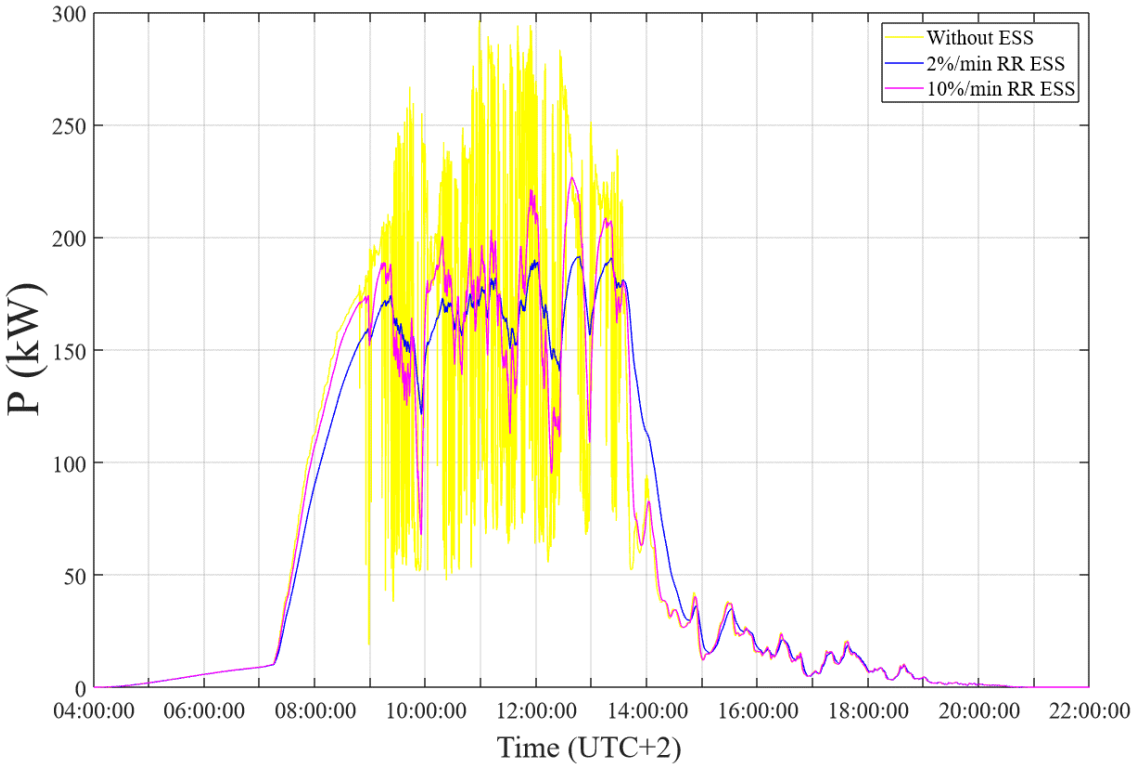

Figure 6.2.10. *Differences of the PV production of the LV feeder in Case 3 without an ESS application and with two RR ESS application modes of PV systems on 7th August 2021.*

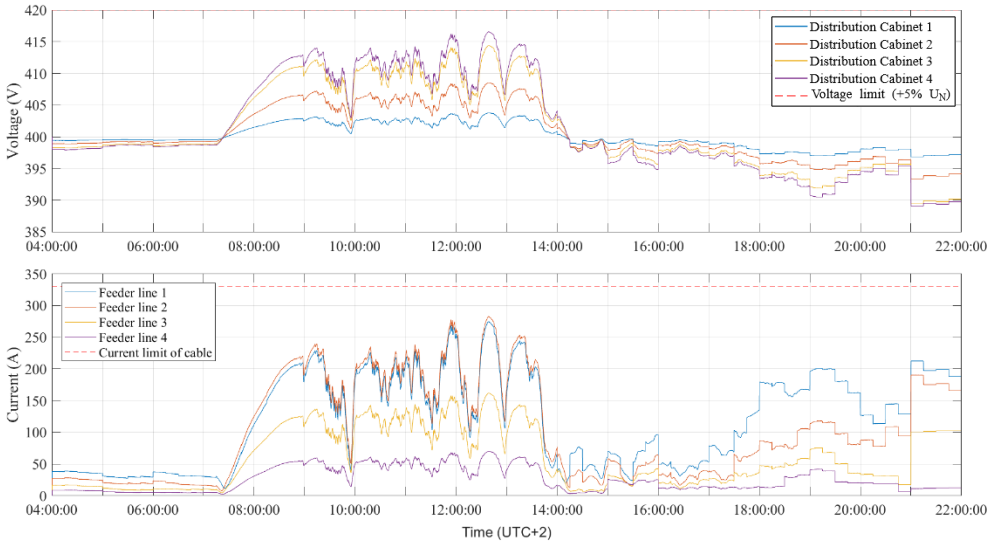

Figure 6.2.11. *Voltage and current levels of the LV feeder during the PV production of Case 3 with the 10 %/min RR limit ESS application on 7th August 2021.*

The voltages and currents with the 10 %/min $\mathrm{RR}_{\mathrm{limit}}$ ESS application on the same simulation date is shown in Figure 6.2.11. The voltage of distribution cabinet 4 is peaking at 413 V and the peak currents of feeder lines 1 and 2 are around the same values with direct electric heating later at night. There are no voltage violations in the household switchboards with the highest voltages of 418 V in the switchboards of S12 and S13. The currents of residential cables peak during the night when the direct electric heating is turned on during both simulation dates, like during previous cases. The voltage and current values of the LV feeder with the use of the 2 %/min $\mathrm{RR}_{\mathrm{limit}}$ ESS application on 7th August 2021 are shown in Figure 6.2.12. There are no voltage violations in the household switchboards with the highest voltages of 415 V in the switchboards of S12 and S13.

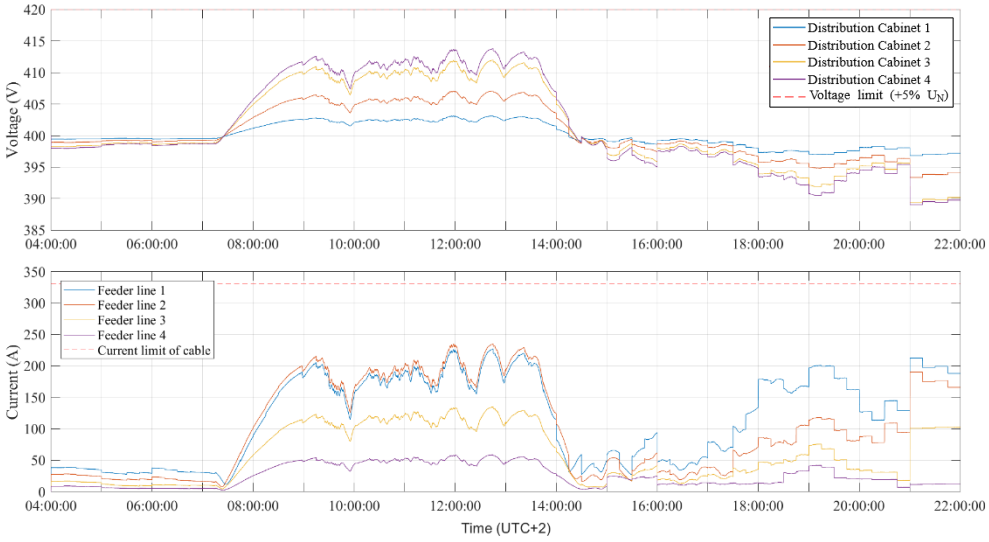

Figure 6.2.12. *Voltage and current levels of the LV feeder during the PV production of Case 3 with the 2 %/min RR limit ESS application mode on 7th August 2021.*

The effectiveness of the ESS modes is confirmed and they maximize PV production without grid violations. The results are similar to the 2 %/min $\mathrm{RR}_{\mathrm{limit}}$ mode. The higher PV production in April 2022 raises grid values but no grid violations occur. The peak voltage is 416 V in the distribution cabinet 4 and the peak RPF currents in feeder lines 1 and 2 are about 83–85% of the rated current of the cables. Both ESS modes effectively stabilize the grid values on 7th August 2021.

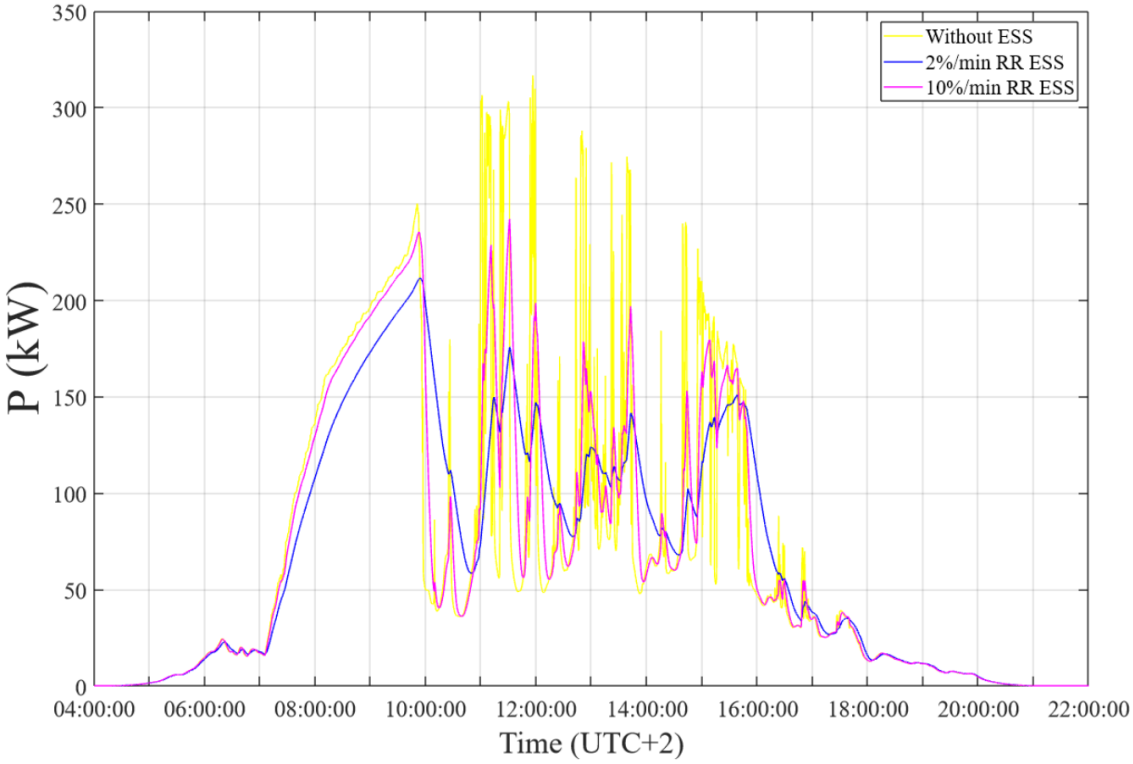

Figure 6.2.13. *Differences of the PV production in Case 3 with the PV capacity without ESS and two ESS application modes of PV systems on 27th April 2022.*

The PV productions under ESS application modes are lower as well in the second simulation date when compared to the PV capacity without an ESS application in Figure 6.2.13. The PV capacity without ESS application and with two ESS modes on 27th April 2022 is shown in Figure 6.2.13. The peak PV production is 210 kW with the 2 %/min $\mathrm{RR}_{\mathrm{limit}}$ and 240 kW with the 10%/ min $\mathrm{RR}_{\mathrm{limit}}$. The voltage and current values of the 2 %/min $\mathrm{RR}_{\mathrm{limit}}$ mode during the second simulation date is shown in Figure 6.2.14. The 2 %/min $\mathrm{RR}_{\mathrm{limit}}$ is more efficient, like in the first simulation date. The ESS application mode effectively lowers the overvoltage and RPF current values in the LV feeder. The peak voltage of 415 V occurs in distribution cabinet 4 and the peak RPF currents are between 77–80 % of the rated current of the cable type in feeder lines 1 and 2. There are no voltage violations in the household switchboards with the highest voltage of 418 V in the switchboard of S12. The grid codes are not violated in either ESS mode. The result values in the morning are like in the previous simulations but are smoother than without an ESS application during the simulation. The difference can be seen especially between 11 and 16 o'clock. The peak voltage occurred at midday and PV production altered greatly in the daytime due to the cloud movement on 27th April 2022 in the previous cases. The 2%/ min $\mathrm{RR}_{\mathrm{limit}}$ mode has balanced the PV production and has helped in keeping grid value changes at a minimum.

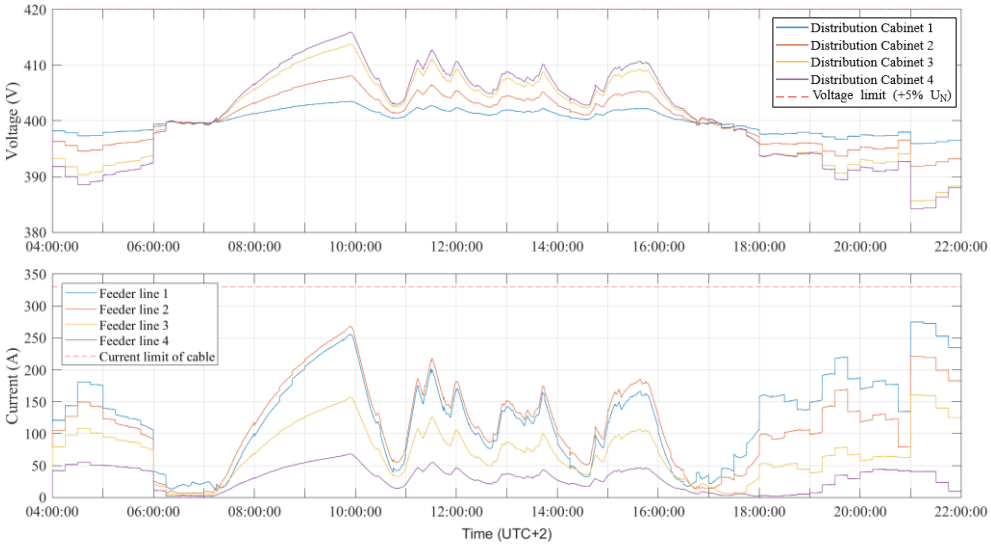

Figure 6.2.14. *Voltage and current levels of the LV feeder with the 2 %/min RR limit ESS application of Case 3 on 27th April 2022.*

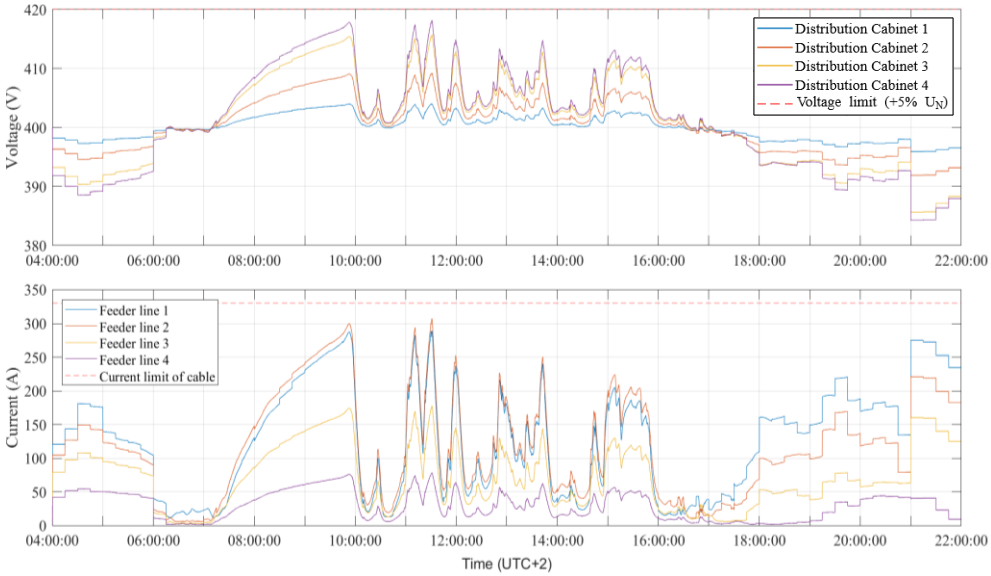

Figure 6.2.15. *Voltage and current levels of the LV feeder with the 10 %/min RR limit ESS application of Case 3 on 27th April 2021.*

The results are different when compared to the 10 %/min $\mathrm{RR}_{\mathrm{limit}}$ mode, as shown in Figure 6.2.15. The grid values alter greatly during daytime like in the previous simulation cases. The peak voltage of 418 V is in the distribution cabinet 4 and the peak RPF currents are between 87–93 % of the rated current of feeder lines 1 and 2. There are voltage violations in the household switchboards with overvoltages of 420 V in both the switchboards of S12 (420.62 V) and S13 (420.29 V). This means that the 10 %/min $\mathrm{RR}_{\mathrm{limit}}$ is not the suitable value for the ESS control due to overvoltages at the end of the LV feeder on 27$^{\mathrm{th}}$ April 2022. The currents of residential cables peak during the night when the direct electric heating is turned on during both simulation dates, like in previous cases.

Installing the ESS application in PV systems is shown to help in avoiding grid violations in the LV feeder. The most effective out of the two $\mathrm{RR_{limit}}$ values in lowering grid values is the 2%/ min $\mathrm{RR_{limit}}$ which can lower overvoltages under the voltage limit and RPF current values in feeder lines over 50 A, even 100 A around 11:30 o'clock on 27th April 2022, when comparing the results of the two ESS modes in Figures 6.2.14 and 6.2.15. The better response time to voltage fluctuations due to the cloud movement on PV modules is another reason why the 2 %/min $\mathrm{RR_{limit}}$ mode should be preferred over the 10%/ min RR mode which caused voltage violations in two switchboards at the end of the LV feeder on 27th April 2022. But overall both modes stabilize the LV feeder. The major concern when selecting between the ESS modes is the investment cost if the total number of PV modules will remain the same in the LV feeder. For both the current PV capacity in Case 3 and an increasing number of PV modules, it should be considered to prefer the 2 %/min $\mathrm{RR_{limit}}$.

6.3 Hosting capacity level

Case 3 has multiple grid violations as shown earlier. But the way of showing grid violations in the individual simulated cases is not an effective way for DSOs or residents to determine the HC level for PV capacity in the LV grid. HC is a new parameter that is determined as the safe level of PV production fed to a distribution grid. HC is the parameter tool characterized by an individual grid with limits and performance factors. HC can be defined after multiple grid factors: peak load of the grid, the transformer rating, the ratio of PV systems per household in an LV grid, yearly energy consumption, etc. The study of Fatima et al. confirms that 47% of the literature uses the peak load in defining HC [63]. This thesis will use the peak load of the LV feeder in defining the total PV capacity related to the load. The goal is to determine the HC in the LV feeder. PV capacity by the peak load of the feeder is determined as

$$\text{PV capacity (\%)} = \frac{\text{PV capacity (W)}}{\text{peak load in the LV feeder}} \cdot 100 = \frac{\sum P_{\mathrm{MPP}}}{P_{\text{peak load}}} \cdot 100. \tag{6.1}$$

P_{MPPT} is 190 W of the NP190-GKg PV module operating in the MPP under STC, as mentioned earlier in 5.1. $P_{\text{peak load}}$ is the peak active power load of the LV feeder. The peak load of 180 kW occurs at 21 o'clock on 27th April 2022 out of two simulation dates, as mentioned earlier in 5.2.2. Using Equation 6.1, PV capacity can be determined from 17 different PV capacity cases during two simulation dates. The HC equals 100% of the PV capacity in the following Figures 6.3.1–6.3.4. PV capacity is calculated by multiplying the number of PV modules in the LV feeder with the MPPT point value of the PV module. The maximum and minimum voltages of the distribution cabinets 3 and 4 are shown in Figure 6.3.1. The dotted red lines present the grid voltage limits of ±5 % U_N.

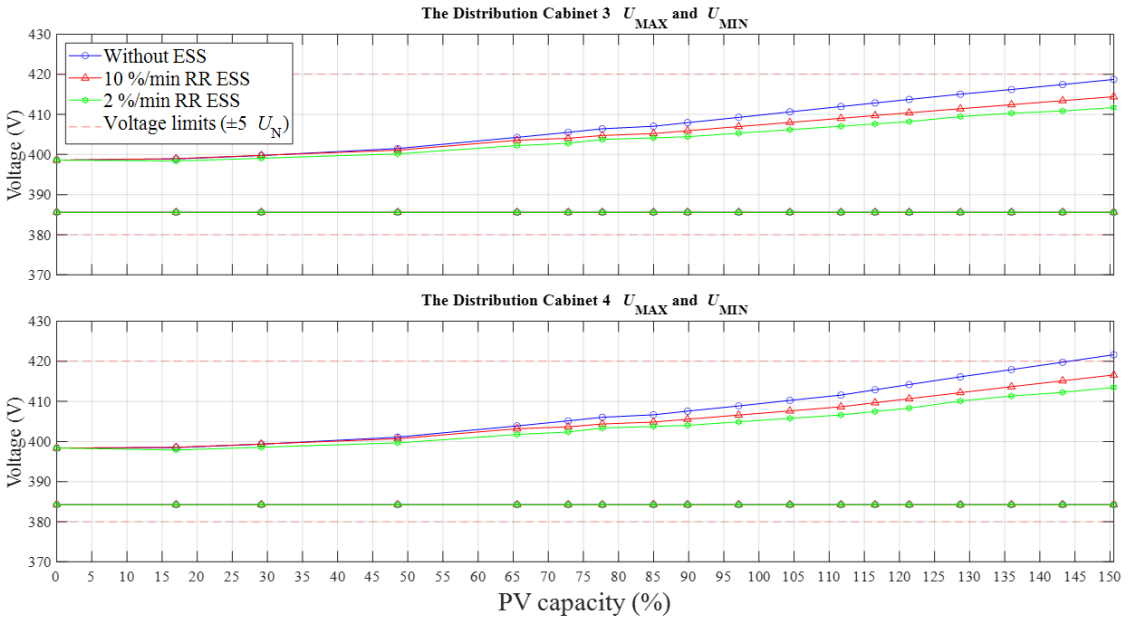

Figure 6.3.1. *Peak and lowest voltages of distribution cabinets 3 and 4 on 7th August 2021. Base case and 17 PV capacity cases in three different ESS modes are shown as the dotted plot lines from left to right in the chronical order in 18 cases.*

The minimum voltages of 385 V and 384 V in distribution cabinets 3 and 4 occurred due to turning on direct electric heating during the night. The highest voltages are under the grid limit of 420 V in the distribution cabinet 3 in all cases. The voltage limit is violated in distribution cabinet 4 with the PV capacity value in the 17th PV capacity case. The distribution cabinet 4 at the end of the LV feeder has smaller loads when compared to voltages in distribution cabinets 1 and 2. The voltage values at the start of the LV feeder never violate the grid limit due to larger loads during the simulations. The voltages are kept under the grid limit in all distribution cabinets using the ESS modes in PV systems. The point voltages in the LV feeder are not the only major concern of the grid operations. Another factor is RPF currents due to the high amount of PV production in the LV feeder. The peak RPF current values during peak PV production must be kept under it.

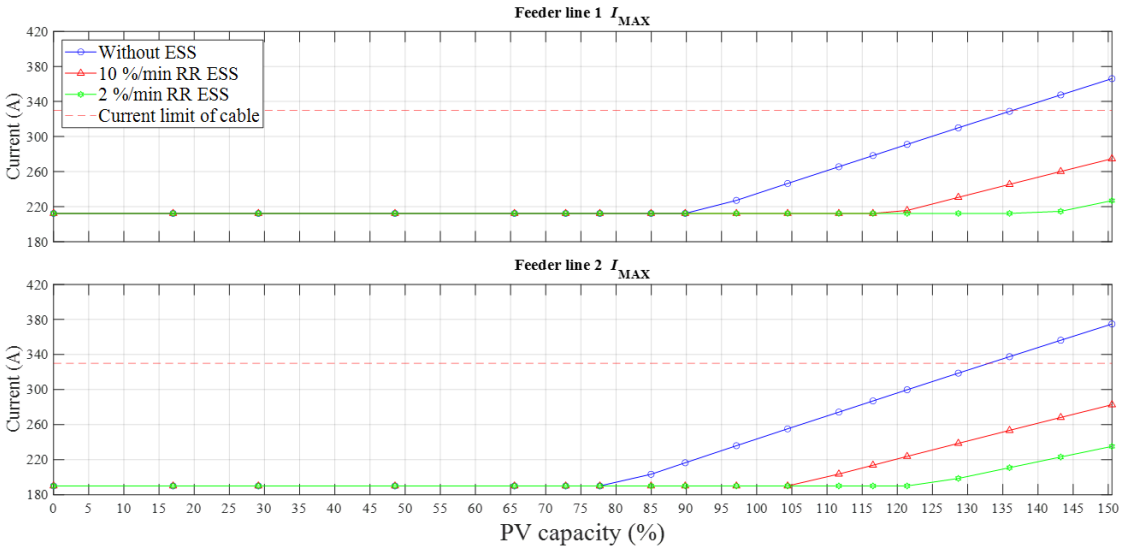

Figure 6.3.2. *The maximum currents of feeder lines 1 and 2 in different PV capacity levels caused by the RPF on 7th August 2021.*

The maximum currents of feeder lines 1 and 2 in the different simulation cases on 7th August 2021 are shown in Figure 6.3.2. The current limits are violated in the last two, 16th and 17th, PV capacity cases in both feeder lines 1 and 2. The PV production is fed toward the transformer and MV grid which causes high RPF currents in feeder line 2 with over 77.69 % PV capacity after the 6th case. The currents are lower in feeder line 1 due to loads of apartment buildings 1–4 connected to distribution cabinet 1. The ESS applications lower the current values under the cable limit in feeder lines 1 and 2 effectively. In the 17th case, the 2 %/min $\mathrm{RR}_{\mathrm{limit}}$ mode lowers the peak current of feeder line 2 over 130 A and the 10 %/min RR mode over 75 A when compared to the situation without an ESS application. Thus, when the ESS applications are not used, the current limit of the cables are violated before voltage violations in the distribution cabinets with the raising PV capacity on 7th August 2021.

The results are similar to the higher PV production on 27th April 2022. The voltages of distribution cabinets 3 and 4 without and with ESS applications on 27th April 2022 are shown in Figure 6.3.3. The minimum voltages in distribution cabinets 3 and 4 are the same as on 7th August 2021. Like on 7th August 2021, the voltage violations occur in distribution cabinet 4 and also in distribution cabinet 3. The violations happen in the lower PV capacities in the three last cases in the distribution cabinet 4. This is due to lower midday loads on 27th April 2022. The voltages are lowered under the grid limits by using ESS integration. Also noticeable is that the voltages of ESS modes in the distribution cabinet 4 of the 17th case are just under 420 V with the 2 %/min $\mathrm{RR}_{\mathrm{limit}}$ ESS is 415 V and the 10 %/min $\mathrm{RR}_{\mathrm{limit}}$ ESS being 418 V. Overvoltages with the 10 %/min $\mathrm{RR}_{\mathrm{limit}}$ ESS occurred in PCCs at the end of the feeder on 27th April 2022 as mentioned earlier. If the PV capacity of the LV feeder were increased unlimitedly, grid violations in distribution cabinets would occur eventually, first with the 10 %/min $\mathrm{RR}_{\mathrm{limit}}$ ESS and later on with the 2 %/min $\mathrm{RR}_{\mathrm{limit}}$ ESS.

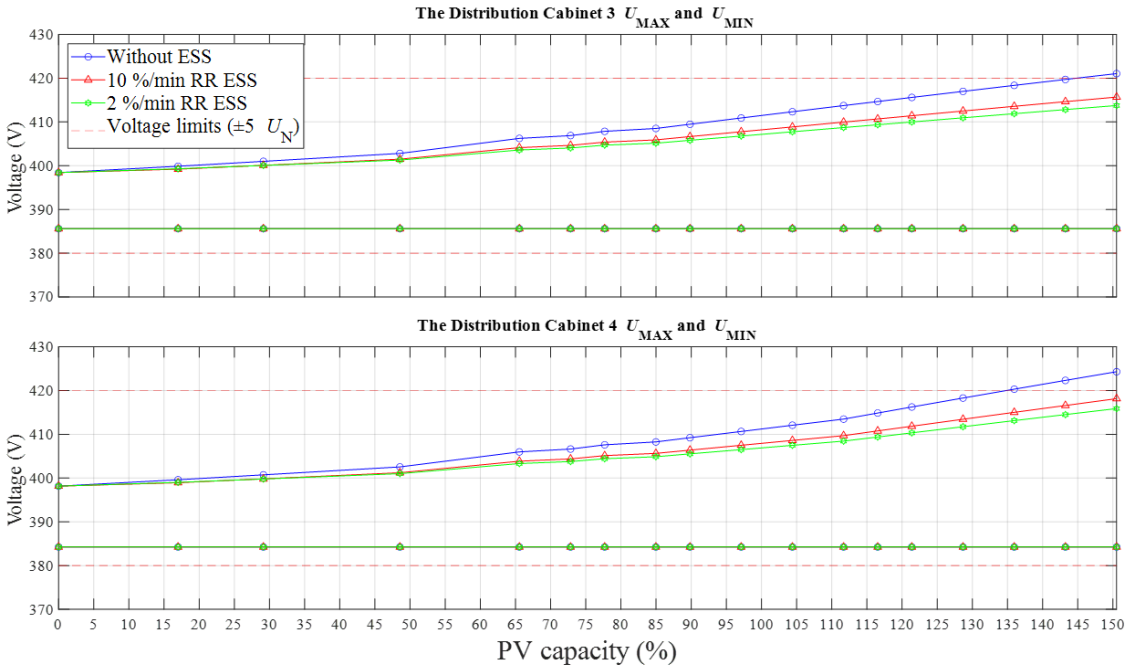

Figure 6.3.3. *Peak voltages of distribution cabinets 3 and 4 caused by RPF in different PV capacity cases on 27th April 2022.*

The current values of feeder lines 3 and 4 under the 17 PV capacity cases are shown in Figure 6.3.4. Similar to the values on 7th August 2021, RPF currents violate the current limit of cables in both feeder lines 1 and 2. But the violations occur already in case 14 in both feeder lines. The results on 27th April 2022 show that the current limit violations occur before the voltage violations in the LV feeder. RPF will occur in feeder line 2 without an ESS application with over 77.69 % PV capacity.

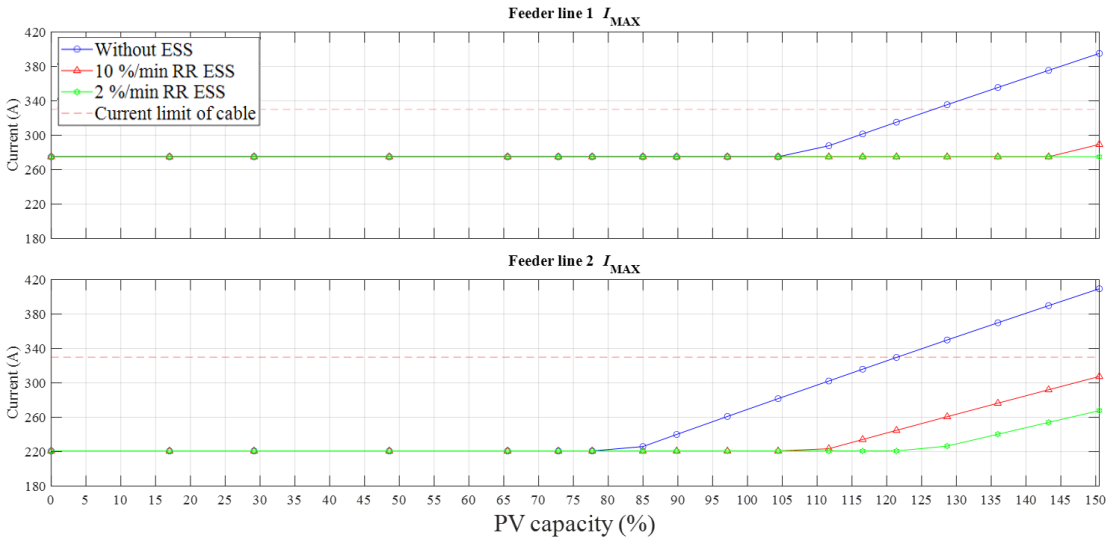

Figure 6.3.4. *The maximum current of feeder lines 3 and 4 caused by RPF with different PV capacity cases on 27th April 2022.*

6.4 Discussion

The topology of the simulated LV grid feeder is simple, short 285 m LV feeder between the transformer and the distribution cabinet 4. The longest line length is 350 m between the transformer and the single-household 12 at the end of the LV feeder. Rapid shading of PV modules during both simulation dates causes fast changes in solar irradiance received by PV modules causing fluctuations in the PV production. The grid operations of the LV feeder cannot react fast enough to this which causes grid violations in the feeder. Higher loads in the LV feeder can lower grid values and prevent grid violations. This can be seen when comparing the results of feeder lines 1 and 2 as the simulated results are lower in feeder line 1. Loads of the apartment buildings without PV production at the beginning of the LV feeder lower the current load of feeder line 1. The short length of the LV feeder will cause thermal damage to the feeder underground cables before overvoltage violations at the end of the feeder. The results of two simulation dates show that the HC of the feeder without ESS applications is 120% of the peak load of the LV feeder. The current limit of feeder line 1 is violated by over 120% PV capacity, as shown in Figure 6.3.4. The voltage violations occur with over 135% PV capacity in distribution cabinets 3 and 4 at the end of the LV feeder, as shown in Figure 6.3.3. RPF occurs with over 77.69 % PV capacity. Grid violations in the feeder lines and distribution cabinets can be avoided by using ESS integration in PV systems. Only using the 10 %/min $\mathrm{RR}_{\mathrm{limit}}$ with the ESSs causes voltage violations over 420 V in the switchboards of residential buildings of S12 and S13.

The HC is 120 % of the LV feeder without an ESS application seems reasonable when comparing the simulation results to the literature back in Chapter 3.3. There was mentioned overall general 70 % HC in the typical European LV grids and 110 % HC when multiple PV systems are installed evenly in a short LV feeder. The simulations result confirms both of these study results. The literature also mentioned the example that lower HC values can overload conductors

and it was the current limit of feeder lines 1 and 2 that were violated before voltage violations at the end of the LV feeder. But the necessity for grid investment due to grid violations came important at 120 % HC during the two simulations dates. This is the opposite of what was stated in the study by Gandhi et al [44] that grid investments become a necessity after 50 % HC. This might be more realistic in grid regions with longer feeders.

The simulations did not include the effect of harmonics in the LV feeder and the choice of rooftop materials on the cell temperatures of PV modules. The THD value of the feeder is affected by the number of PV inverters and could violate the grid code limits with a lower PV capacity than in the simulation results. Cell temperatures of PV modules on rooftops do not take into account rooftop materials, like metal sheeting, that will increase or decrease operation temperatures depending on current weather conditions. Temperatures drop under the freezing temperature during winter which lowers the cell temperature of modules. Lower cell temperatures increase PV production but temperatures rise in summer which will decrease the PV production of modules. The PV modules of the research plant in the Hervanta Campus are placed in the fixed position with a large space behind the modules to enable better cooling of the modules. PV modules of the simulation model are placed on the line with rooftops with small air gaps. Smaller air gaps will increase the cell temperatures of the modules on a sunny day. Another factor is the separate shading conditions of PV systems. The simulations used the constant 10 m/s wind speed from the west that was simulated by the PV data values starting ±10 s depending on the placement of PV systems. In general, shading conditions, and thus PV production, alter more in real life.

Increasing HC means that an ESS application may be a necessity for new PV system installations in the LV feeder. $\mathrm{RR}_{\mathrm{limit}}$ is determined by the PV capacity in the LV feeder and a lower $\mathrm{RR}_{\mathrm{limit}}$ of ESS mode means increasing the battery capacities of the ESS installations. This raises the investment costs of new PV systems in the LV feeder and makes the situation more preferable for older PV systems without a control tool, like APC or RPC tools in a PV inverter. It can be said that “first come, first served” is the situation for PV installations. Residents who are the first ones to install PV modules on their rooftops in their neighborhood and the grid region have the best chances not to be demanded to invest in an ESS application or other grid control tools installed in or next to their PV systems when high PV penetration levels cause grid issues. Most likely, new grid codes for PV systems are determined to better restrict grid violations due to PV production. But problems of high PV penetration levels must first become major issues for distribution grid operations to gain larger attention. This may take years but increasing the level of new PV installations in LV grids will speed up the process.

For further study, an LV grid with household PV production should be simulated with multiple feeders of a shared transformer and more complex load profiles, like a medium-scaled industry at the MV level of the distribution grid. Also, a higher PV capacity could be simulated by installing more PV modules on all possible rooftop areas in the LV feeder. The four apartment buildings with 4 separate apartments did not have PV production during the simulations. And north parts of the rooftops of the existing households with PV systems are available for more PV modules.

7 CONCLUSIONS

The rising trend of installing household PV systems has caused new challenges and issues to the operation of the distribution grid. DSOs have noticed and informed about issues caused by the high power capacities of PV systems connected to the grid. These issues mainly concern voltage stability and violations of the thermal current capacity of grid lines. Secondary factors include injecting harmonics from power electronic components, like PV inverters, phase voltage unbalances due to single-phase PV systems and altering load levels of the local distribution grid. This thesis was done to better understand the characteristics and electrical phenomena of household PV systems in LV grids and what kind of role ESS applications can have in maximizing PV production and stabilizing local grid operation states.

PV systems consist of two main components: modules and an inverter. PV cells in PV modules produce DC from solar irradiance which is transformed to AC form and injected into the grid by the inverter. The value of output is affected mainly by two factors: global irradiance received by the PV cells and the cell temperature of the PV modules. PV system topologies can be connected to a grid by either single-phase or three-phase connections. Production of 3-phase PV systems is mainly limited by a thermal limit capacity of grid lines. Most PV systems purchased by consumers are single-phase grid-connected and most of the new PV installations have been connected to LV grids. A high level of production of single-phase PV systems causes voltage phase unbalances, high phase currents, poorer PQ values and injecting harmonics into the grid. Production of single-phase PV systems is mostly affected by grid code limits and the current threshold of grid components, like the current limitation of windings of a transformer.

The electric power grid is a crucial part of stabilized and evolving society. Household PV systems are a newer technology and there is no general and reliable definition for safe PV production in the distribution grid. Literature uses different descriptions of HC. A level of PV production can be defined by multiple factors referring to PV system characteristics, like capacity, the annual energy or the number of PV production points in the feeder. Other definitions include grid components, like the transformer rating, peak load or the annual consumption of the grid feeder. This thesis used HC defined by the peak load which is 180 kW in the simulated case study. The restrictive factors of HC include poor PF, VUF and THD values in the grid. Generally, the 15% level of PV penetration will not cause any major grid issues. Characteristics of LV feeders, line lengths, number and capacity of residential loads, cause HC per an individual feeder to alter greatly. HC can be increased by different grid control tools. APC is the basic on/off switch-type controller that is non-preferable due to lost PV production when the PV production surpasses HC which causes grid violation. RPC is a reactive power control tool that helps to stabilize and avoid voltage limit violations. But RPC does not have the same efficiency as in transmission grids due to a low X/R ratio of the distribution grid. OLTC and OfLTC are voltage control tools that can increase the level of HC in the feeder by lowering or increasing voltage levels by changing taps of the secondary windings of a transformer. OfLTC tools can be operated only during a non-load

state of a feeder. An OLTC tool can cause undervoltages when all the phase voltages are lowered due to a single-phase overvoltage. This is why the single-phase voltage control of OLTC is recommended. Literature also stated that 3-phase grid connections in PV systems should be preferred when using an OLTC application in a feeder transformer. Hybrid solutions, like RPC or single-phase connection, with OLTC have been confirmed to increase HC in the grid but their effects may cause issues, like increasing VUF value in the grid.

ESSs are used frequently for smoothing and controlling power fluctuations in injecting PV production into distribution grids. Many nations, especially those with weak distribution grids, have included the power control of PV systems in their grid codes. The power control is either defined by using a RR limit on injected power, Denmark at 100 kW/s and Ireland at 30 MW/min, or the capacity of the PV system (%), Germany and Puerto Rico with 10%/ min, according to the stated time. Adding the grid code about PV production smoothing seems to become a necessity with the rising number of household PV installations. ESS technologies alter greatly based on price, capacity and operation attributes, like cycle life and response time. PHES and CAES technologies have higher capacities but their use is restricted due to large physical sizes and high investment costs. RFB, flywheel and BESS technologies are small- and medium-scale storage technologies with faster response time and easier installations but alter greatly by price and performance. The most likely ESS applications used in household PV systems are BESSs. Popular BESS technologies are lead-acid and Li-ion batteries. Using a single ESS technology based on performance is non-preferable and hybrid ESSs are recommended to better respond to rapid changes in PV productions and grid control solutions. Different ESS algorithms are used to better respond grid demands and maximize PV production. Two general ESS topologies are de-centralized, located next to PV systems, and centralized, the ESS application in a single point like next to a transformer, topologies. The number of PV systems in the grid region, distances and separate shading conditions between PV modules and systems are key factors in choosing a correct topology.

Injecting PV production from household PV systems located in the suburban LV feeder was simulated by using the measurement data of the research PV power plant of the Hervanta campus of Tampere University. The general factors in PV production of the research plant and the instruments of the weather station were presented. The research plant consists of 69 PV modules of which the string of 23 PV modules data was used in the simulations. Three data types were used: the measured data without an ESS application and two ESS $\mathrm{RR}_{\mathrm{limit}}$ values: 2 %/min and 10 %/min. All PV systems had 3-phase grid connections and all PV modules were facing south during the simulations. The LV feeder had 8 apartment and 13 single-household buildings. Heating was the major power demand of the LV feeder. Two simulation dates were used: 7th August 2021 and 27th April 2022. These dates had different load profiles due to heating in different seasons and the peak load was 180 kW on the evening of 27th April 2022. The peak load value was used in determining the HC values during the simulations.

Three different PV capacity cases were simulated. The integrated PV active power production was increased by adding PV capacity of a single building starting from the transformer. The LV feeder safe limits were violated in Case 3. The thermal capacity of feeder line 2 was

violated with over 120% PV penetration concerning PV capacity in the feeder which is the threshold of the LV feeder. Next, the thermal capacity of feeder line 1 and the overvoltage limit of 5% U_N of distribution cabinets 3 and 4 were violated. The violations were not quick and lasted for several minutes. The violations were avoided by using the 2 %/min $\mathrm{RR}_{\mathrm{limit}}$of ESS applications integrated into the PV systems but there were overvoltages in the switchboards of two single-household buildings when using the 10 %/min $\mathrm{RR}_{\mathrm{limit}}$ on 27th April 2021. The RR limit did not cause grid violations on 7th August 2021. If the PV capacity of the LV feeder was to be increased, the violations would also occur using the 10%/ min $\mathrm{RR}_{\mathrm{limit}}$ of the ESS application. The simulation results showed that the LV feeder can threshold a large amount of injected power from PV systems due to the topology of the feeder. The line lengths were reasonably short, 3-phase grid connections were used and the feeder had a high load profile. All of these factors increased the HC level in the feeder but grid investments, like ESSs, are needed to increase HC more. High grid investment costs will eventually make owners of PV systems and DSOs reconsider if increasing HC unlimitedly is a good financial choice.

The simulations were simple when considering the subject. The technology of PV systems and issues are harder than what was simulated. Only 3-phase grid connections were used due to the simulation component limitation. This is not ideal when most new PV installations in distribution grids use single-phase grid connections. PV systems have many factors which can cause grid issues and violations if not recognized and answered properly. Household PV systems in LV grids are still gaining the attention of larger crowds and the technology has not gained commercial maturity. The role of distribution grids as more than the downstream power flow solution for residential consumption must be re-considered to better adapt to larger PV productions in the future. A more stabilized PV system with a multi-operational inverter helps in avoiding grid violations. The proper method could be adding demand for ESS solutions in medium- and large-scale PV systems in the Finnish grid code. The capacity scale of ESS demand could be determined using a threshold of distribution grids and feeders. Other methods could include favoring grid regions with larger consumption and 3-phase grid connections in PV systems to avoid grid violations, like the thermal capacity of conductors and VUF, during peak PV production. But this thesis is just a small introduction to the field of study that needs more studying, simulating and testing before the commercial maturity of household PV systems is achieved.

REFERENCES

[1] I. Lindell, *Sähkön pitkä historia*. in Otatieto-sarja. Helsinki: Otatieto / Helsinki University Press, 2009, 454 p.

[2] X. Lu and F. Anariba, “Fostering Innovation through an Active Learning Activity Inspired by the Baghdad Battery,” *J. Chem. Educ.*, vol. 91, no. 11, pp. 1929–1933, 2014, doi: 10.1021/ed400869c.

[3] J. Elovaara, *Sähköverkot. II, Verkon suunnittelu, järjestelmät ja laitteet*. in Otatieto. Helsinki: Otatieto Helsinki University Press, 2011, 551 p.

[4] K. Fekete, Z. Klaic, and L. Majdandzic, “Expansion of the residential photovoltaic systems and its harmonic impact on the distribution grid,” *Renew. Energy*, vol. 43, pp. 140–148, 2012, doi: 10.1016/j.renene.2011.11.026.

[5] B. Ren, M. Zhang, S. An, and X. Sun, “Local control strategy of PV inverters for overvoltage prevention in low voltage feeder,” IEEE, 2016, pp. 2071–2075. doi: 10.1109/ICIEA.2016.7603930.

[6] N. Efkarpidis, T. De Rybel, and J. Driesen, “Technical assessment of centralized and localized voltage control strategies in low voltage networks,” *Sustain. Energy Grids Netw.*, vol. 8, pp. 85–97, 2016, doi: 10.1016/j.segan.2016.09.003.

[7] T. Aziz and N. Ketjoy, “PV Penetration Limits in Low Voltage Networks and Voltage Variations,” *IEEE Access*, vol. 5, pp. 16784–16792, 2017, doi: 10.1109/ACCESS.2017.2747086.

[8] Z. Wang and G. Yang, “Static Operational Impacts of Residential Solar PV Plants on the Medium Voltage Distribution Grids—A Case Study Based on the Danish Island Bornholm,” *Energ. Basel*, vol. 12, no. 8, pp. 1458-, 2019, doi: 10.3390/en12081458.

[9] A. El-Naggar and I. Erlich, “Control approach of three-phase grid connected PV inverters for voltage unbalance mitigation in low-voltage distribution grids,” *IET Renew. Power Gener.*, vol. 10, no. 10, pp. 1577–1586, 2016, doi: 10.1049/iet-rpg.2016.0200.

[10] R. Torquato, D. Salles, C. Oriente Pereira, P. C. M. Meira, and W. Freitas, “A Comprehensive Assessment of PV Hosting Capacity on Low-Voltage Distribution Systems,” *IEEE Trans. Power Deliv.*, vol. 33, no. 2, pp. 1002–1012, 2018, doi: 10.1109/TPWRD.2018.2798707.

[11] T. Oliveira, P. Carvalho, P. Ribeiro, and B. Bonatto, “PV Hosting Capacity Dependence on Harmonic Voltage Distortion in Low-Voltage Grids: Model Validation with Experimental Data,” *Energ. Basel*, vol. 11, no. 2, pp. 465-, 2018, doi: 10.3390/en11020465.

[12] M. J. Weisshaupt, B. Schlatter, P. Korba, E. Kaffe, and F. Kienzle, “Evaluation of Measures to Operate Urban Low Voltage Grids Considering Future PV Expansion,” *IFAC Pap.*, vol. 49, no. 27, pp. 336–341, 2016, doi: 10.1016/j.ifacol.2016.10.714.

[13] J. D. Watson, N. R. Watson, D. Santos-Martin, A. R. Wood, S. Lemon, and A. J. Miller, “Impact of solar photovoltaics on the low-voltage distribution network in New

Zealand," *IET Gener. Transm. Distrib.*, vol. 10, no. 1, pp. 1–9, 2016, doi: 10.1049/iet-gtd.2014.1076.

[14] D. Torres Lobera, A. Mäki, J. Huusari, K. Lappalainen, T. Suntio, and S. Valkealahti, "Operation of TUT Solar PV Power Station Research Plant under Partial Shading Caused by Snow and Buildings," *Int. J. Photoenergy*, vol. 2013, pp. 1–13, Aug. 2013, doi: 10.1155/2013/837310.

[15] "ABB Conversations > Power at your fingertips." https://www.abb-conversations.com/2014/08/power-at-your-fingertips/ (accessed Sep. 15, 2022).

[16] "Future of Photovoltaic." https://www.irena.org/publications/2019/Nov/Future-of-Solar-Photovoltaic (accessed Mar. 21, 2023).

[17] J. Martins, S. Spataru, D. Sera, D.-I. Stroe, and A. Lashab, "Comparative Study of Ramp-Rate Control Algorithms for PV with Energy Storage Systems," *Energies*, vol. 12, no. 7, Art. no. 7, Jan. 2019, doi: 10.3390/en12071342.

[18] A. Arshad, M. Lindner, and M. Lehtonen, "An Analysis of Photo-Voltaic Hosting Capacity in Finnish Low Voltage Distribution Networks," *Energ. Basel*, vol. 10, no. 11, pp. 1702-, 2017, doi: 10.3390/en10111702.

[19] "Aurinkosähkön kapasiteetti kasvoi Suomessa yli 100 megawattia vuonna 2021," *Energiavirasto*, Jun. 20, 2022. https://energiavirasto.fi/-/aurinkosahkon-kapasiteetti-kasvoi-suomessa-yli-100-megawattia-vuonna-2021 (accessed Sep. 16, 2022).

[20] "Utajärven pikkukuntaan suunnitellaan Suomen suurinta aurinkovoimalaa: 350 000 paneelin tuotanto vastaisi jopa 40 000 ihmisen vuotuista kulutusta," *Yle Uutiset*, Sep. 07, 2022. https://yle.fi/uutiset/3-12611567 (accessed Sep. 09, 2022).

[21] H. Bagheri Tolabi, M. H. Ali, and M. Rizwan, "Simultaneous Reconfiguration, Optimal Placement of DSTATCOM, and Photovoltaic Array in a Distribution System Based on Fuzzy-ACO Approach," *IEEE Trans. Sustain. Energy*, vol. 6, no. 1, pp. 210–218, 2015, doi: 10.1109/TSTE.2014.2364230.

[22] K. F. Katiraei and J. R. Agüero, "Solar PV Integration Challenges," *IEEE Power Energy Mag.*, vol. 9, no. 3, pp. 62–71, 2011, doi: 10.1109/MPE.2011.940579.

[23] A. Cabrera-Tobar, E. Bullich-Massagué, M. Aragüés-Peñalba, and O. Gomis-Bellmunt, "Review of advanced grid requirements for the integration of large scale photovoltaic power plants in the transmission system," *Renew. Sustain. Energy Rev.*, vol. 62, pp. 971–987, Sep. 2016, doi: 10.1016/j.rser.2016.05.044.

[24] S. K. Sharma, A. Chandra, M. Saad, S. Lefebvre, D. Asber, and L. Lenoir, "Voltage Flicker Mitigation Employing Smart Loads With High Penetration of Renewable Energy in Distribution Systems," *IEEE Trans. Sustain. Energy*, vol. 8, no. 1, pp. 414–424, 2017, doi: 10.1109/TSTE.2016.2603512.

[25] H. Cheung, A. Hamlyn, L. Wang, C. Yang, and R. Cheung, "Investigations of impacts of distributed generations on feeder protections," in *2009 IEEE Power & Energy Society General Meeting*, Jul. 2009, pp. 1–7. doi: 10.1109/PES.2009.5275220.

[26] M. D. Archer and R. Hill, *Clean electricity from photovoltaics*. in Series on photoconversion of solar energy ; v. 1. London: Imperial College Press, 2001, 870 p.

[27] M. Azab, "Intra-minutes technical impacts of PV grid integration on distribution network operation of a rural community under extreme PV power delivery," *Energy*

Syst. Berl. Period., vol. 11, no. 1, pp. 213–245, 2018, doi: 10.1007/s12667-018-0307-7.

[28] M. D. Archer and M. A. Green, *Clean electricity from photovoltaics*, Second edition. in Series on Photoconversion of Solar Energy, Volume 4. London, England: Imperial College Press, 2015, 706 p.

[29] J. L. Gray, "The Physics of the Solar Cell," in *Handbook of Photovoltaic Science and Engineering*, 2nd Edition.Chichester, UK: John Wiley & Sons, 2011, pp. 1–1. doi: 10.1002/9780470974704.ch3.

[30] F. Vignola, *Solar and infrared radiation measurements*, 1st edition. in Energy and the environment. Boca Raton, Fla: CRC Press, 2012, 409 p. doi: 10.1201/b12367.

[31] K. Lappalainen and J. Kleissl, "Analysis of the cloud enhancement phenomenon and its effects on photovoltaic generators based on cloud speed sensor measurements," *J. Renew. Sustain. Energy*, vol. 12, no. 4, p. 043502, Jul. 2020, doi: 10.1063/5.0007550.

[32] D. Torres Lobera, "Measuring Actual Operating Conditions of a Photovoltaic Power Generator", Master of Science Thesis, Tampere University of Technology, 2011, 116 p. Available: https://trepo.tuni.fi/handle/123456789/6897

[33] W. Issaadi and S. Issaadi, *Photovoltaic systems: design, performance and applications*. in Electrical engineering developments. New York: Nova Science Publishers, 2018, 345 p.

[34] J. Schnabel, "Compensation of PV Generator Power Fluctuations Using Energy Storage Systems," Master of Science Thesis, Tampere University of Technology, 2015, 57 p. Available: https://trepo.tuni.fi/handle/123456789/23276

[35] K. Lappalainen, *Output Power Variation and Mismatch Losses of Photovoltaic Power Generators Caused by Moving Clouds*, dissertation, Tampere University of Technology, Publication 1506, 2017, 116 p. Available: https://trepo.tuni.fi/handle/10024/115030

[36] K. Lappalainen and S. Valkealahti, "Analysis of shading periods caused by moving clouds," *Sol. Energy*, vol. 135, pp. 188–196, 2016, doi: 10.1016/j.solener.2016.05.050.

[37] A. Luque and S. Hegedus, *Handbook of photovoltaic science and engineering*, 2nd ed. Chichester, West Sussex, U.K: Wiley, 2011, 1170 p.

[38] R. R. Boros and I. Bodnár, "Grid and PV Fed Uninterruptible Induction Motor Drive Implementation and Measurements," *Energ. Basel*, vol. 15, no. 3, pp. 708-, 2022, doi: 10.3390/en15030708.

[39] "Best Research-Cell Efficiency Chart." https://www.nrel.gov/pv/cell-efficiency.html (accessed Sep. 12, 2022).

[40] J. A. Candanedo and A. K. Athienitis, "A systematic approach for energy design of advanced solar houses," in *2009 IEEE Electrical Power & Energy Conference (EPEC)*, Oct. 2009, pp. 1–6. doi: 10.1109/EPEC.2009.5420363.

[41] S. M. Ahsan, H. A. Khan, A. Hussain, S. Tariq, and N. A. Zaffar, "Harmonic Analysis of Grid-Connected Solar PV Systems with Nonlinear Household Loads in Low-Voltage Distribution Networks," *Sustain. Basel Switz.*, vol. 13, no. 7, pp. 3709-, 2021, doi: 10.3390/su13073709.

[42] M. A. Eltawil and Z. Zhao, “Grid-connected photovoltaic power systems: Technical and potential problems—A review,” *Renew. Sustain. Energy Rev.*, vol. 14, no. 1, pp. 112–129, Jan. 2010, doi: 10.1016/j.rser.2009.07.015.

[43] K. Lappalainen and S. Valkealahti, “Sizing of energy storage systems for ramp rate control of photovoltaic strings,” *Renew. Energy*, vol. 196, pp. 1366–1375, Aug. 2022, doi: 10.1016/j.renene.2022.07.069.

[44] O. Gandhi, D. S. Kumar, C. D. Rodríguez-Gallegos, and D. Srinivasan, “Review of power system impacts at high PV penetration Part I: Factors limiting PV penetration,” *Sol. Energy*, vol. 210, pp. 181–201, 2020, doi: 10.1016/j.solener.2020.06.097.

[45] B. Uzum, A. Onen, H. M. Hasanien, and S. M. Muyeen, “Rooftop Solar PV Penetration Impacts on Distribution Network and Further Growth Factors—A Comprehensive Review,” *Electron. Basel*, vol. 10, no. 1, pp. 55-, 2021, doi: 10.3390/electronics10010055.

[46] R. Salcedo, X. Ran, F. de León, D. Czarkowski, and V. Spitsa, “Long Duration Overvoltages due to Current Backfeeding in Secondary Networks,” *IEEE Trans. Power Deliv.*, vol. 28, no. 4, pp. 2500–2508, Oct. 2013, doi: 10.1109/TPWRD.2013.2273897.

[47] F. M. Camilo, V. F. Pires, R. Castro, and M. E. Almeida, “The impact of harmonics compensation ancillary services of photovoltaic microgeneration in low voltage distribution networks,” *Sustain. Cities Soc.*, vol. 39, pp. 449–458, May 2018, doi: 10.1016/j.scs.2018.03.016.

[48] M. Wajahat, H. A. Khalid, G. M. Bhutto, and C. Leth Bak, “A Comparative Study into Enhancing the PV Penetration Limit of a LV CIGRE Residential Network with Distributed Grid-Tied Single-Phase PV Systems,” *Energ. Basel*, vol. 12, no. 15, pp. 2964-, 2019, doi: 10.3390/en12152964.

[49] T. Aziz and N. Ketjoy, “Enhancing PV Penetration in LV Networks Using Reactive Power Control and On Load Tap Changer With Existing Transformers,” *IEEE Access*, vol. 6, pp. 2683–2691, 2018, doi: 10.1109/ACCESS.2017.2784840.

[50] L. Hietalahti, *Sähkövoimatekniikan perusteet*, 1. p. Tammertekniikka, 2013, 302 p.

[51] J. Elovaara, *Sähköverkot. I, Järjestelmätekniikka ja sähköverkon laskenta*. in Otatieto. Helsinki: Otatieto Helsinki University Press, 2011, 520 p.

[52] A. Kharrazi, V. Sreeram, and Y. Mishra, “Assessment techniques of the impact of grid-tied rooftop photovoltaic generation on the power quality of low voltage distribution network - A review,” *Renew. Sustain. Energy Rev.*, vol. 120, pp. 109643-, 2020, doi: 10.1016/j.rser.2019.109643.

[53] S. Dalhues, Y. Zang, O. Pohl, F. Rewald, F. Erlemeyer, D. Schmid, J. Zwartscholten, Z. Hagemann, C. Wagner, D. G. Mayorga, H. Liu, M. Zhang, J.Liu, C. Rehtanz, Y. Li and Y. Cao, “Research and practice of flexibility in distribution systems: A review,” *CSEE J. Power Energy Syst.*, vol. 5, no. 3, pp. 285–294, 2019, doi: 10.17775/CSEEJPES.2019.00170.

[54] “EstLink 2 - toinen tasasähköyhteys Suomen ja Viron välillä,” *Fingrid*, Jun. 22, 2017. https://www.fingrid.fi/kantaverkko/suunnittelu-ja-rakentaminen/arkisto/estlink-2/ (accessed Sep. 09, 2022).

[55] “Electricity system of Finland,” *Fingrid*, May 19, 2017. https://www.fingrid.fi/en/grid/power-transmission/electricity-system-of-finland/ (accessed May 04, 2022).

[56] “Electricity networks - Energiateollisuus.” https://energia.fi/en/energy_sector_in_finland/energy_networks/electricity_networks (accessed May 05, 2022).

[57] J. Tahkolahti, “Pohjoisen ennätyspakkanen katkaisi voimajohdon,” *Helsingin Sanomat*, Jan. 28, 1999. https://www.hs.fi/kotimaa/art-2000003774770.html (accessed May 02, 2022).

[58] R. Tonkoski, L. A. C. Lopes, and T. H. M. El-Fouly, “Coordinated Active Power Curtailment of Grid Connected PV Inverters for Overvoltage Prevention,” *IEEE Trans. Sustain. Energy*, vol. 2, no. 2, pp. 139–147, Apr. 2011, doi: 10.1109/TSTE.2010.2098483.

[59] L. Kütt, E. Saarijärvi, M. Lehtonen, H. Mõlder, and T. Vinnal, “Harmonic load of residential distribution network — Case study monitoring results,” in *2014 Electric Power Quality and Supply Reliability Conference (PQ)*, Jun. 2014, pp. 93–98. doi: 10.1109/PQ.2014.6866791.

[60] C. Long and L. F. Ochoa, “Voltage Control of PV-Rich LV Networks: OLTC-Fitted Transformer and Capacitor Banks,” *IEEE Trans. Power Syst.*, vol. 31, no. 5, pp. 4016–4025, 2016, doi: 10.1109/TPWRS.2015.2494627.

[61] J. Hirvonen, J. Jokisalo, J. Heljo, and R. Kosonen, “Towards the EU Emission Targets of 2050: Cost-Effective Emission Reduction in Finnish Detached Houses,” *Energ. Basel*, vol. 12, no. 22, pp. 4395-, 2019, doi: 10.3390/en12224395.

[62] “Virransyöttöjärjestelmä ylijännitesuojalaitteilla SPD,” *Surge Protection Device*, Apr. 12, 2018. https://www.lsp-international.com/fi/power-supply-system/ (accessed Sep. 14, 2022).

[63] S. Fatima, V. Püvi, and M. Lehtonen, “Review on the PV Hosting Capacity in Distribution Networks,” *Energ. Basel*, vol. 13, no. 18, pp. 4756-, 2020, doi: 10.3390/en13184756.

[64] T. Verschueren, K. Mets, B. Meersman, M. Strobbe, C. Develder, and L. Vandevelde, “Assessment and mitigation of voltage violations by solar panels in a residential distribution grid,” IEEE, 2011, pp. 540–545. doi: 10.1109/SmartGridComm.2011.6102381.

[65] G. Fernández, N. Galan, D. Marquina, D. Martínez, and A. Sanchez, “Photovoltaic Generation Impact Analysis in Low Voltage Distribution Grids,” *Energ. Basel*, vol. 13, no. 17, pp. 4347-, 2020, doi: 10.3390/en13174347.

[66] BHEL, *Transformers.*, 2nd ed. New York: McGraw-Hill Education LLC, 2003, 614 p.

[67] B. S. Guru, *Electric Machinery and Transformers*, 3rd ed. Oxford University Press Incorporated, 2001, 720 p.

[68] P. Jusner, E. Schwaiger, A. Potthast, and T. Rosenau, “Thermal stability of cellulose insulation in electrical power transformers – A review,” *Carbohydr. Polym.*, vol. 252, pp. 117196–117196, 2021, doi: 10.1016/j.carbpol.2020.117196.

[69] J. K. Kaldellis, “Chapter 13 - Photovoltaic-Energy Storage Systems for Remote Small Islands,” in *Solar Energy Storage*, Elsevier Ltd, 2015, pp. 291–326. doi: 10.1016/B978-0-12-409540-3.00013-X.

[70] S. Kikuchi, M. Machida, J. Tamura, M. Imanaka, and J. Baba, “Hosting capacity analysis of many distributed photovoltaic systems in future distribution networks,” IEEE, 2017, pp. 1–5. doi: 10.1109/ISGT-Asia.2017.8378408.

[71] P. B. Kitworawut, D. T. Azuatalam, O. C. Unigwe, and A. J. Collin, “An investigation into the technical impacts of microgeneration on uk-type LV distribution networks,” IEEE, 2016, pp. 124–129. doi: 10.1109/ICRERA.2016.7884478.

[72] T. Khatib and L. Sabri, “Grid Impact Assessment of Centralized and Decentralized Photovoltaic-Based Distribution Generation: A Case Study of Power Distribution Network with High Renewable Energy Penetration,” *Math. Probl. Eng.*, vol. 2021, pp. 1–16, 2021, doi: 10.1155/2021/5430089.

[73] J. Bird, “35 - Maximum power transfer theorems and impedance matching,” in J. Bird (ed.) *Electrical Circuit Theory and Technology*, Second Edition.Elsevier Ltd, 2003, pp. 617–630. doi: 10.1016/B978-0-08-050516-9.50039-6.

[74] J. C. Hernández, M. J. Ortega, and A. Medina, “Statistical characterisation of harmonic current emission for large photovoltaic plants: Characterisation of harmonic current in PV,” *Int. Trans. Electr. Energy Syst.*, vol. 24, no. 8, pp. 1134–1150, 2014, doi: 10.1002/etep.1767.

[75] J. Hu, M. Marinelli, M. Coppo, A. Zecchino, and H. W. Bindner, “Coordinated voltage control of a decoupled three-phase on-load tap changer transformer and photovoltaic inverters for managing unbalanced networks,” *Electr. Power Syst. Res.*, vol. 131, pp. 264–274, 2016, doi: 10.1016/j.epsr.2015.10.025.

[76] E. Yao, P. Samadi, V. W. S. Wong, and R. Schober, “Residential Demand Side Management Under High Penetration of Rooftop Photovoltaic Units,” *IEEE Trans. Smart Grid*, vol. 7, no. 3, pp. 1597–1608, 2016, doi: 10.1109/TSG.2015.2472523.

[77] F. Katiraei and J. R. Agüero, “Solar PV Integration Challenges,” *IEEE Power Energy Mag.*, vol. 9, no. 3, pp. 62–71, May 2011, doi: 10.1109/MPE.2011.940579.

[78] D. E. Mawarni, M. M. V. M. Ali, P. H. Nguyen, W. L. Kling, and M. Jerele, “A case study of using OLTC to mitigate overvoltage in a rural european low voltage network,” IEEE, 2015, pp. 1–5. doi: 10.1109/UPEC.2015.7339875.

[79] N. K. Singh, M. Z. C. Wanik, A. A. Jabbar, and A. Sanfilippo, “Enhancing PV hosting Capacity of a Qatar Remote Farm Network using Inverters Ability to Regulate Reactive Power-a Case Study,” IEEE, 2019, pp. 1–5. doi: 10.1109/ISGTEurope.2019.8905545.

[80] M. Juelsgaard, C. Sloth, R. Wisniewski, and J. Pillai, “Loss minimization and voltage control in smart distribution grid,” presented at the IFAC Proceedings Volumes (IFAC-PapersOnline), 2014, pp. 4030–4037. doi: 10.3182/20140824-6-za-1003.00090.

[81] R. Tonkoski and L. A. C. Lopes, “Impact of active power curtailment on overvoltage prevention and energy production of PV inverters connected to low voltage residential feeders,” *Renew. Energy*, vol. 36, no. 12, pp. 3566–3574, Dec. 2011, doi: 10.1016/j.renene.2011.05.031.

[82] D. Garozzo and G. M. Tina, “Evaluation of the Effective Active Power Reserve for Fast Frequency Response of PV with BESS Inverters Considering Reactive Power Control,” *Energ. Basel*, vol. 13, no. 13, pp. 3437-, 2020, doi: 10.3390/en13133437.

[83] Y. Ding, Y. Li, C. Liu, and Z. Sun, “Chapter 2 - Solar Electrical Energy Storage,” in *Solar Energy Storage*, Elsevier Ltd, 2015, pp. 7–25. doi: 10.1016/B978-0-12-409540-3.00002-5.

[84] K. C. Divya and J. Østergaard, “Battery energy storage technology for power systems—An overview,” *Electr. Power Syst. Res.*, vol. 79, no. 4, pp. 511–520, Apr. 2009, doi: 10.1016/j.epsr.2008.09.017.

[85] F. Rahman, M. A. Baseer, and S. Rehman, “Chapter 4 - Assessment of Electricity Storage Systems,” in *Solar Energy Storage*, Elsevier Ltd, 2015, pp. 63–114. doi: 10.1016/B978-0-12-409540-3.00004-9.

[86] B. Sørensen, “Chapter 1 - Introduction and Overview,” in *Solar Energy Storage*, Elsevier Ltd, 2015, pp. 1–4. doi: 10.1016/B978-0-12-409540-3.00001-3.

[87] D. Sharafi, A. Dowdy, J. Landsberg, P. Bryant, D. Ward, J. Eggleston, and G. Liu, “Wildfires Down Under: Impacts and Mitigation Strategies for Australian Electricity Grids,” *IEEE Power Energy Mag.*, vol. 20, no. 1, pp. 52–63, 2022, doi: 10.1109/MPE.2021.3122732.

[88] S. Prakash and S. Mishra, “VSC Control of Grid Connected PV for Maintaining Power Supply During Open-Phase Condition in Distribution Network,” *IEEE Trans. Ind. Appl.*, vol. 55, no. 6, pp. 6211–6222, Nov. 2019, doi: 10.1109/TIA.2019.2932697.

[89] Y. Sun, Z. Zhao, M. Yang, D. Jia, W. Pei, and B. Xu, “Overview of energy storage in renewable energy power fluctuation mitigation,” *CSEE J. Power Energy Syst.*, vol. 6, no. 1, pp. 160–173, Mar. 2020, doi: 10.17775/CSEEJPES.2019.01950.

[90] F. M. Camilo, R. Castro, M. E. Almeida, and V. Fernão Pires, “Assessment of over-voltage mitigation techniques in low-voltage distribution networks with high penetration of photovoltaic microgeneration,” *IET Renew. Power Gener.*, vol. 12, no. 6, pp. 649–656, 2018, doi: 10.1049/iet-rpg.2017.0482.

[91] E. McKenna, M. McManus, S. Cooper, and M. Thomson, “Economic and environmental impact of lead-acid batteries in grid-connected domestic PV systems,” *Appl. Energy*, vol. 104, pp. 239–249, 2013, doi: 10.1016/j.apenergy.2012.11.016.

[92] Prysmian Group. "AXMK-PLUS - 1 kV verkonrakennuskaapelit" 1000872datasheet. February 2019.

[93] A. Woyte, V. Van Thong, R. Belmans, and J. Nijs, “Voltage fluctuations on distribution level introduced by photovoltaic systems,” *IEEE Trans. Energy Convers.*, vol. 21, no. 1, pp. 202–209, Mar. 2006, doi: 10.1109/TEC.2005.845454.

ATTACHMENTS

Table A.1. *Cable information in the simulation model [92].*

Cable type	R (Ω /km) [NxN matrix]	*L* (H/km) [NxN matrix]	*C* (F/km) [NxN matrix]	U_N (kV)	The current capacity (A)
Prysmian AXMK-PLUS 4G185	[0.2 0.6]	[0.26e-3 4.1264e-3]	[0.28e-6 7.751e-9]	1	330
Prysmian AXMK-PLUS 4G25	[1.5 4.5]	[0.28e-3 4.1264e-3]	[0.29e-6 7.751e-9]	1	100